1963

Overload behavior of prestressed concrete beams with web reinforcement, February 1963

J. M. Hanson

C. L. Hulsbos

PRESTRESSED CONCRETE BRIDGE MEMBERS

PROGRESS REPORT NO. 25

OVERLOAD BEHAVIOR OF PRESTRESSED CONCRETE BEAMS WITH WEB REINFORCEMENT

John M. Hanson
C. L. Hulsbos

Part of an Investigation Sponsored by:

PENNSYLVANIA DEPARTMENT OF HIGHWAYS
U.S. DEPARTMENT OF COMMERCE
BUREAU OF PUBLIC ROADS
REINFORCED CONCRETE RESEARCH COUNCIL

Lehigh University

Bethlehem, Pennsylvania

Fritz Engineering Laboratory Report No. 223.25

February, 1963

ACKNOWLEDGEMENTS

This work has been carried out in the Department of Civil Engineering at Fritz Engineering Laboratory, under the auspices of the Institute of Research of Lehigh University, as part of an investigation sponsored by: Pennsylvania Department of Highways; U.S. Department of Commerce, Bureau of Public Roads; and the Reinforced Concrete Research Council.

The authors wish to express their thanks to Mr. Frank Holmes, Mr. Dundar Kocaoglu, Mr. Wilfred Chen, and Mr. Dick Miller for their work on various stages of the project.

TABLE OF CONTENTS

1. INTRODUCTION

1.1 Object and Scope

In general, an ultimate strength study of a concrete structure must be based upon a consideration of the following five factors: static strength, fatigue strength, stability, deflection, and durability. To be satisfactory, a structure must have the desired degree of safety with respect to each of these factors.

For pretensioned prestressed beams, stability, deflection, and durability are generally factors of lesser importance. The ultimate static strength is usually the factor of paramount importance. However, where many repeated loads of large magnitude can be expected, the fatigue strength of the member may be of equal importance.

Knowledge of the strength of prestressed beams requires an understanding of the physical behavior of these members under load. Within ordinary working ranges in which the prestressed beam is not cracked, the response to load is approximately linear and the behavior can be evaluated by the familiar formulas of structural mechanics.

Strength outside of the elastic range, however, must be evaluated in terms of the various phenomena of the overload behavior of the member, as follows:

(1) Flexural cracking load
(2) Inclined cracking load
    (a) Flexure shear cracking
    (b) Diagonal tension cracking
(3) Ultimate load
    (a) Flexural strength
    (b) Shear strength
    (c) Fatigue strength

Each of these terms will be defined in Section 1.2.

This investigation was undertaken to study the ultimate shear strength of pretensioned prestressed I-beams with web reinforcement. Ultimate shear strength, however, depends upon the inclined cracking strength in its evaluation, and upon the ultimate flexural and fatigue strength in the definition of its limits. Therefore a study of ultimate shear strength must be a study

of all of the phenomena associated with the overload behavior of a prestressed member. The objective of this investigation is twofold: (1) to provide information pertaining to shear strength which will be immediately useful in the design of this type of member, and (2) to develop information which may serve as a basis for a rational analytical evaluation of shear strength of prestressed beams with web reinforcement.

The results of eighteen tests on simply supported beams subjected to a symmetrical two point loading, designated as the E Test Series, are presented in this report. Sixteen of the tests were static tests, conducted for the purpose of evaluating the static overload behavior of prestressed I-beams with web reinforcement. The remaining two tests were repeated load tests, conducted for the purpose of determining if a prestressed I-beam, once overloaded so that inclined cracks would form, could subsequently be critical in fatigue of the web reinforcement.

The principal variables in the static tests were the shear span to effective depth ratio, which varied between 2.54 and 6.39, and percentage of web reinforcement. The majority of the static tests, however, were conducted on a shear span to effective depth ratio of 3.39, for which the web reinforcement percentage was varied from a maximum of 1.22 to a minimum of zero. Corresponding to this particular shear span, the percentage of web reinforcement required according to the ACI - ASCE Joint Committee 323 Report,[1] hereafter referred to as the TRPC, is 0.85.

1.2 Definitions

Flexural cracking load. In general, the magnitude of load causing the formation of a flexural crack anywhere along the length of the prestressed beam is defined as the flexural cracking load; however, a flexural cracking load may be associated with flexural cracking at any specific section along the length of the member. For the symmetrically loaded test beams in the E Series, the magnitude of the shear due to the externally applied load causing a flexural crack anywhere along the length of the test member, V_c^f, is taken as the measure of load causing flexural cracking.

Inclined cracking load. The inclined cracking load is defined as the

load causing the formation of the first non-vertical crack anywhere along the length of the prestressed beam as a result of the combined effect of shear and moment. Inclined cracking may be of two types, flexure shear and diagonal tension.

Flexure shear cracking. A flexure shear crack is a flexural crack that becomes inclined and extends, with increasing load, in the direction of increasing moment. For the beams in the E Series, the magnitude of shear due to the externally applied load causing the initial formation of a significant flexure shear crack, V_c^{fs}, is taken as the measure of load causing flexure shear cracking. A significant flexure shear crack is defined as one which forms at a distance approximately equal to or greater than the effective depth of the member in the direction of decreasing moment from the concentrated load point.

Diagonal tension cracking. The diagonal tension crack is an inclined crack that initiates suddenly from an interior point in a prestressed beam. For beams in the E Series, the magnitude of the shear due to the externally applied load causing the formation of a diagonal tension crack, V_c^{dt}, is taken as the diagonal tension cracking load.

Ultimate load. The ultimate load of a prestressed member is the load carried by the member at failure. For the beams in the E Series, the measure of ultimate load is the shear due to the externally applied load, V_u. Principal modes of failure associated with the ultimate load are flexure, shear, and fatigue.

Flexural strength. The flexural strength is the moment capacity associated with the flexure failure mechanism.

Shear strength. The shear strength is the shear associated with a shear failure mechanism which results from the development and extension of inclined cracking. Excluded from the definition of shear strength are any apparent shear failures due to poor dimensional proportioning, i.e., bond failures in the web reinforcement and strand, insufficient bearing at the reaction, etc.

Fatigue strength. The fatigue strength is the load and number of cycles associated with a fatigue failure mechanism.

1.3 Notation

The following notation has been used throughout this report. Notation used only in one location, i.e., for example, in conjunction with the discussion of a specific figure, is not included; rather it is fully explained where used.

a	Length of shear span
A	Area of beam cross-section
A_v	Area of vertical stirrup
b	Width of top flange of I-beam
b'	Web width of I-beam
c	Horizontal component of resultant force in concrete compression region
d	Depth from concrete top fibers to centroid of prestressing strand
e	Distance from centroid of prestressing strand to center of gravity of the beam cross-section
E_c	Modulus of elasticity of concrete
f_u	Ultimate stress in stirrups
f_y	Yield stress of stirrups
f'_c	Ultimate compressive strength of concrete
f'_r	Modulus of rupture strength of concrete
f'_s	Ultimate stress of prestressing strand
f'_t	Flexural tensile strength of concrete
F	Resultant force in prestressing strand
F_i	Initial prestress force, before transfer
h	Total depth of I-beam
I	Moment of inertia of beam cross-section
ℓ_e	Distance from the junction of web and top flange to the lowest point at which the web reinforcement may be regarded as effective.
L	Span length, center to center of bearing
M	Moment
M_u	Static ultimate moment
M_c^f	Flexural cracking moment
N	Number of cycles of applied loading

P	Concentrated load
Q	Moment, about the center of gravity, of the area of the cross-section on one side of the horizontal section on which the shearing stress is desired
Q^{tf}	Q for a section taken at the junction of web and top flange
Q^{cg}	Q for a section taken at the center of gravity of the beam cross-section
Q^{bf}	Q for a section taken at the junction of web and bottom flange
r	Percentage of web reinforcement, $100\ A_v/b's$
s	Spacing of vertical stirrups
V	Shear
V_c	Amount of V carried by concrete after inclined cracking
V_w	Amount of V carried by stirrups after inclined cracking
V_u	Shear in test beams at ultimate load
V_c^f	Shear in test beams causing flexural cracking
V_c^{dt}	Shear in test beams causing diagonal tension cracking
V_c^{fs}	Shear in test beams causing flexure shear cracking
w	Uniform load
Z^b	Section modulus with respect to stress in bottom fibers
Z^t	Section modulus with respect to stress in top fibers
α	Dimensionless factor which, when multiplied by L, locates P
β	Dimensionless factor which, when multiplied by d, determines the horizontally projected length of an inclined crack
θ	Angle, with respect to the horizontal, of the compressive stress trajectory
σ_t	Maximum principal tensile stress in the web at the diagonal tension-cracking load
σ_t^{cg}	Values of σ_t at the center of gravity of the beam cross-section

2. TEST SPECIMENS

2.1 Description

A doubly symmetric I-shaped cross section with a depth to flange width ratio (h/b) of 2 and a flange to web width ratio (b/b') of 3 was used for all eighteen beam specimens. Each beam specimen was 17'-6" in length, providing a test span of 15'-0" and an overhang at each reaction of 1'-3". Details of the cross section and an elevation view of the test beams are shown in Fig. 1.

Size, spacing (s), and percentage of web reinforcement (r), based on the web width, is given in the outline of tests in Table 1. Except for E.13 and E.14, each stirrup consisted of either one or two U-shaped bars, referred to as S or D. Where only one bar was used, each successive bar was placed so that the U opened to the opposite side of the test beam. In E.13 and E.14 inverted L-shaped bars were used, and each stirrup consisted of two bars. The letter F following E.10 and E.11 indicates repeated load test. All other tests were static tests.

Six 7/16" diameter strands were used as the prestressing elements in each test beam. All strands were straight throughout the length of the test beam, and each strand was pretensioned to a nominal initial force of 18.9 kips, providing a total initial design prestress force of 113.4 kips. Assuming losses of 8% in the prestress force at transfer, the initial stresses in the top and bottom concrete fibers, based on the transformed section and neglecting dead weight, are 210 psi tension and 2150 psi compression, respectively.

2.2 Materials

Ready-mixed concrete was used in the fabrication of the test beams, having a cement to sand to coarse aggregate ratio of approximately 1 to 1.85 to 2.33. The mix contained 7.5 bags per cubic yard of Type III portland cement. The maximum size of the coarse aggregate was 3/4". Gradation of the aggregate conformed to Pennsylvania Department of Highways Specifications. Mixes were made in either 2 or 2.5 cubic yard batches, sufficient

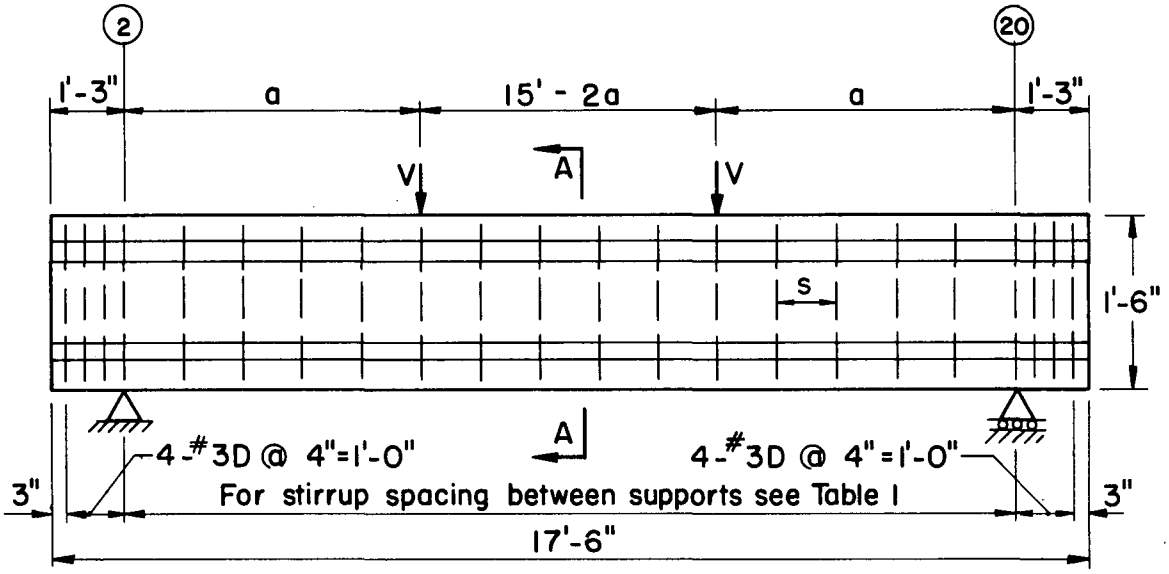

ELEVATION

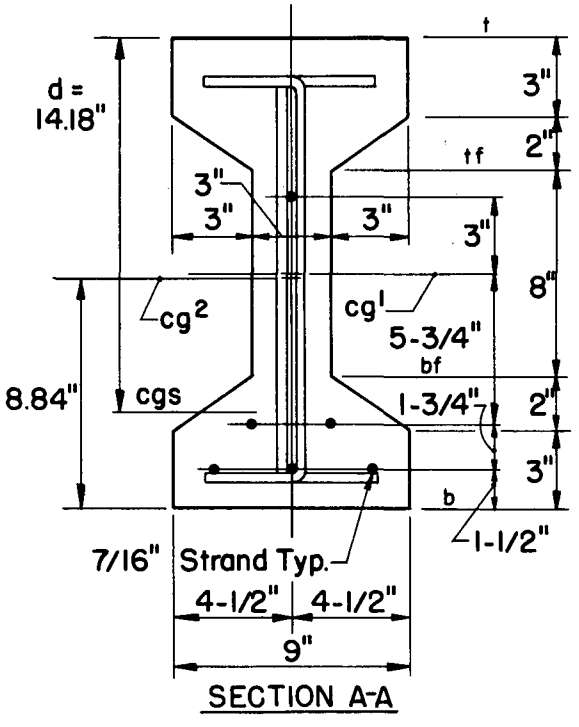

SECTION A-A

SECTION PROPERTIES		
PROPERTY	CONCRETE SECTION[1]	TRANSFORMED SECTION[2]
A	102.0 in.^{2}	105.3 in.^{2}
I	3854 in.^{4}	3986 in.^{4}
Z^t	428.2 in.^{3}	435.2 in.^{3}
Z^b	428.2 in.^{3}	450.9 in.^{3}
Q^{tf}	262.5 in.^{3}	270.9 in.^{3}
Q^{cg}	286.5 in.^{3}	298.5 in.^{3}
Q^{bf}	262.5 in.^{3}	276.3 in.^{3}

Fig. 1 Details of test beams

Table 1. Outline of Tests

Shear Span (a)	Size and Spacing (s) of Web Reinforcement	Web Reinforcement Percentage (r)	Test Beam
3'-0"	#2D at 8.75"	0.374	E.14
	#2D at 8.75"	0.374	E.15
4'-0"	None	0	E.4
	#3D at 6"	1.22	E.5
	#3D at 8"	0.917	E.6
	#3D at 10"	0.733	E.7
	#3S at 6"	0.611	E.8
	#3S at 8"	0.458	E.9
	#3S at 6"	0.611	E.10F
	#3S at 8"	0.458	E.11F
	#3S at 10"	0.367	E.12
	#2D at 8.75"	0.374	E.13
	#2S at 6"	0.272	E.16
	#2S at 8"	0.204	E.17
	#2S at 10"	0.163	E.18
5'-0"	None	0	E.3
6'-0"	None	0	E.2
7'-6"	None	0	E.1

to cast 3 test beams in one pour. Slump varied between 2-1/4" and 2-3/4" for all mixes except for the mix used to cast E.1, E.2, and E.3, which had a slump of 1-1/2". Concrete strength at the time of test of all beam specimens was approximately 7000 psi.

The prestressing strand was 7/16" diameter seven wire uncoated stress relieved high tensile strength strand manufactured by John A. Roebling's Sons Corporation. A stress-strain curve for the strand, determined from a tension test conducted in the laboratory, is shown in Fig. 2. Failure occurred in the testing machine grips at an ultimate load of 26.3 kips. The stress-strain curve in Fig. 2 was virtually identical with the stress-strain curve provided by the manufacturer, which indicated the strand to have an ultimate load of 27.5 kips, corresponding to an ultimate stress (f'_s) equal to 252.5 ksi, and 5.1 percent elongation in 24 in. The surface of the strand was free from rust, and care was taken to avoid getting any grease on the strand during the fabrication operation.

The web reinforcement was fabricated from hot rolled No. 2 or No. 3 deformed bars. For the No. 2 bar, the yield point stress (f_y) was 59,500 psi and the ultimate stress (f_u) was 85,700 psi, based on an area of 0.049 sq. in. For the No. 3 bar, f_y was 55,500 psi and f_u was 82,700 psi, based on an area of 0.11 sq. in. The values of f_y and f_u for the No. 2 and No. 3 bars are an average of 12 and 3 tension tests, respectively.

2.3 Fabrication

The test beams were fabricated in a prestressing bed on the laboratory test floor. The length of the bed was sufficient to permit three beams to be cast end to end.

The sequence of operations in casting the test specimens was as follows: tensioning the strands, positioning the web reinforcement, form erection, pouring the concrete, curing, form removal, instrumentation, and prestress release.

Two 50 ton mechanical jacks were used to tension the strands to approximately the desired value of 113.4 kips. A special hydraulic jacking arrangement

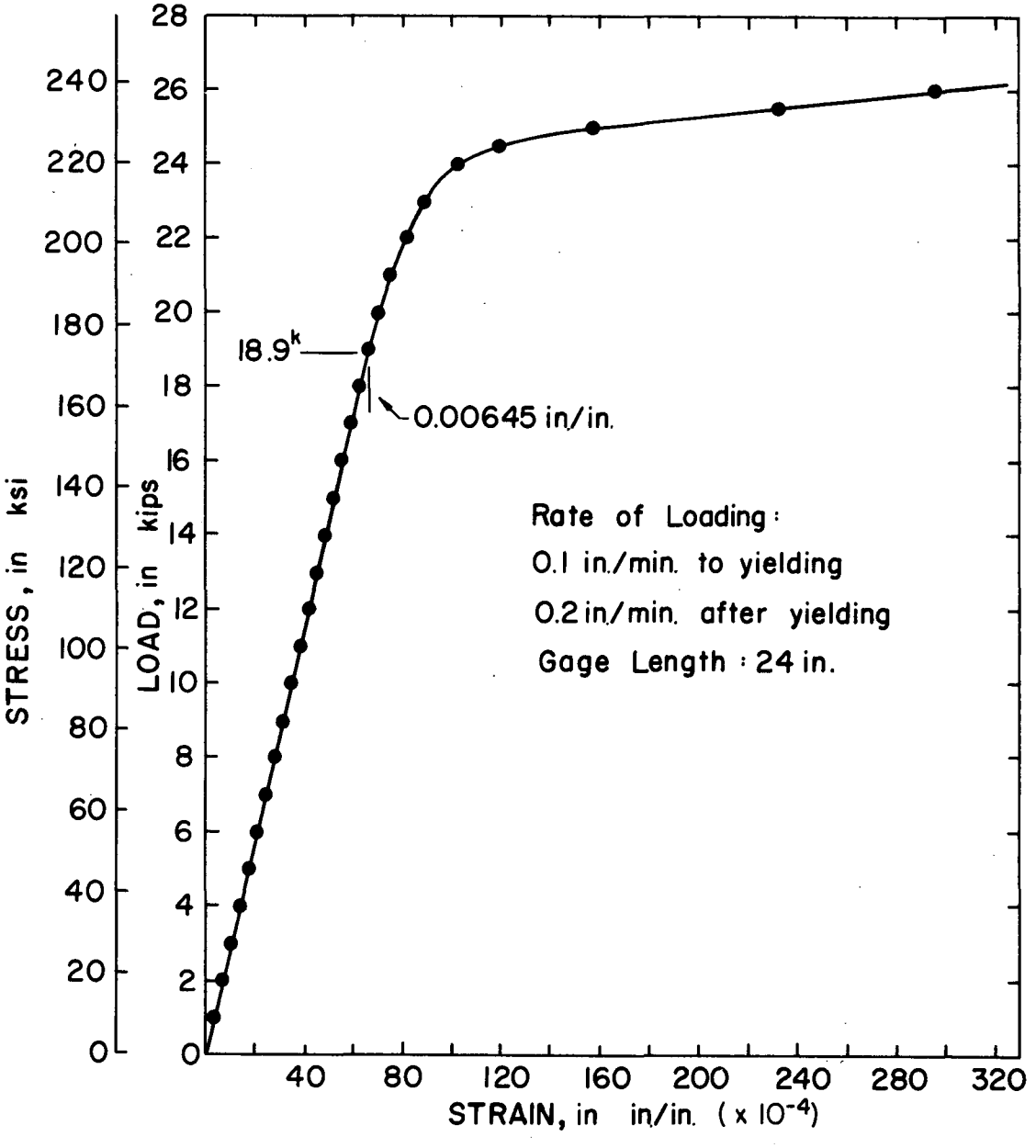

Fig. 2 Stress-strain curve for prestressing strand

was subsequently used to adjust the tension in individual strands if required. The tension was measured by means of load cells placed on each strand; for all of the strands tensioned, the average variation from the desired value of 18.9 kips per strand was less than 0.2 kips. The total initial prestress force, as obtained by reading the load cells just prior to pouring the concrete, is given in Table 2.

Also given in Table 2 is the total prestress force determined by reading the same load cells seven days after the concrete was poured, just prior to releasing the prestress force into the test beams. In all but one set of beams the force in the strands increased between the time of casting and the time of prestress release, possibly due to shrinkage of the specimens exerting an additional force on the prestressing strand.

Table 2. Prestress Force at Casting and Release

Test Beams	Total Prestress Force (kips)		Per Cent Change
	At Casting	At Release	
E.1, E.2, & E.3	113.7	115.6	+1.7
E.4, E.5, & E.6	113.9	119.4	+4.8
E.7, E.8, & E.9	114.9	116.5	+1.4
E.10, E.11, & E.12	113.7	117.3	+3.3
E.13, E.14, & E.15	113.5	113.1	-0.4
E.16, E.17, & E.18	113.3	121.4	+7.1

Wire ties were used to secure the web reinforcement to the strand. In addition, it was found necessary to use a wire tie between successive projecting elements of the stirrups, in the compression flange area, to prevent movement of the stirrups during the pouring operation.

Wood forms were used to cast the test beams. Dimensional checks made on the finished product indicated that, in general, dimensions were maintained within 1/8", and consequently the nominal dimensions of the cross

section given in Fig. 1 were used in all calculations. With each test beam were cast six or more standard concrete cylinders in waxed cardboard forms, and three 6" x 6" by 3'-0" modulus of rupture beam specimens in steel forms. Vibrators were used to place the concrete in both the test beams and the modulus of rupture specimens; the cylinders were rodded.

All specimens were cured by covering with wet burlap and plastic sheeting for five days, after which the forms were stripped. Instrumentation, in the form of Whittemore targets described in the next section, was positioned on the test beams on the sixth day. On the seventh day after casting the prestress force was slowly released into the beams. The specimens were subsequently stored in the laboratory until the time of testing.

2.4 Instrumentation and Loading Apparatus

The test set-up and principal instrumentation employed on the test beams is indicated in Fig. 3. Loads for all test beams were symmetrically applied using two 55 kip Amsler hydraulic jacks bolted to a steel test frame. Vertical deflections were measured by both Ames dial gages and level readings.

Deformation data was taken using a 10 inch Whittemore Strain Gage. The gage points were made in the laboratory by cutting 1/16 inch aluminum plate into 3/8 inch square pieces. Prior to cutting, each individual target was center punched and drilled with a No. 56 drill. The drilled holes did not go through the aluminum plate, but were made deep enough to clear the end of the points of the Whittemore. The aluminum targets were cemented to the test beams with an epoxy type resin known as Armstrong Adhesive A-6.

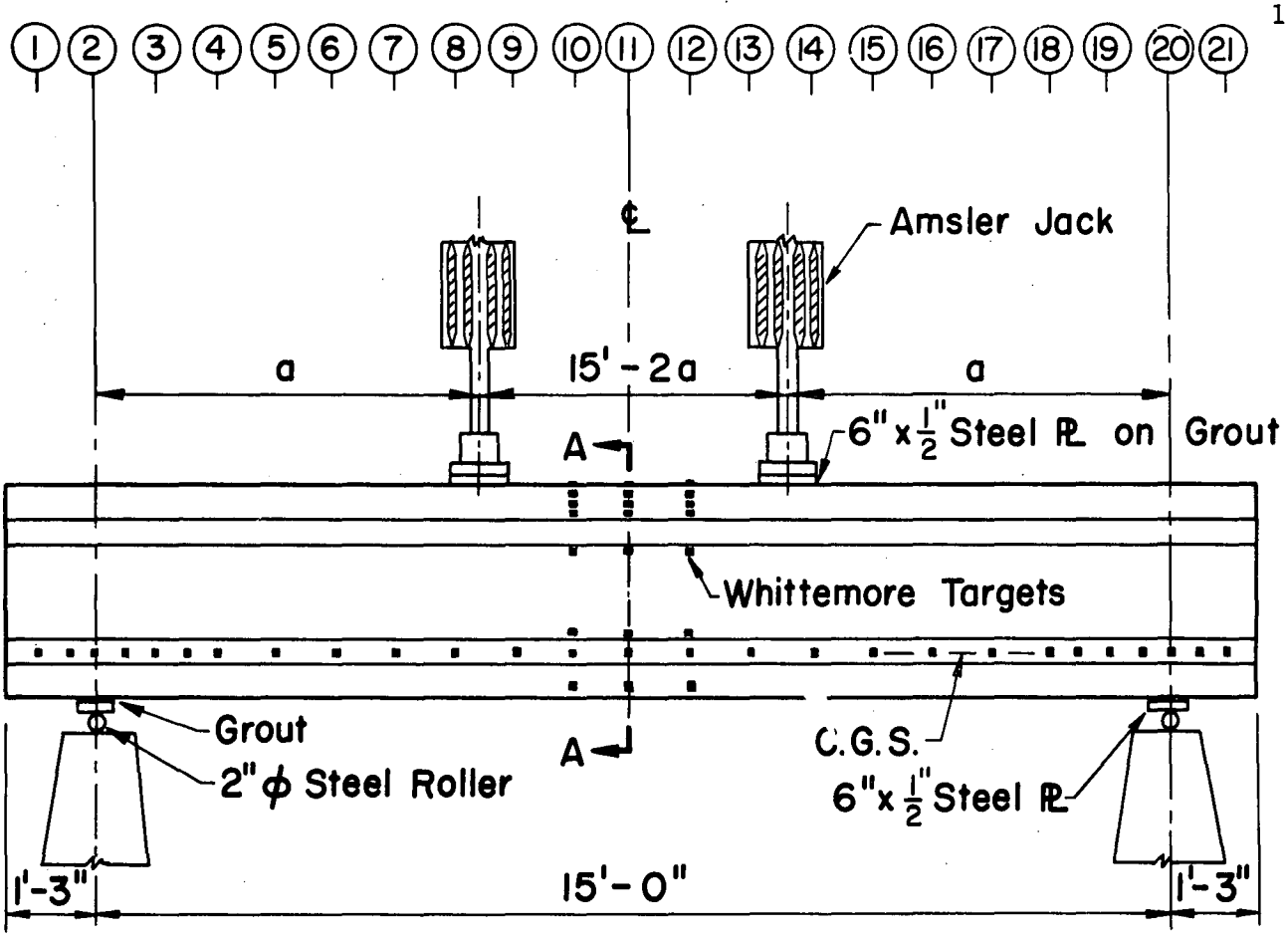

ELEVATION

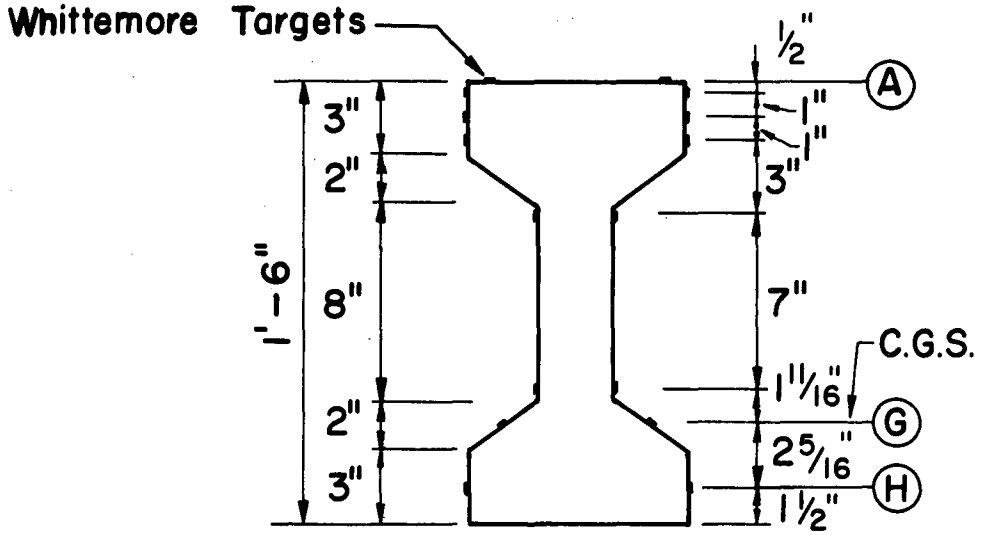

SECTION A – A

Fig. 3 Test set-up and principal instrumentation

3. PROCEDURE AND RESULTS

3.1 General

The tests carried out in this investigation may be considered as divided into three groups: static tests, repeated load tests, and re-loaded static tests.

The static tests, E.1 through E.18 with the exception of E.10 and E.11, were tests carried directly to the ultimate capacity of the member. The majority of these tests were carried out on a 4'-0" shear span; however, two were carried out on a shear span of 3'-0", and one each on shear spans of 5'-0", 6'-0", and 7'-6". These test results are presented in Section 3.4.

The repeated load tests, E.10 and E.11, were first statically loaded on a 4'-0" shear span, to approximately 77% of their ultimate flexural capacity. This was sufficient to cause diagonal tension inclined cracking in both shear spans of both beams. Repeated loadings were subsequently applied which varied from a minimum of approximately 19% to a maximum of 44% and 68%, in the case of E.10, and 58%, in the case of E.11, of the ultimate flexural capacity of the test beam. Section 3.5 contains the results of these tests.

The re-loaded static tests were conducted on the remaining intact portion of selected beams after the specimen had already been tested in either the static or fatigue test group. The results of these tests are presented in Section 3.6.

Section 3.2 contains the results of tests on cylinder and modulus of rupture specimens to determine the properties of the concrete associated with the test beams at the time of prestress release and at the time of test. Section 3.3 presents the results of strain measurements taken to determine prestress losses, and to determine the prestress transfer distance at the end of the test beams.

3.2 Properties of the Concrete

Standard cylinder tests were conducted to determine the ultimate compressive strength of the concrete (f'_c) associated with the test beams at the

time of prestress release and at the time of test. Strains were measured on selected cylinders with a compressometer to determine the modulus of elasticity (E_c) of the concrete. For comparison, values of E_c were also determined from the load deflection curves of the test beams.

As a measure of the tensile strength of the concrete, modulus of rupture tests were conducted to determine the modulus of rupture strength of the concrete (f'_r) associated with the test beams at the time of test.

Cylinder tests associated with the time of prestress release were always carried out on the same day that the prestress force was released, generally within an hour or two of the actual operation. Cylinder and modulus of rupture tests associated with the time of test were carried out either on the same day, or in a very few instances, on the day following the testing of the beam specimen. Where these tests were repeated load tests, which were carried out over a period of several days, the cylinder and modulus of rupture tests were conducted on either the first or second day. The values of f'_c, f'_r, and E_c determined from these tests are given in Table 3. In general, each value is an average of three tests. As a typical example, the results of three cylinder tests associated with E.5 at the time of test are shown in Fig. 4.

3.3 Prestress Data

For both the static and repeated load test specimens, data was taken to determine experimentally the elastic and inelastic losses in the prestress force, and the distance from the ends of the test beams, at the level of the center of gravity of the prestressing strand, to the point at which 85% of the prestress force was effective. This was accomplished by taking Whittemore readings on the surface of the test beams along line G shown in Fig. 3. Readings were taken just prior to releasing the prestress force, after the release of the prestress force, and again just prior to the actual testing of the specimen. The difference between these readings, converted to concrete strain, can be plotted against location along the length of the test beam, a typical example of which is shown for E.5 in Figs. 5a and 5b.

Table 3. Properties of the Concrete

Beam No.	At Transfer			At Test				
	Age (days)	f'_c (psi)	E_c^1 (ksi)	Age (days)	f'_c (psi)	f'_r (psi)	E_c^1 (ksi)	E_c^2 (ksi)
E.1	7	5600	3100	67	7030	690	4000	4600
E.2	7	5640	3100	62	6690	740	3600	4200
E.3	7	5690	3100	56	6720	660	3500	4300
E.4	7	5500	3200	55	6960	700	3900	4700
E.5	7	5530	3100	60	6610	670	3800	4600
E.6	7	5440	3200	62	7100	730	4100	4500
E.7	7	5900	3800	62	7230	800	4100	4700
E.8	7	5680	3400	70	6970	650	4400	4700
E.9	7	5630	3500	74	7140	720	4200	4700
E.10	7	6160	3600	228	7360	950	4400	5100
E.11	7	6410	3600	245	7790	960	4200	5000
E.12	7	5590	3300	68	7020	680	3900	4700
E.13	7	6130	3700	27	7320	630	4400	4500
E.14	7	5670	3600	47	6780	680	4100	4700
E.15	7	5730	3500	35	6940	670	4300	4600
E.16	7	5650	3300	64	6950	610	3700	4500
E.17	7	5400	3300	57	6580	600	3800	4300
E.18	7	5520	3200	52	6640	580	3600	4500
Ave.		5720	3400		7000	710	4000	4600

Note: Modulus of elasticity values are designated E_c^1 if determined from cylinder tests and E_c^2 if determined from load-deflection curve of the test beam.

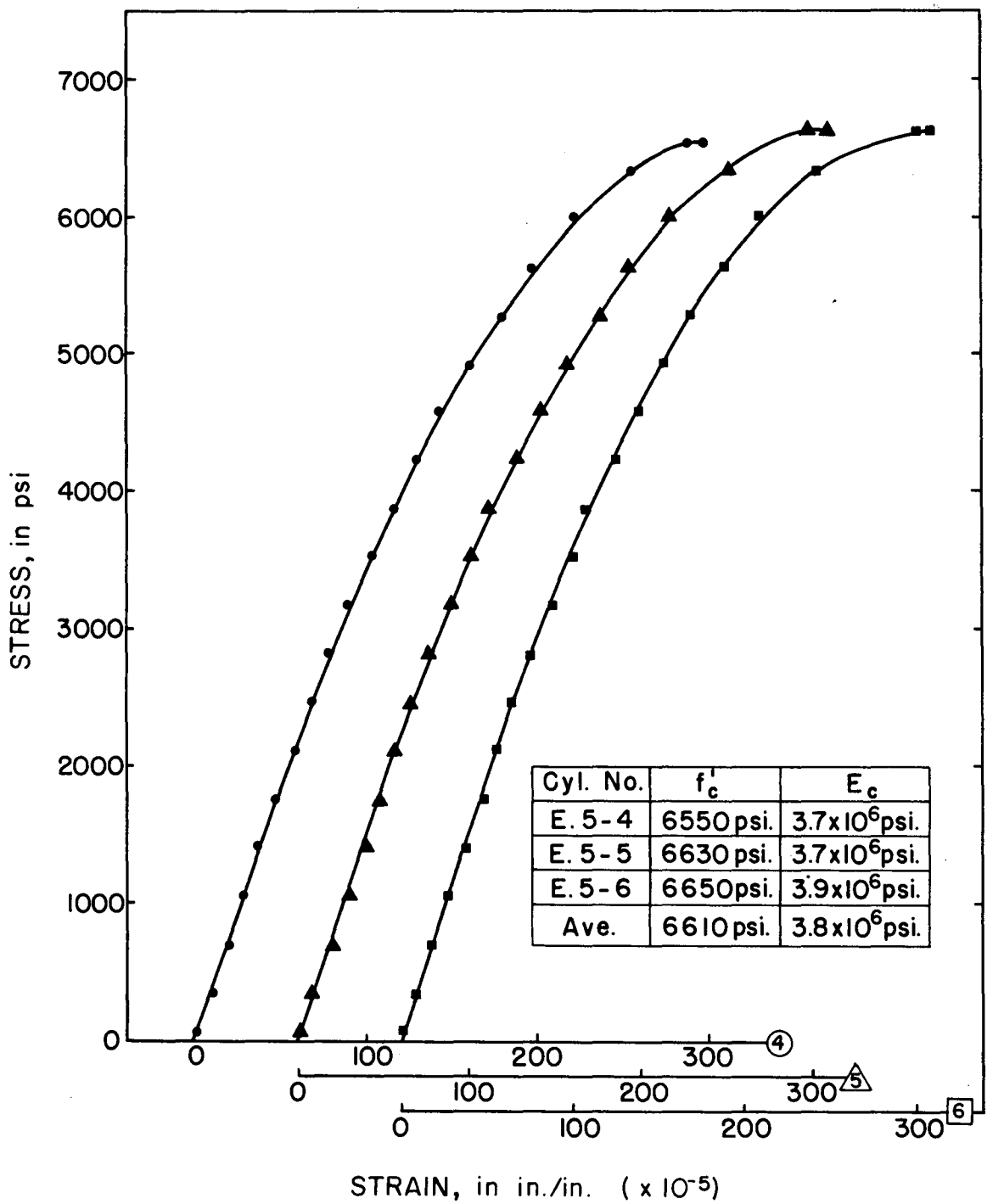

Fig. 4 Cylinder tests for E.5 (at test)

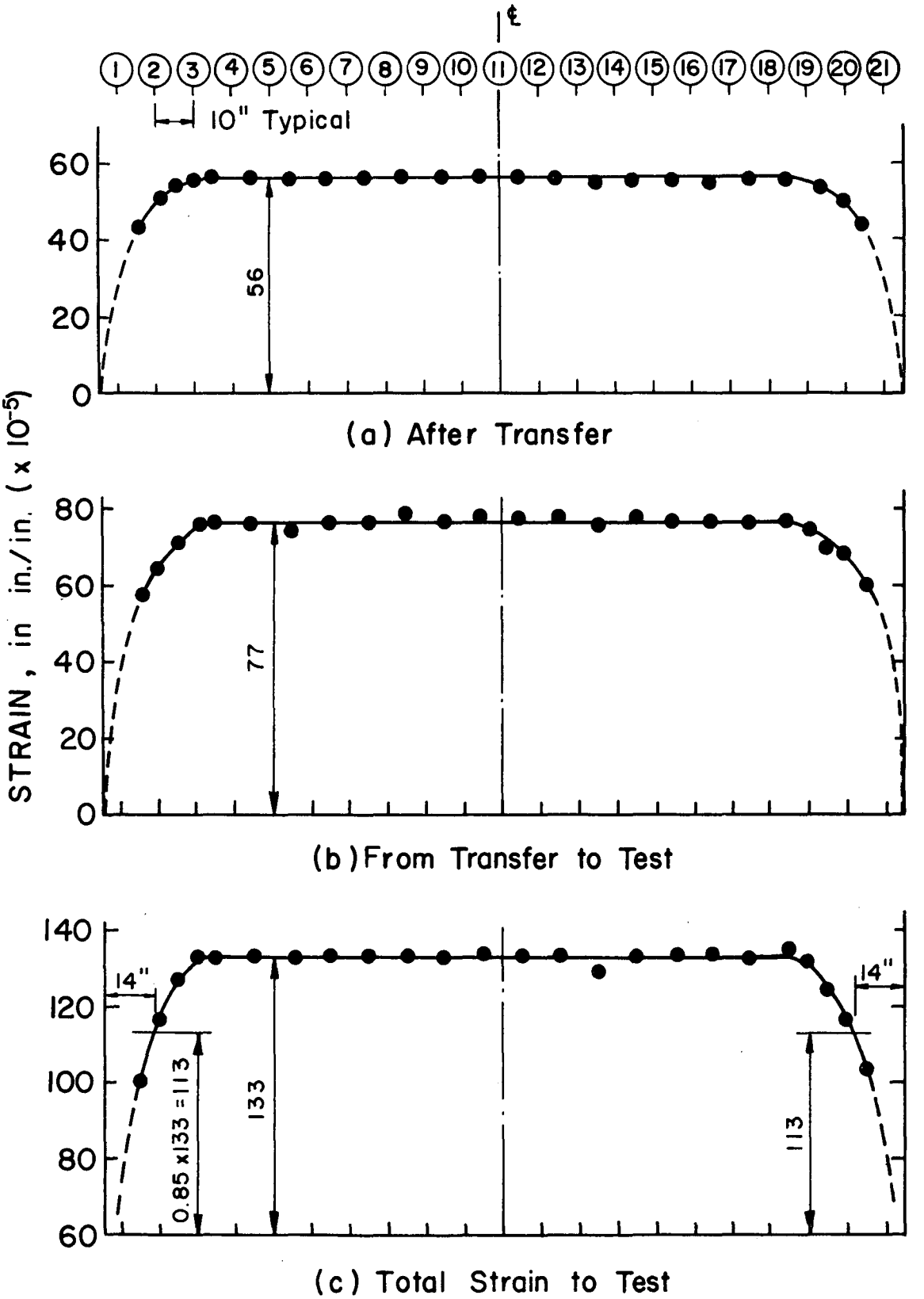

Fig. 5 Concrete strain along C.G.S. from before transfer to test

Assuming that the concrete strain measured on the surface of the test beam at the level of the center of gravity of the strand is equal to the average strain loss in the prestressing strand, the loss in the prestress force can be determined from the stress-strain curve of the strand. The strain determined from the difference in the Whittemore readings before and after release of the prestress force was considered to be the elastic loss. Similarly the strain determined from the difference in the readings after release of the prestress force and just prior to testing was considered to be the inelastic loss. The results of this work are presented in Table 4.

The distance from the end of the beam at the level of the center of gravity of the strand to the point at which 85% of the prestress force was developed was determined by plotting the total concrete strain at the time of test along the length of the beam. An example of this is shown for E.5 in Fig. 5c. Transfer distances determined in this way for all of the test beams are given in Table 4.

3.4 Static Tests

The beams in this group, E.1 through E.18 with the exception of E.10 and E.11, were loaded to ultimate failure in one load cycle. Load was symmetrically applied in shear increments of 2 kips, except when near loads at which cracking was expected, in which case the shear increment was reduced to 1 kip.

Data taken during the test included primarily load-deflection readings, strain measurements by Whittemore readings, and a log of the loads at which flexural cracking, inclined cracking, and ultimate failure took place. In addition, crack patterns were marked on the test beams after the application of each load increment. After failure the test beams were photographed.

The principal results of this group of tests are presented in Table 5. Convenient parameters for comparing the two principal variables in this investigation, length of shear span and amount of web reinforcement, are tabulated as the shear span to effective depth ratio $(\frac{a}{d})$ and the web reinforcement index $(rf_y/100)$. The experimentally determined shears at flexural cracking, inclined diagonal tension cracking, and at failure are given as V_c^f, V_c^{dt}, and

Table 4. Prestress Data

Beam No.	Initial Prestress Force F_i (kips)	Losses			Prestress Force At Test F (kips)	Transfer Distance	
		Elastic (%)	Inelastic (%)	Total (%)		End (2) (in.)	End (20) (in.)
E.1	113.7	8.4	12.9	21.3	89.4	11	9
E.2	113.7	8.5	12.7	21.2	89.5	12	14
E.3	113.7	9.0	12.3	21.3	89.4	14	17
E.4	113.9	8.8	11.3	20.1	91.0	11	12
E.5	113.9	8.6	11.9	20.5	90.6	14	14
E.6	113.9	8.5	12.3	20.8	90.2	16	16
E.7	114.9	8.1	11.8	19.9	92.0	13	15
E.8	114.9	8.1	11.8	19.9	92.0	14	15
E.9	114.9	8.1	12.7	20.8	91.0	17	15
E.10	113.7	8.4	15.3	23.7	86.7	15	15
E.11	113.7	8.3	15.4	23.7	86.7	14	16
E.12	113.7	8.5	12.3	20.8	90.0	12	15
E.13	113.5	7.8	7.1	14.9	96.6	15	14
E.14	113.5	7.6	7.3	14.9	96.6	10	11
E.15	113.5	7.3	7.9	15.2	96.3	13	11
E.16	113.3	8.2	11.0	19.2	91.6	13	15
E.17	113.3	8.4	10.2	18.6	92.4	14	13
E.18	113.3	8.5	9.9	18.4	92.6	15	15
Ave.	113.8	8.3	11.5	19.8	91.4	13.5	14.0

Table 5. Static Test Results

Test Beam	$\frac{a}{d}$	$\frac{rf_y}{100}$ (psi)	Shear, V				Nominal Shear Stress At Ult. Load $v_u = \frac{V_u}{b'd}$ (psi)	Mode of Failure
			At Flexural Cracking V_c^f (kips)	At Diagonal Tension Cracking		At Ult. Load V_u (kips)		
				End (2) V_c^{dt} (kips)	End (20) V_c^{dt} (kips)			
E.1	6.35	0	14.4	----	20.4	16.2	381	S
E.2	5.08	0	16	----	23.9	20.8	489	S
E.3	4.23	0	20	26	----	23.1	542	S
E.4	3.39	0	24.4	30	----	30.8	724	S
E.5	3.39	676	24	31.8	28	42.0	988	F
E.6	3.39	508	24	30	28	41.8	984	F
E.7	3.39	406	25	28	28	41.1	965	F
E.8	3.39	339	23.3	28.2	27.2	41.2	968	F
E.9	3.39	254	24	28	28	41.2	968	F
E.12	3.39	204	24	30	30	41.2	968	F
E.13	3.39	222	24	30.6	29.2	41.7	981	F
E.14	2.54	222	33	33.8	32.3	53.8	1263	B
E.15	2.54	222	32	33	34	55.7	1310	F
E.16	3.39	162	24	30	30	39.9	939	F
E.17	3.39	121	24	26	29.4	38.0	894	S
E.18	3.39	97	24	27.1	31.5	38.7	911	S

V_u, respectively, determined according to the definitions in Section 1.2. Modes of failure are indicated by S for shear, F for flexure, and B for bond failure in stirrups.

For example, Figs. 6a and 6b show an overall view and a closer view of the right side, respectively, of the test beam E.12. The crack patterns are marked so as to indicate extent of cracking for the value of shear marked on the beam, and the dark lines marked on the web of the test beams, perpendicular to the longitudinal axis, indicate the location of the web reinforcement. The values of V_c^f and V_c^{dt} can be readily determined from Fig. 6b as 24 kips and 30 kips, respectively. The mode of failure may be observed to be flexure.

Inclined diagonal tension cracking occurred in all of the test beams. This cracking was in all instances characterized by its sudden appearance and by its initiation from an interior point in the web of the test beams. Because the hydraulic loading apparatus was of the type which controlled the displacement introduced into the test beams and measured the corresponding applied force, a further characteristic of the diagonal tension cracking was a noticeable drop off in the measured applied load at the instant the diagonal tension cracking formed. In general, the amount of load drop off was greater for tests with the greater a/d ratios.

In the test beams without web reinforcement, E.1 through E.4, the diagonal tension cracking load was in effect the ultimate load. Although the test beams did not collapse with the formation of diagonal tension cracking, their appearance indicated extreme instability, particularly for the three test beams with the greater a/d ratios. As a consequence of this instability, these four test beams were unloaded after the diagonal tension cracks formed. They were subsequently re-loaded to complete failure, characterized by a total loss of load carrying capacity. These final values of ultimate load are given as V_u in Table 5; however the value of V_c^{dt} for these four test beams may be more appropriately regarded as the ultimate load.

The state of cracking in the test beams at the time of formation of the inclined diagonal tension cracks was reconstructed from photographs of the test beams, and is presented in Appendix I. These figures are elevation views of the test beams in both the static and repeated load test group,

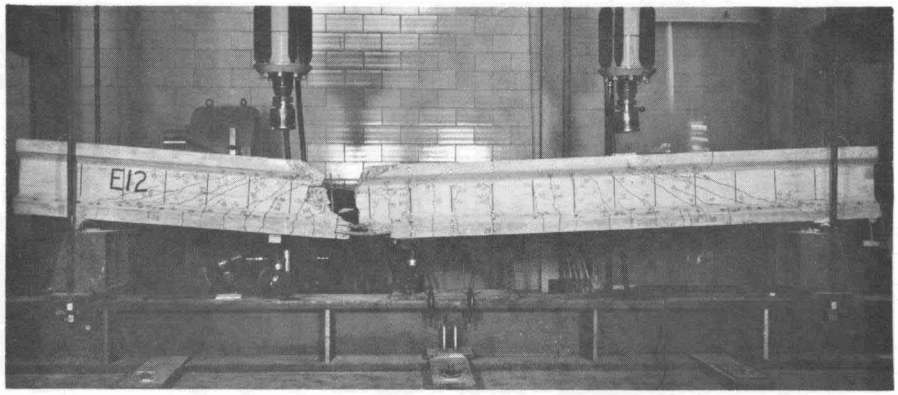

a. Elevation view, end (2) on right

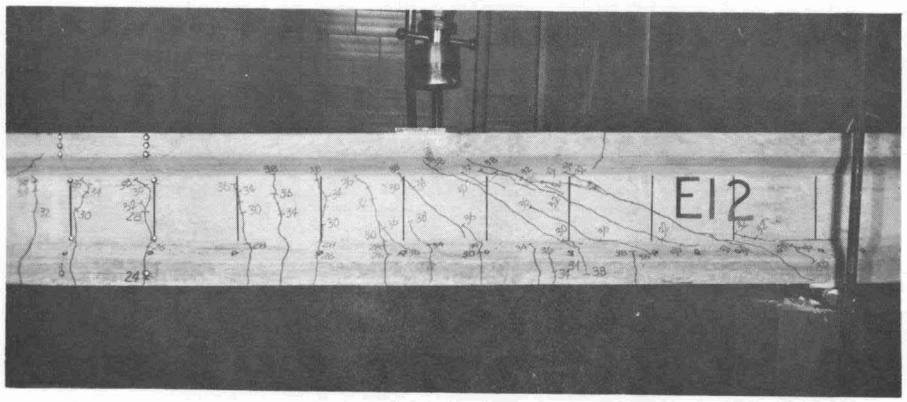

b. View of end (2)

Fig. 6 E.12 after failure

the two beams in the repeated load test group being included because the first load cycle causing inclined cracking may be regarded as a static test. Note that in the case of test beams without web reinforcement, diagonal tension cracking occurred on only one side of the test beams, since failure was synonymous with the diagonal tension cracking load. For test beams with web reinforcement, however, there was substantial load carrying capacity beyond diagonal tension cracking; consequently diagonal tension cracking would form, at different loads, in both shear spans.

In the figures in Appendix I, all cracking prior to the formation of diagonal tension cracking is indicated by solid heavy lines. The suddenly appearing diagonal tension cracking is indicated by dashed heavy lines, and the magnitude of the applied load shear causing this diagonal tension cracking is indicated by the applied load at one of the two load points. Also shown in the figures, in the conventional way, is the location of the vertical web reinforcement.

The principal stresses (calculated at the intersection points of the grid lines and the junction of the web and top flange, the center of gravity of the concrete section, and the junction of the web and bottom flange) and compressive stress trajectories shown in the shear span of the test beams in Appendix I were determined using the familiar procedures of structural mechanics, based on the assumptions of an uncracked section and no stress concentrations. For such test beams as, for example, E.14, there was no cracking in the shear span prior to diagonal tension cracking, and therefore the given principal stresses represent the state of stress just prior to cracking, at least so far as the assumptions stated are correct. However, for such test beams as, for example, E.3, flexure shear cracking occurred in the shear span prior to the suddenly forming diagonal tension cracking; therefore the principal stresses in the region of the flexure shear cracking do not represent the state of stress at the time of diagonal tension cracking. The principal stresses given are based on the section properties of the transformed cross-section, include the very slight effect of the dead weight of the test beam, and utilize the experimentally determined value of the prestress force at the time of test given in Table 4.

Examination of the figures in Appendix I suggest that there may be three test beams, E.1, E.2, and E.3, which have a lower value of the inclined

cracking load than the value of the diagonal tension cracking load given in Table 5. Pictures of these three test beams are shown in Figs. 7a, 7b, and 7c. From these pictures values of V_c^{fs} in agreement with the definition of significant flexure shear cracking in Section 1.2 may be approximately determined; the values selected are given in Table 5A. The value of V_c^{fs} equal to 26 kips for E.3 is the same as the value of V_c^{dt} given in Table 5. In this case the diagonal tension crack formed while holding the load on E.3 constant at a shear of 26 kips, during the time that the experimental readings were being taken and crack patterns marked. A significant flexure shear crack, however, had formed just prior to reaching the shear of 26 kips.

Table 5A. Flexure Shear Cracking

Test Beams	a/d	V_c^{fs} (kips)
E.1	6.35	17.5
E.2	5.08	22
E.3	4.23	26

Modes of failure of the test beams were classified in Table 5 as flexure, shear, or bond. The flexural failures were all similar, being characterized by crushing of the concrete in the compression zone and sudden complete collapse of the test beam. Test beam E.5 may be regarded as typical of the flexural failures; pictures of this failure are shown in Fig. 8.

The shear failures were quite dissimilar. Consider first the beams without web reinforcement, E.1 through E.4. As previously noted, the formation of diagonal tension cracking caused the beam to appear unstable, but did not trigger a collapse mechanism. Subsequent un-loading and re-loading to complete failure led to a collapse mechanism characterized in all four cases by crushing of concrete in the lower portion of the web and by the apparently simultaneous development of a tension crack in the top flange. The failure in E.4 typifies this description, and a picture of this particular failure mechanism is shown in Fig. 9. The failure in test beams E.1 through E.3 was similar to that shown in Fig. 9 for E.4, and the failure region in all cases

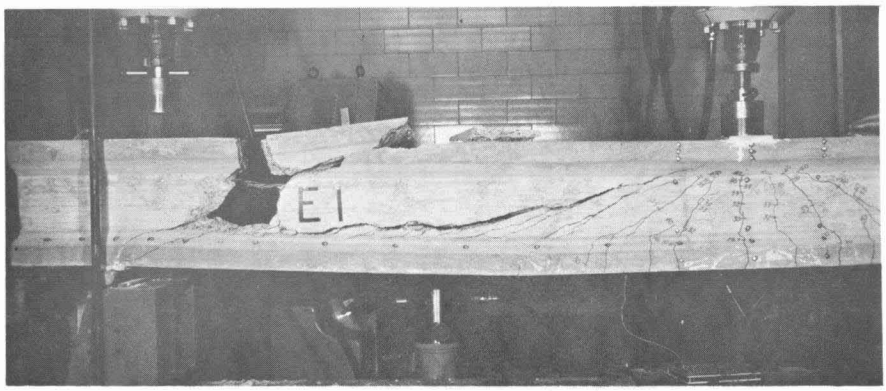

a. Beam E.1

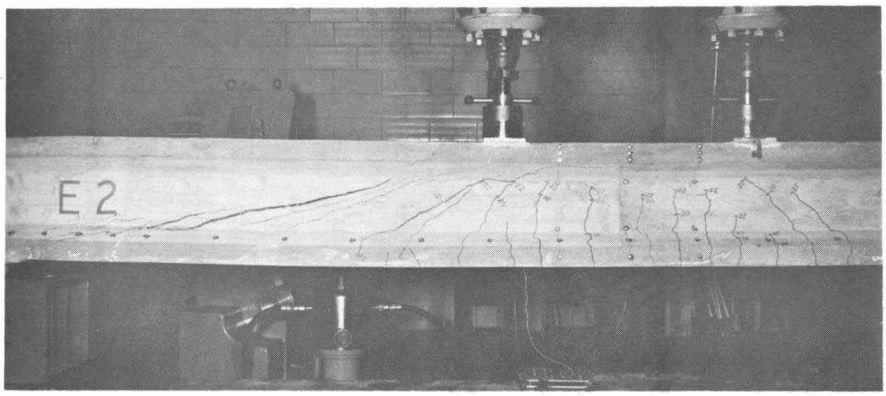

b. Beam E.2

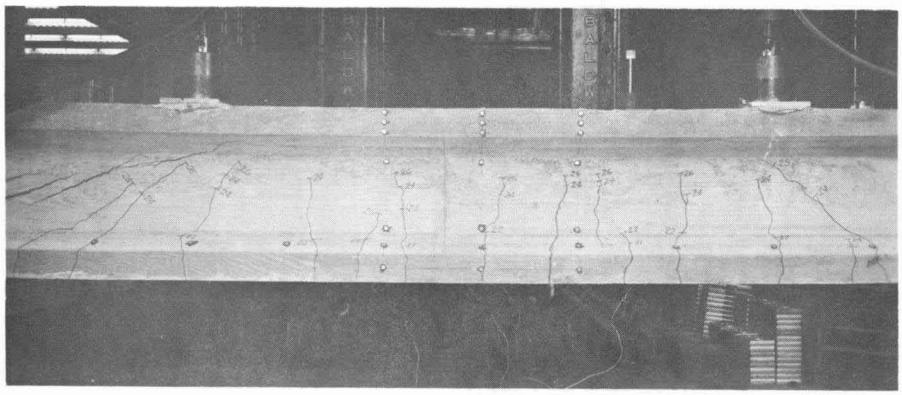

c. Beam E.3

Fig. 7 E.1, E.2 and E.3 after failure

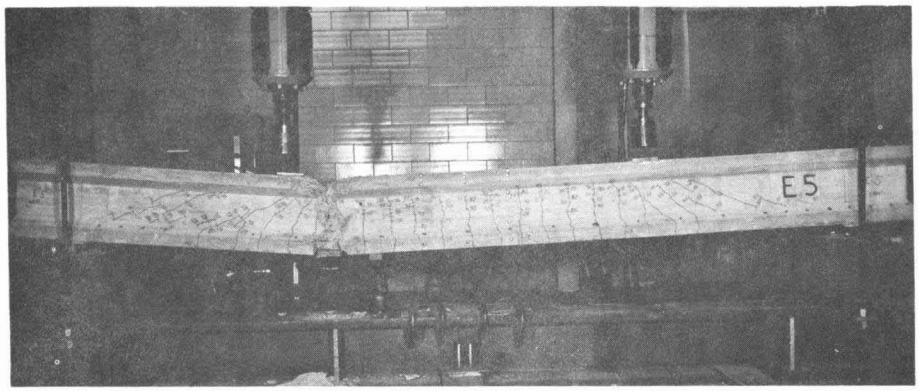

a. Elevation view, end (2) on right

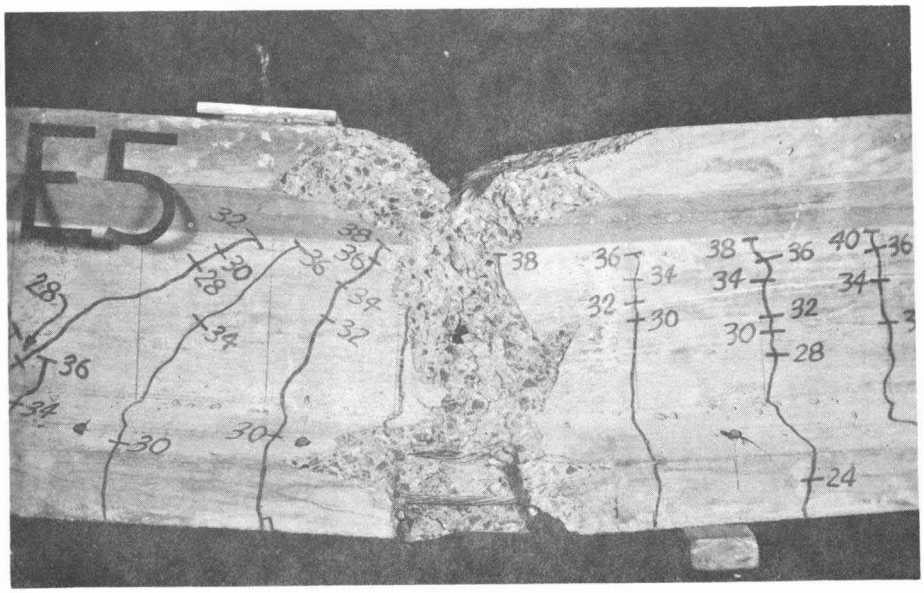

b. View of failure region

Fig. 8 Flexural failure in E.5

was located approximately a distance equal to the effective depth of the specimen from the reaction.

Two beams with web reinforcement, E.17 and E.18 failed in shear. An overall view, and a close-up view of the shear span in which the failure occurred, are shown for both of these beams in Figs. 10 and 11, respectively. Note that only the close-up view of E.18 is taken in the test set-up. The other three pictures were taken after the beams were removed from the test set-up, and artificial means are used to indicate the approximate location of the reactions and load points.

The shear failure in E.17 was gradual and non-violent, being characterized by crushing of concrete in the web. No stirrups were broken. In contrast, the shear failure in E.18 was sudden and violent. Examination of E.18 after failure showed that the second and third stirrup from the reaction had fractured. Because of the suddenness of the failure, it was considered most probable that the shear failure mechanism was triggered by fracture of the web reinforcement. However, as an examination of the close-up view of E.18 in Fig. 11 indicates, it is possible that the first stirrup from the support failed in bond, thereby causing the fracture of the second and third stirrup.

As noted in Section 2.1, beams E.13 and E.14 had inverted L-shaped stirrups for web reinforcment, in contrast to the U-shaped stirrups used in the other test beams. Beam E.13 failed in flexure, since the web reinforcement was able to increase the load carrying capacity of the member from the inclined cracking load to the full flexural capacity of the section. However, E.14 failed in shear apparently due to a bond failure in the web reinforcement. As can be seen from the close-up view of the failure region in Fig. 12, the second stirrup from the reaction had insufficient embedment below the point at which it was crossed by an inclined crack to develop the strength of the stirrup, thereby triggering the shear failure. The failure mechanism for E.14 was therefore described in Table 5 as a bond failure in the stirrups.

Load-deflection curves for each test beam in the static test group are presented in Appendix II. On each curve is indicated the shear at which the first flexural crack was observed, V_c^f, and the shear at which the inclined diagonal tension cracking formed, V_c^{dt}.

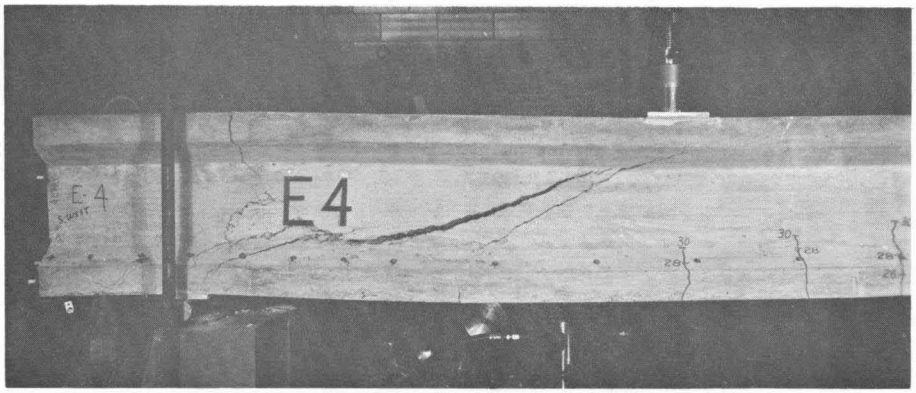

Fig. 9 Shear failure in E.4

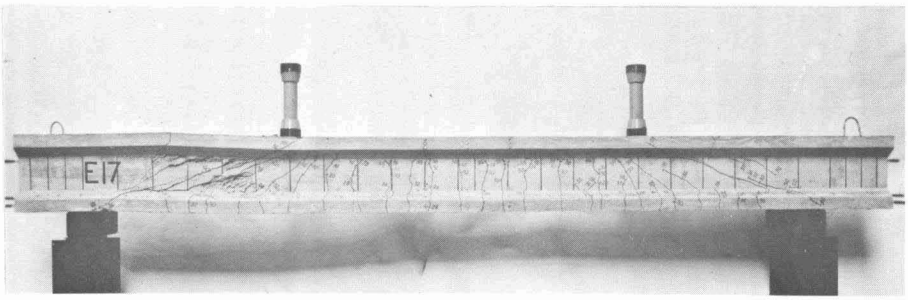

a. Elevation view, end (2) on left

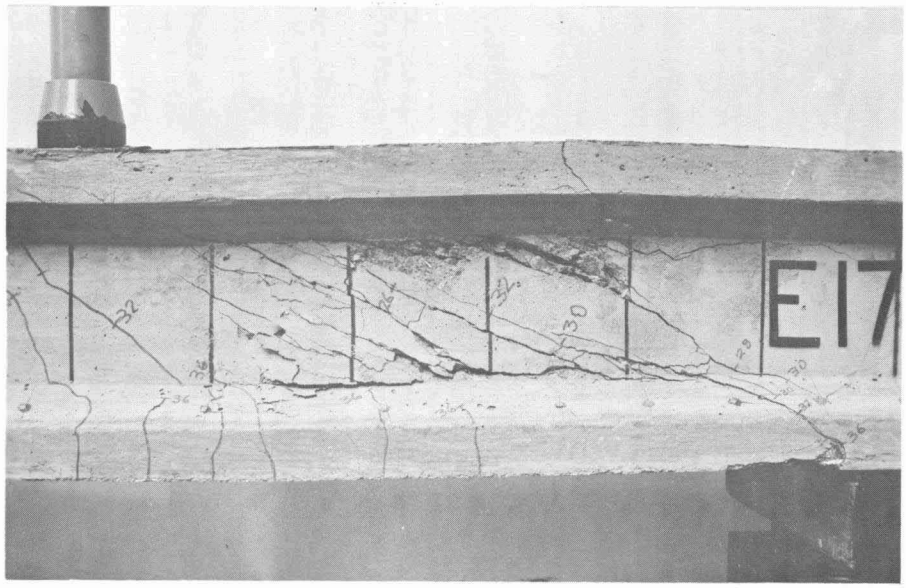

b. Opposite side view of failure region

Fig. 10 Shear failure in E.17

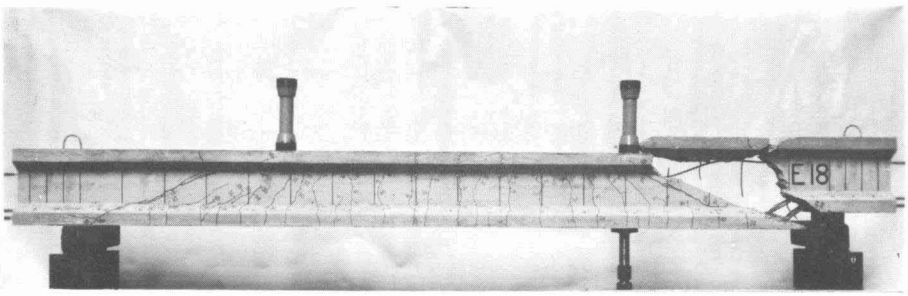

a. Elevation view, end (2) on right

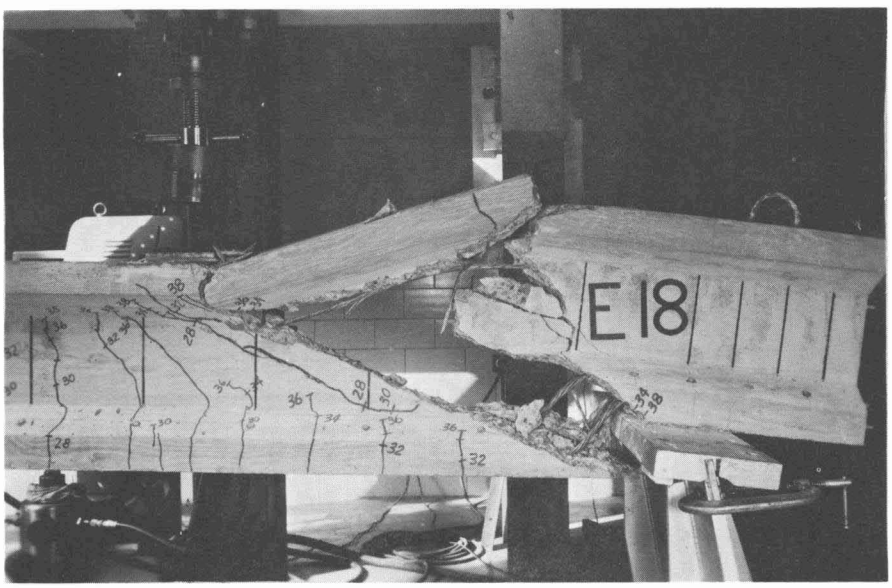

b. View of failure region

Fig. 11 Shear failure in E.18

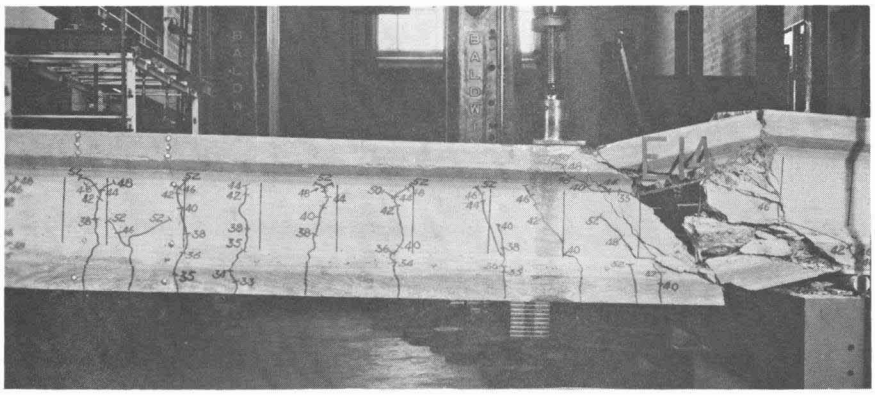

a. Part elevation view, end (20) on right

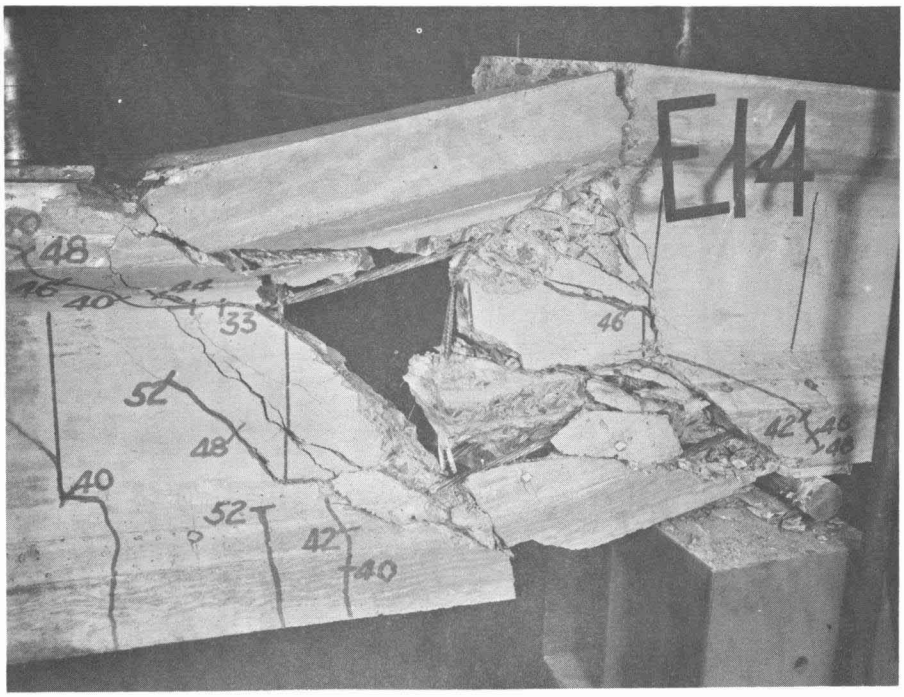

b. View of failure region

Fig. 12 Failure region in E.14

Strain measurements were taken at selected intervals during the course of a beam test. With reference to Fig. 3, the Whittemore targets can be separated into two groups. Let the first group be considered to consist of the set of targets on the C.G.S., i.e. on the horizontal line G, and the second group the set of targets on vertical lines 10, 11, and 12.

The first group of targets was intended, in addition to the use described in Section 3.3, to show the variation in concrete deformation with load along the C.G.S.. Accordingly strain data for E.16, which failed in flexure, and E.17 and E.18, which failed in shear, are presented in Figs. 13, 14, and 15, respectively. Data taken for the other test beams are not reported. In these figures, the variation in concrete deformation along the C.G.S. is given for three values of shear: V equal to 24 kips, 32 kips, and 38 kips. For all three test beams, the flexural cracking load, V_c^f, was equal to 24 kips; therefore the deformation at this load may be regarded as concrete strain. At V equal to 32 kips, inclined diagonal tension cracking had occurred for all three beams, and flexural cracking had extended across the C.G.S. The deformations for V equal to 38 kips are, in all three cases, indicative of the deformations at ultimate load.

The second group of targets was intended to give the deformation at a vertical section in the constant moment region of the test beams. The results obtained for all of the test beams were very similar. Test beam E.5 may be regarded as typical; the data for this beam are plotted in Fig. 16. Each plotted point is an average of readings between lines 10-11 and 11-12 on both sides of the member. Note that this plot includes data taken before and after transfer, as well as prior to and during the test. In Fig. 16, the strains before and after transfer, from transfer to test, and during the test are plotted separately, i.e. for example, the strain from after transfer to test is measured between the vertical zero line and the indicated line.

In Fig. 17, the data in Fig. 16 has been used to determine the elastic strain distribution in E.5 just prior to testing, i.e. at V equal to zero, and corresponding to selected magnitudes of shear during the test. The strain distribution determined from the Whittemore readings before and after transfer was assumed to be elastic strain. This was corrected to approximately indicate the elastic strain just prior to testing by evaluating the effect of the change in prestress force due to the inelastic losses occurring from after transfer

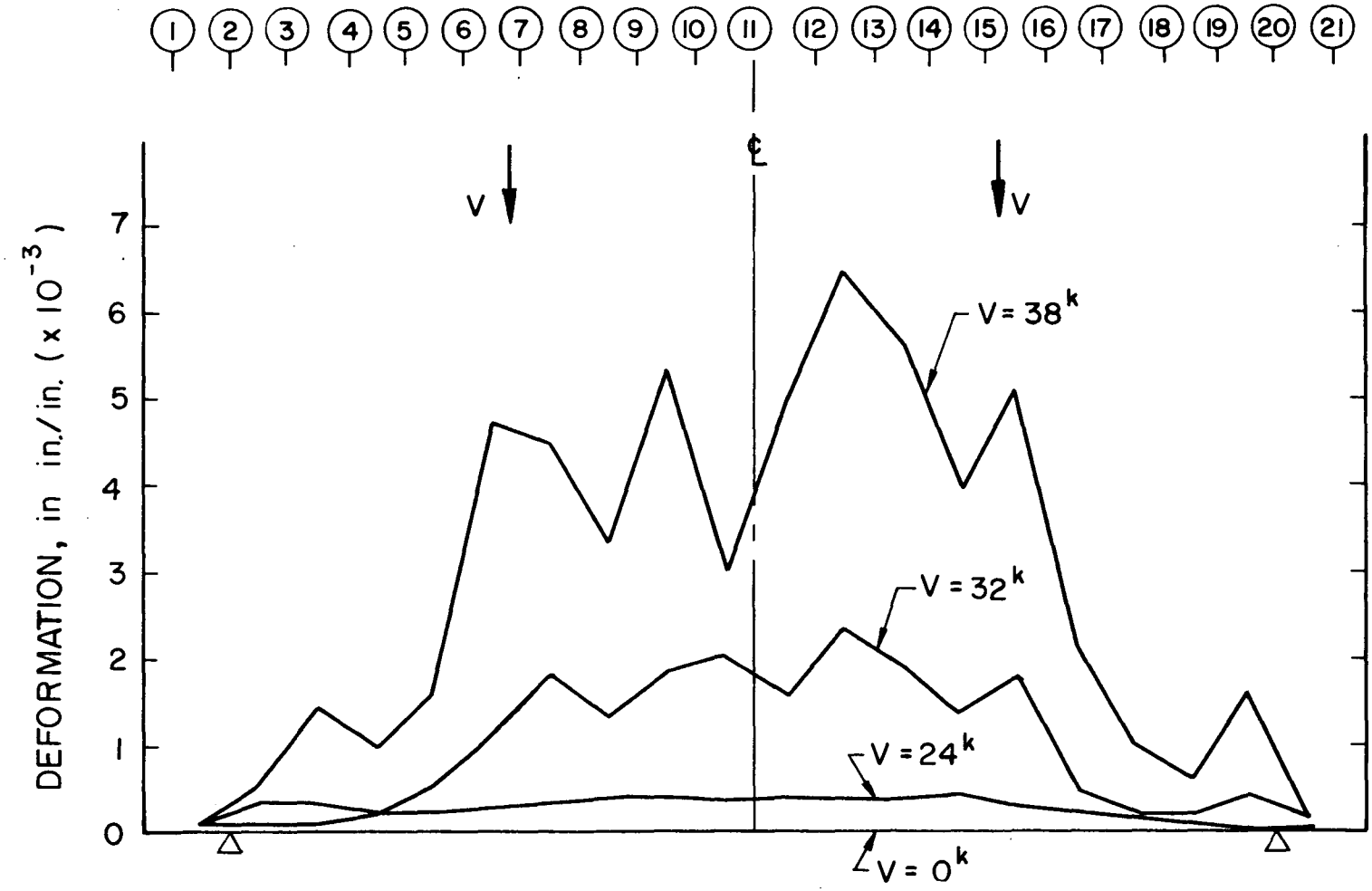

Fig. 13 Concrete deformation along C.G.S. during test of E.16

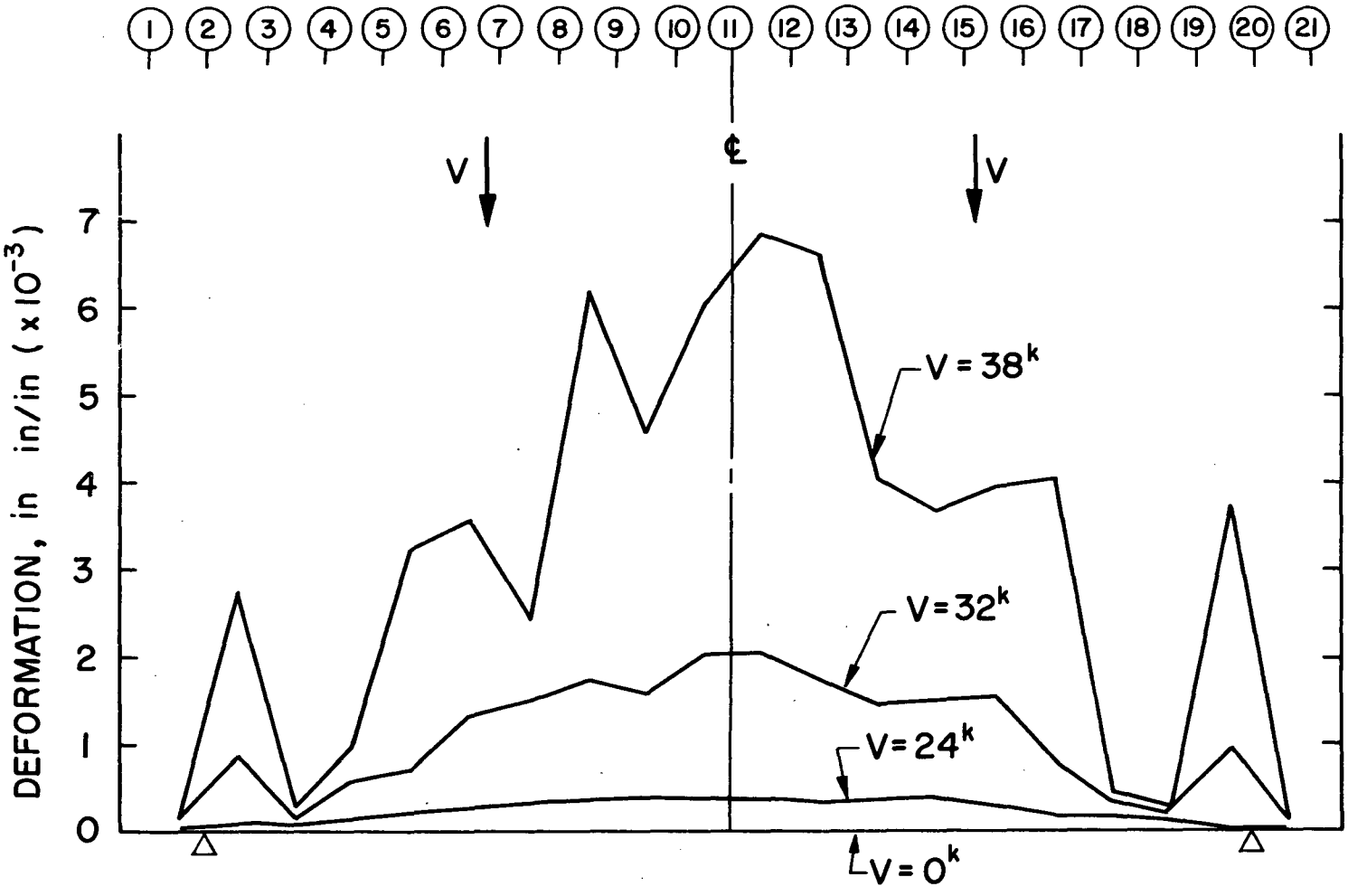

Fig. 14 Concrete deformation along C.G.S. during test of E.17

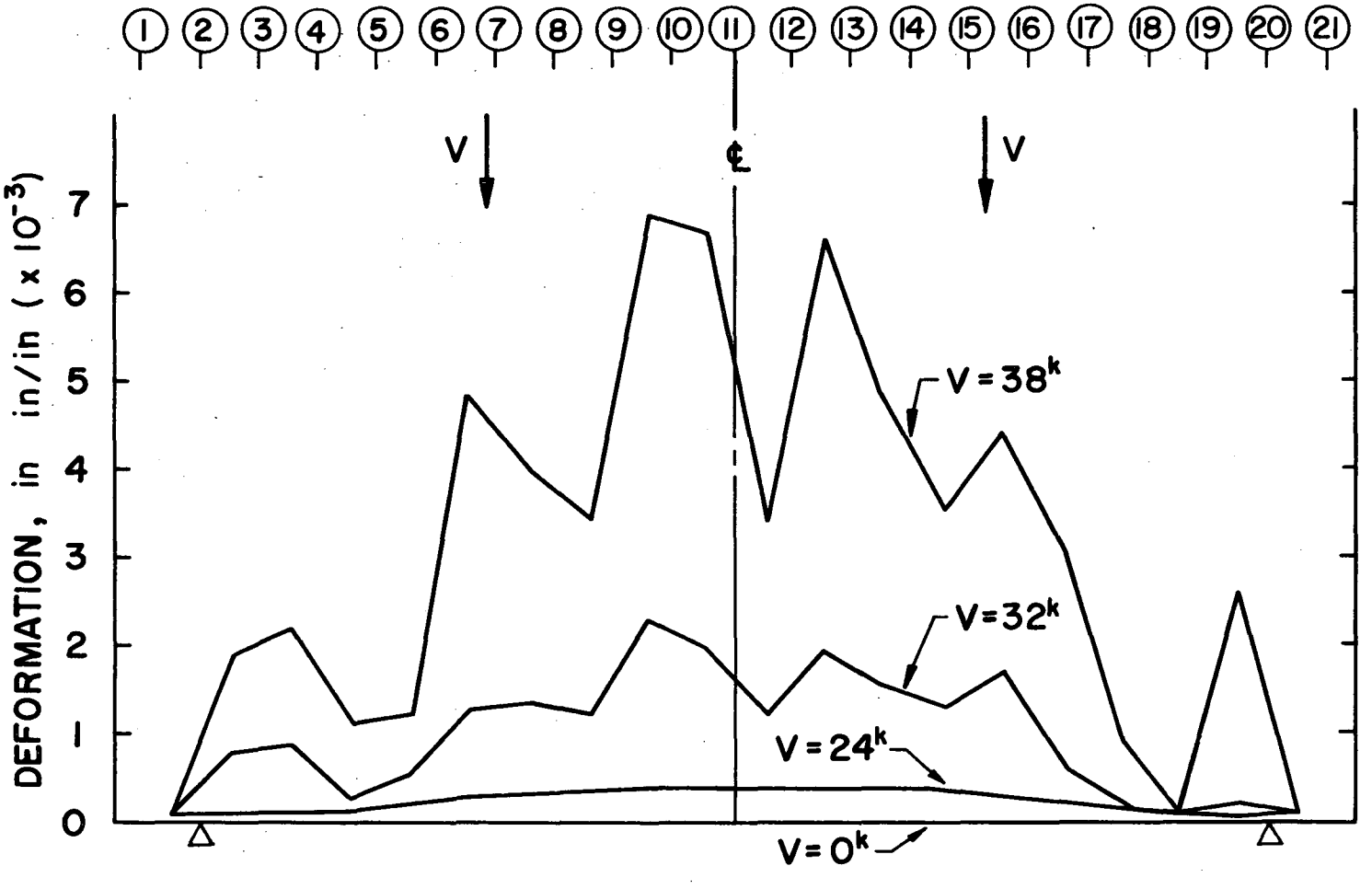

Fig. 15 Concrete deformation along C.G.S. during test of E.18

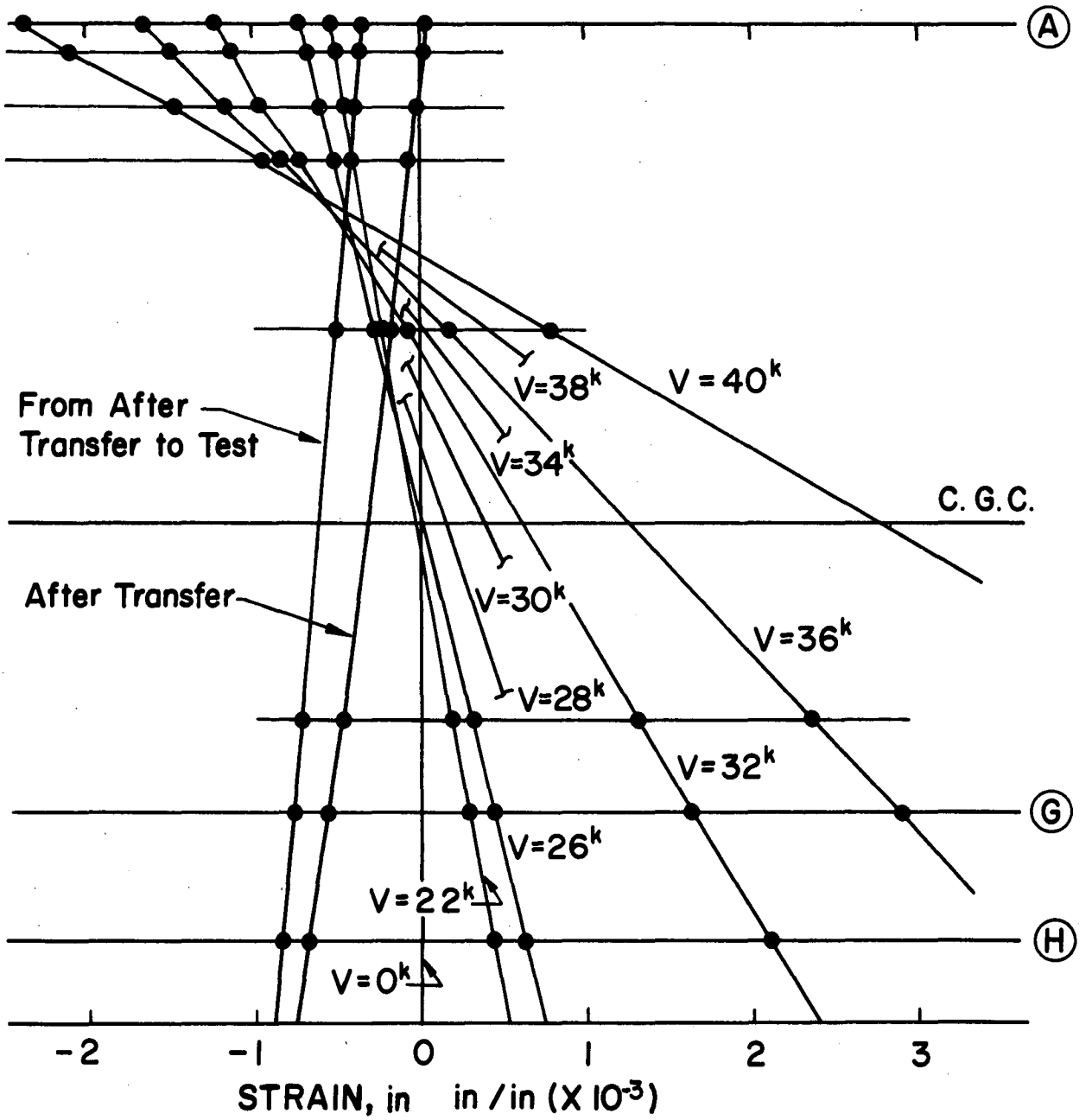

Fig. 16 Strain distribution of E.5

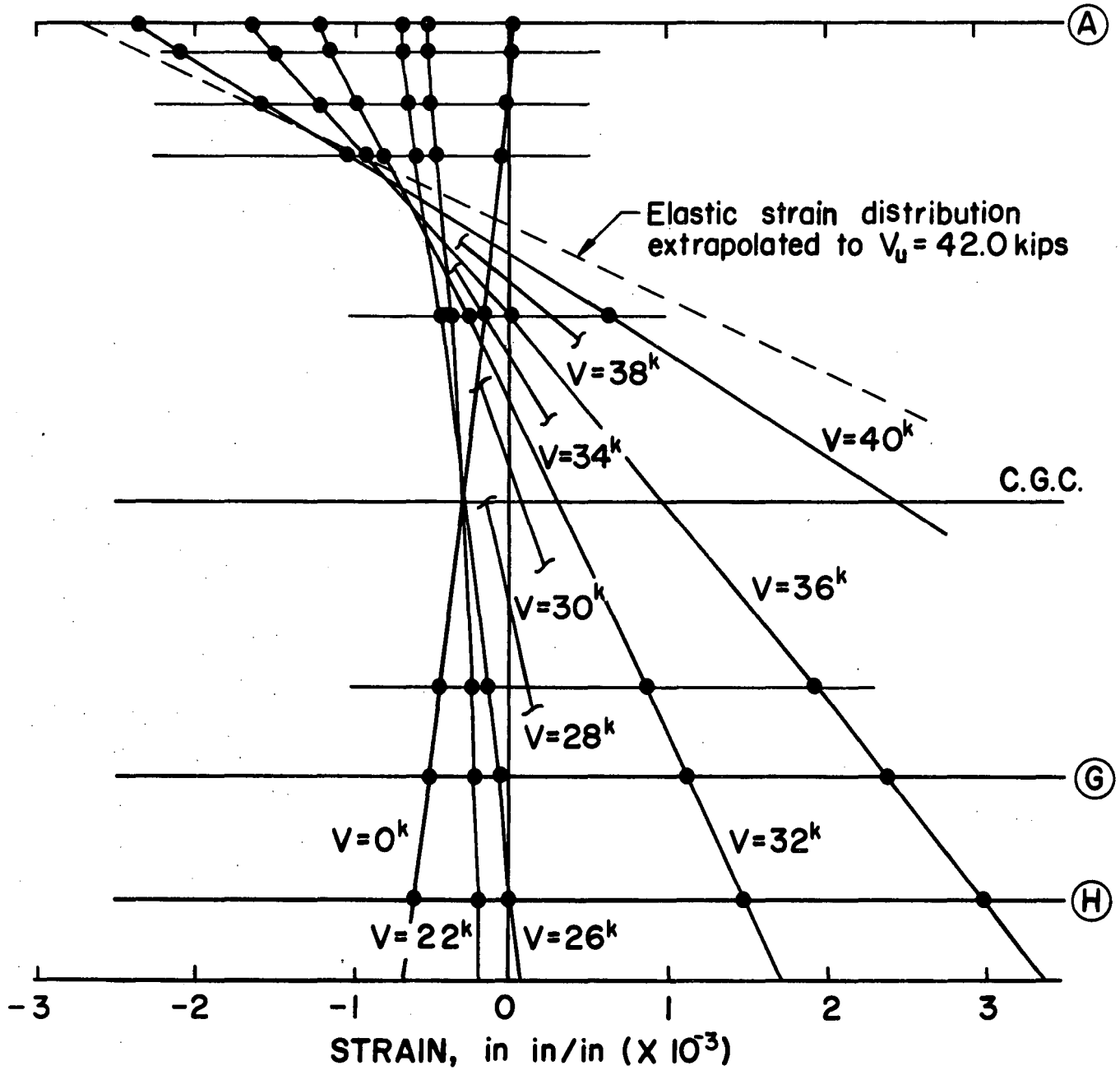

Fig. 17 Elastic strain history of E.5

to time of test. The deformation corresponding to the different increments of shear were then added to the elastic strain at V equal to zero. From Fig. 17, the strain in the top fibers of the test beams, ϵ_u, and the approximate location of the neutral axis at failure can be determined by extrapolation to the ultimate load, V_u equal to 42.0 kips.

Values of ϵ_u, determined as indicated in the preceding paragraph, and ultimate moment, M_u, are given in Table 6 for those test beams failing in flexure. The values of M_u include an allowance of 2.9 ft.-kips for dead load moment. The average experimental ultimate moment of these nine beams was 168.2 ft.-kips. For comparison, the calculated ultimate flexural capacity using the TRPC method, assuming all of the strand concentrated at the C.G.S. and taking f'_c equal to 6920 psi (average concrete strength of test excluding E.10 and E.11) and f'_s equal to 252.2 ksi, was 164.5 ft.-kips.

Table 6. Beams Failing in Flexure

Test Beam	ϵ_u (in./in.)	M_u (ft.-kips)
E.5	0.0027	170.9
E.6	0.0027	170.1
E.7	0.0028	167.3
E.8	0.0025	167.7
E.9	0.0025	167.7
E.12	0.0028	167.7
E.13	0.0025	169.7
E.15	0.0025	170.0
E.16	0.0028	162.5

3.5 Repeated Load Tests

Two beams, E.10 and E.11, were first symmetrically loaded on a 4 ft. shear span to a load sufficient to cause diagonal tension inclined cracking, and then subsequently subjected to repeated loadings of a lesser magnitude. The loading history for the two test beams is summarized in Table 7.

Table 7. Loading History

Test Beam	Loading Cycle N	V_{min} (kips)	V_{max} (kips)	Remarks
E.10 (a/d=3.39)	1	0	32	Initial static test: V_c^f = 24 kips; V_c^{dt} = 30 kips, both ends
	2 - 6	0,8	18	Static tests
	7 - 3,200,000	8	18	Repeated load test at 250 cpm.
	3,200,001 - 4,000,000	8	18	Repeated load test at 500 cpm.
	4,000,001 - 4,526,900	8	28	Repeated load test at 250 cpm. Fatigue failure in one wire of bottom strand at N=4,526,900
E.11 (a/d=3.39)	1	0	32	Initial static test: V_c^f = 24 kips; V_c^{dt} = 30 kips end (2), 28 kips end (20)
	2 - 5	0,8	24	Static tests
	6 - 2,007,500	8	24	Repeated load test at 250 cpm. Fatigue failure in stirrup, end (2), at N = 2,007,500.

Both beams were initially loaded to a maximum shear of 32 kips, using exactly the same procedure as employed for the static beam tests presented in Section 3.4, and the comparable values of V_c^f and V_c^{dt} for these initial static tests are given in Table 7. The beams were then unloaded, and subsequently subjected to several additional static tests to determine the load deflection response of the cracked member. In addition, Whittemore readings were taken using primarily the group of targets on lines 10, 11 and 12. Also, a location along the diagonal tension crack was arbitrarily selected at which the variation in width of the crack with load was measured.

The 0,8 kip notation for V_{min} indicates that either of these values of shear correspond to the minimum load in the static load cycle. For example, in the case of E.10 beginning with the second load cycle, the load was varied from zero to a maximum of 18 kips shear and then back to zero. At this point E.10 was permitted to rest overnight. Beginning with the third load cycle on the second day of the test, the load was taken from zero to 18 kips shear, and then back to 8 kips shear. The subsequent fourth through sixth static tests continued in the 8 to 18 kip range, after which the repeated loading was applied.

Static tests, similar to those described above, were conducted at selected intervals during the repeated loadings. Rest periods, in general for overnight, were permitted after a static test.

The repeated loading for both beams was applied at the rate of 250 cycles per minute, except for the load cycles between 3,200,001 and 4,000,000 applied to E.10, when the loading rate was increased to 500 cycles per minute. The magnitude of the maximum load applied in the repeated load cycle was controlled by the known load deflection response to the member determined from the preceding static tests; i.e., the magnitude of the repeated loading was adjusted so that the maximum deflection of the test beam while subjected to the repeated loading was the same as the deflection in the static test at the maximum load. The tests on E.10 and E.11 extended over a period of 16 and 9 days, respectively.

As indicated in Table 7, the repeated loading applied to E.10 for the first 4,000,000 load cycles ranged between 8 and 18 kips shear, which corresponds to 19% and 44%, respectively, of the applied load shear required to develop the flexural capacity of the member. At N equal to 4,000,000 there was no indication of structural damage in the member, which prompted the decision to change the loading range to between 8 and 28 kips shear, corresponding to 19% and 68% of the ultimate capacity. Failure in E.10 occurred at N equal to 4,526,900 load cycles as a fatigue fracture in one wire of one of the bottom strands.

The load-deflection curve for E.10 at N equal to 1, 2, 4,000,000 and 4,400,000 is shown in Fig. 18. Between N equal to 2 and N equal to 4,000,000 the load deflection diagrams obtained from the static tests remained essentially unchanged. Between N equal to 4,000,000 and N equal to 4,400,000 the

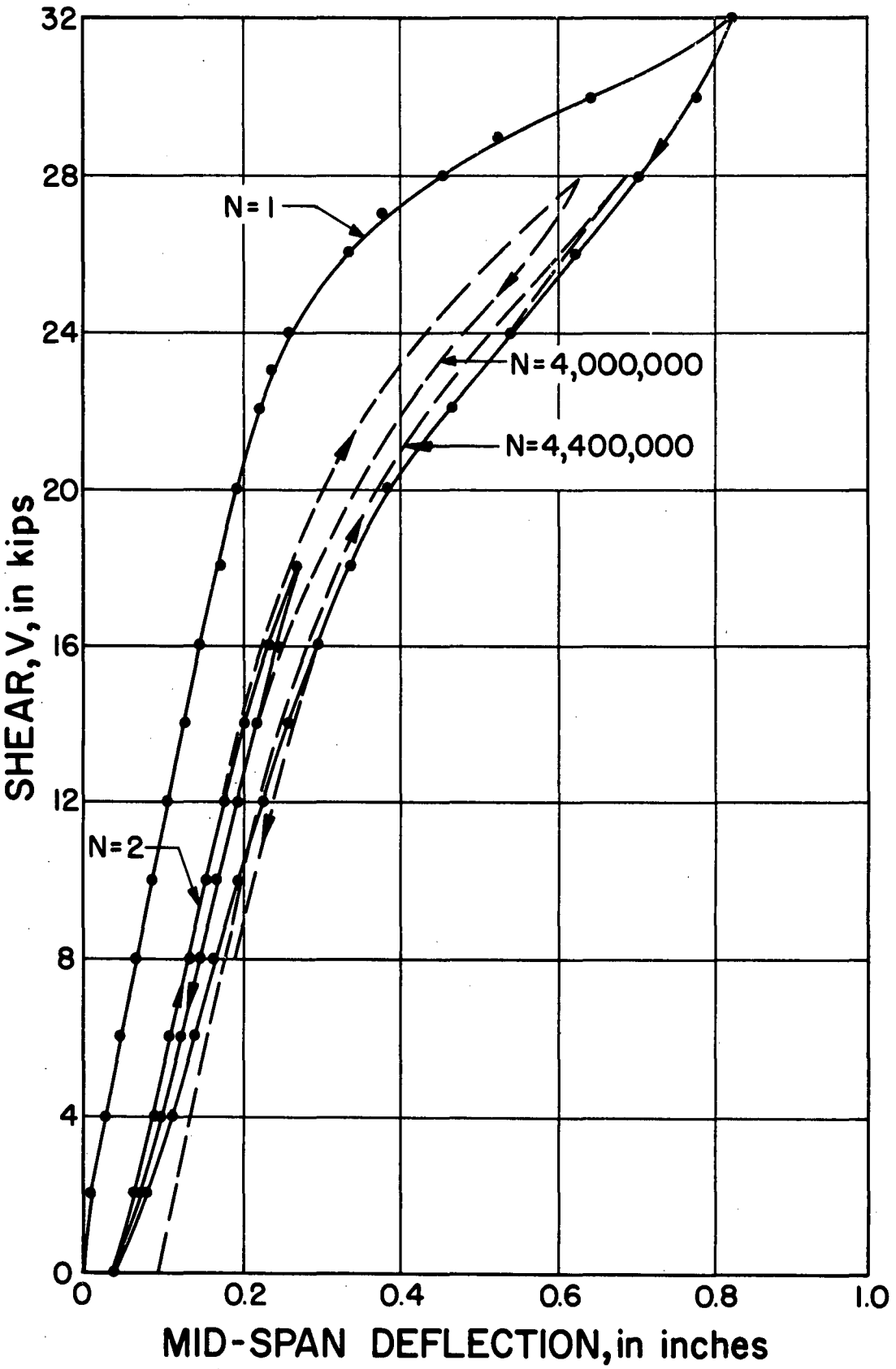

Fig. 18 Load-deflection curve for E.10

load deflection diagram continually moved to the right. The load deflection data obtained is summarized by the Deflection - N diagram shown for E.10 in Fig. 19, where corresponding to 0,8,18 and 28 kips shear mid-span deflection is plotted against the N at which the static test was conducted.

In Fig. 20, the variation in width of the diagonal crack at an arbitrarily selected point is plotted against N. The Whittemore readings were used to determine the variation in concrete strain in the top fibers (line A), at the C.G.S. (line G), and at the level of the lowest strand (line H), for N corresponding to the indicated values of shear, as shown in Figs. 21, 22, and 23, respectively. Each point plotted in these figures is an average of four readings, i.e., an average of the readings between lines 10-11 and 11-12 on both sides of the member.

A close-up view of the failure region in E.10 is shown in Fig. 24. The vertical line of targets is line 12. The failure was characterized by a sudden increase in the deflection of the test beam, and a noticeable opening of the flexure crack in the region where the fatigue fracture of the strand occurred.

The repeated loading applied to E.11 varied between 8 and 24 kips shear, corresponding to 19% and 58% of the static ultimate shear. Failure in E.11 occurred at N equal to 2,007,500 load cycles as a fatigue fracture of the web reinforcement.

Load-deflection curves for E.11 at N equal to 1, 2, and 1,900,000 are shown in Fig. 25. The variation in mid-span deflection between N equal to 1 and 1,900,000 is given in the Deflection - N diagram, for values of shear equal to 0, 8, and 24 kips, in Fig. 26. The variation in width of the diagonal crack at an arbitrarily selected location with N is shown in Fig. 27. Variation in concrete strain in the top fibers (line A), at the C.G.S. (line G), and at the level of the lowest strand (line H), with N for the indicated values of shear is shown in Figs. 28, 29, and 30, respectively.

Close-up views of both sides of the failure region for E.11 are shown in Fig. 31. The first visual evidence of structural damage was the noticeable increase in width of the diagonal crack, at approximately N equal to 1,500,000 cycles. Subsequently, noticeable extension of the diagonal cracking occurred, particularly in the region of the tension flange. The last static test was

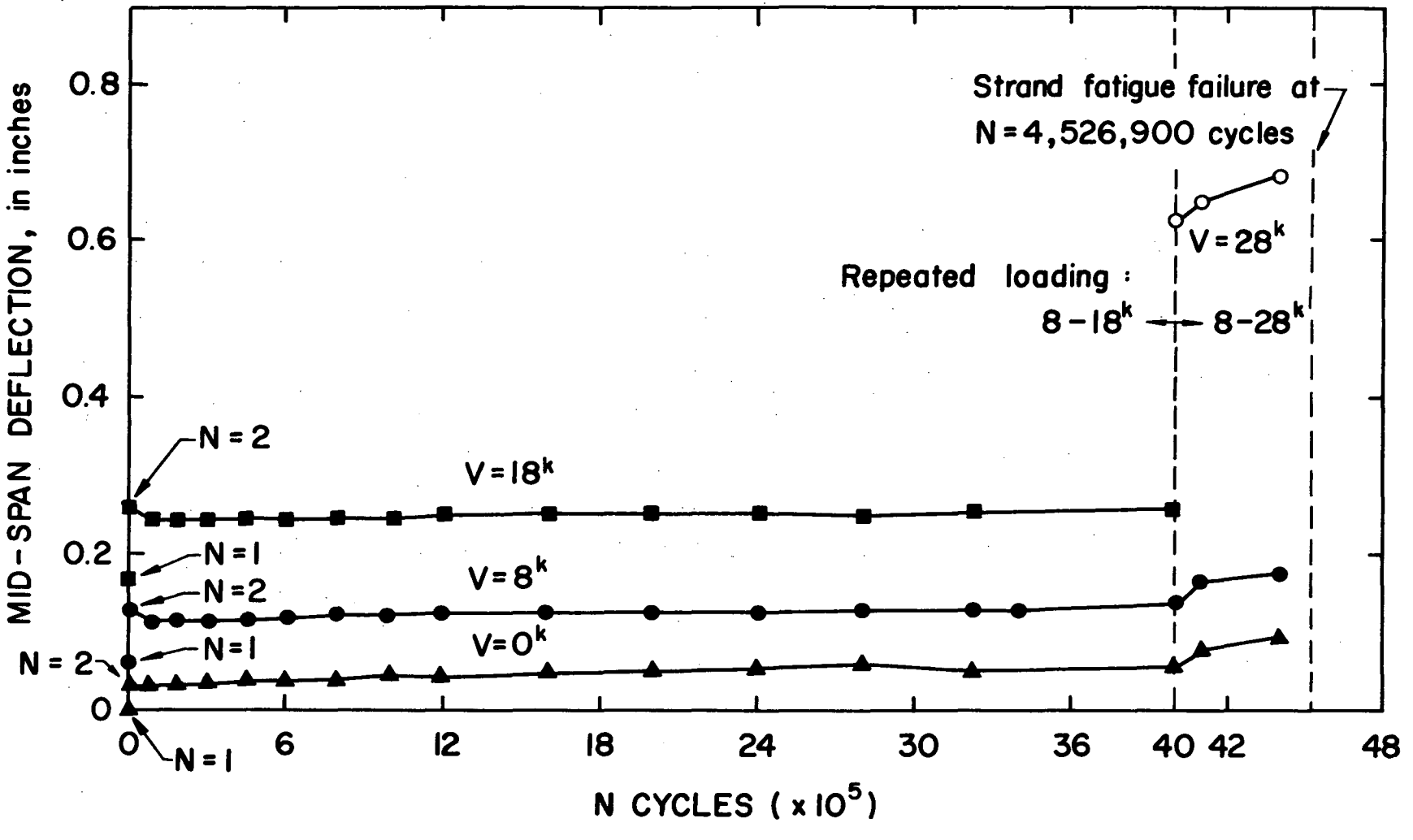

Fig. 19 Deflection-N curves for E.10

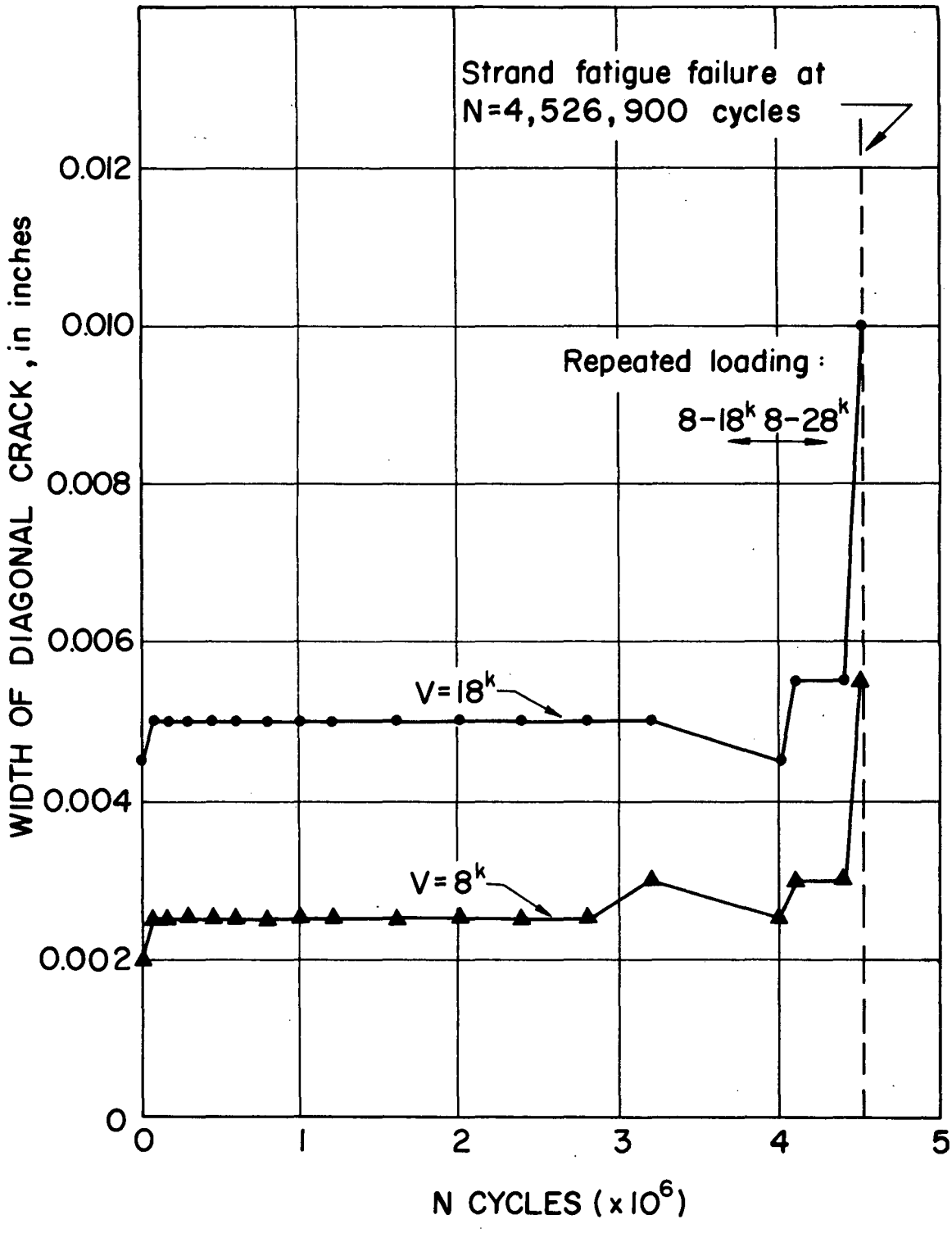

Fig. 20 Variation in width of diagonal crack with N for E.10

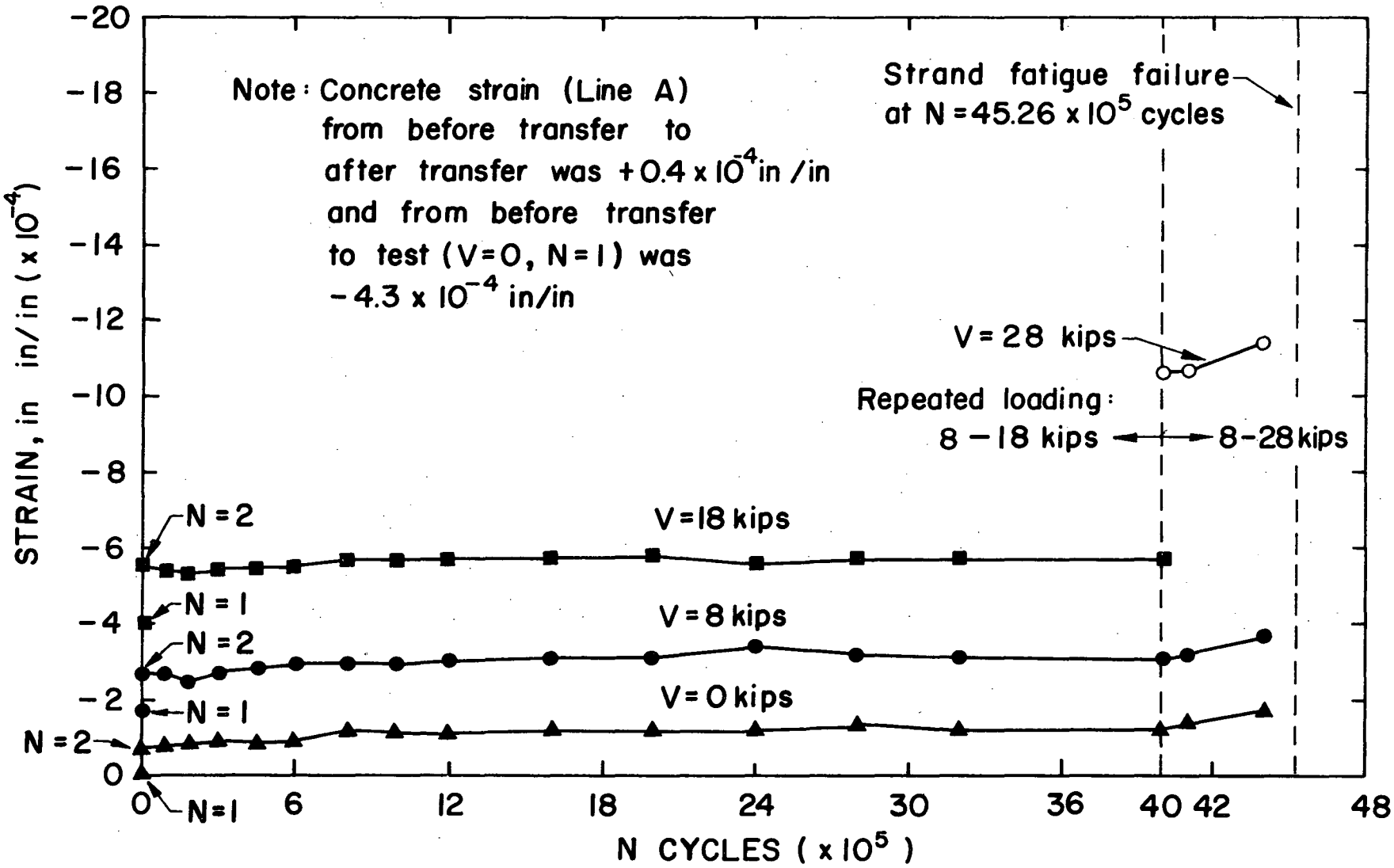

Fig. 21 Variation in concrete strain of top fiber during test of E.10

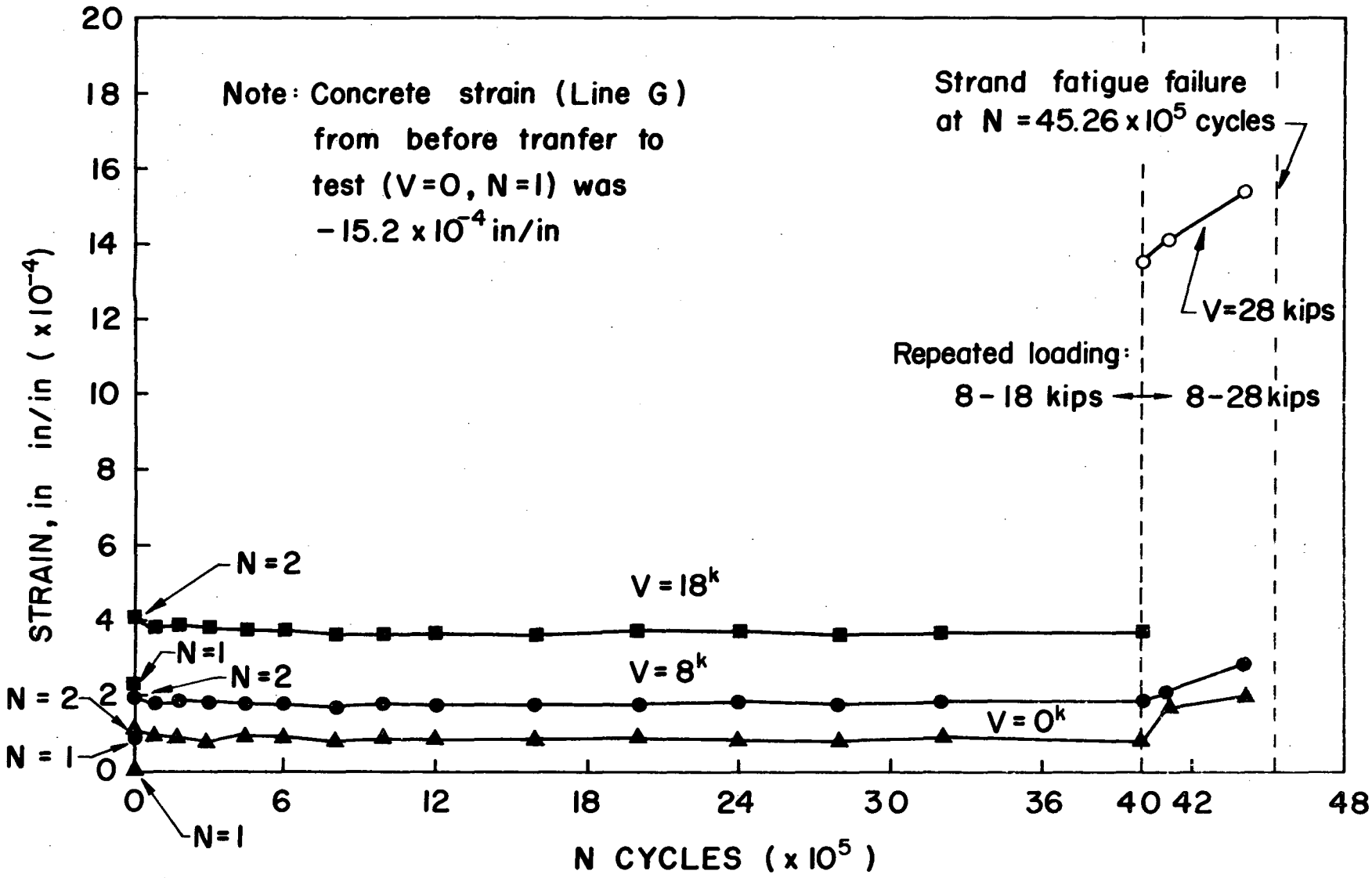

Fig. 22 Variation in concrete strain at level of C.G.S. during test of E.10

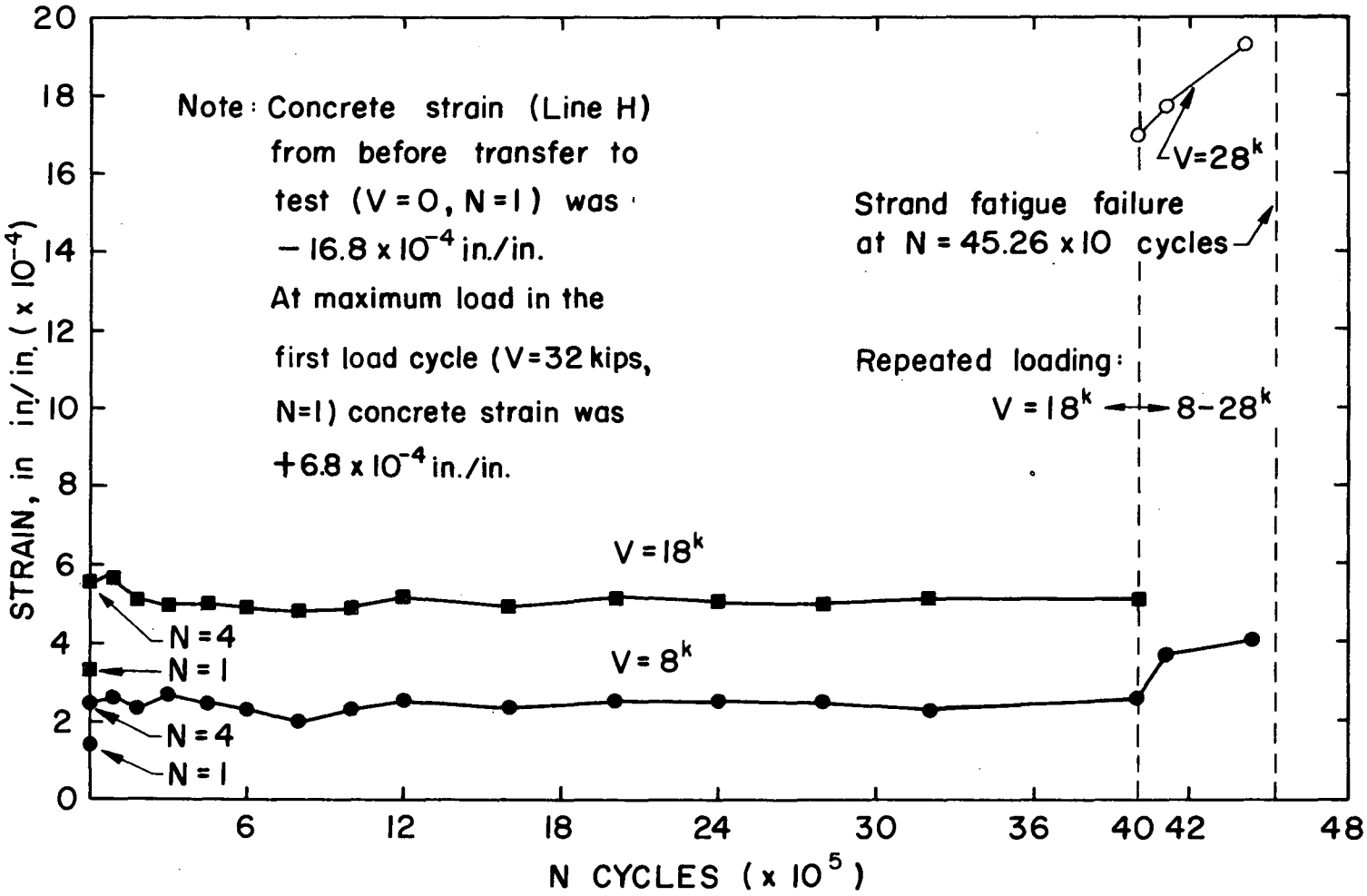

Fig. 23 Variation in concrete strain at level of lower strand during test of E.10

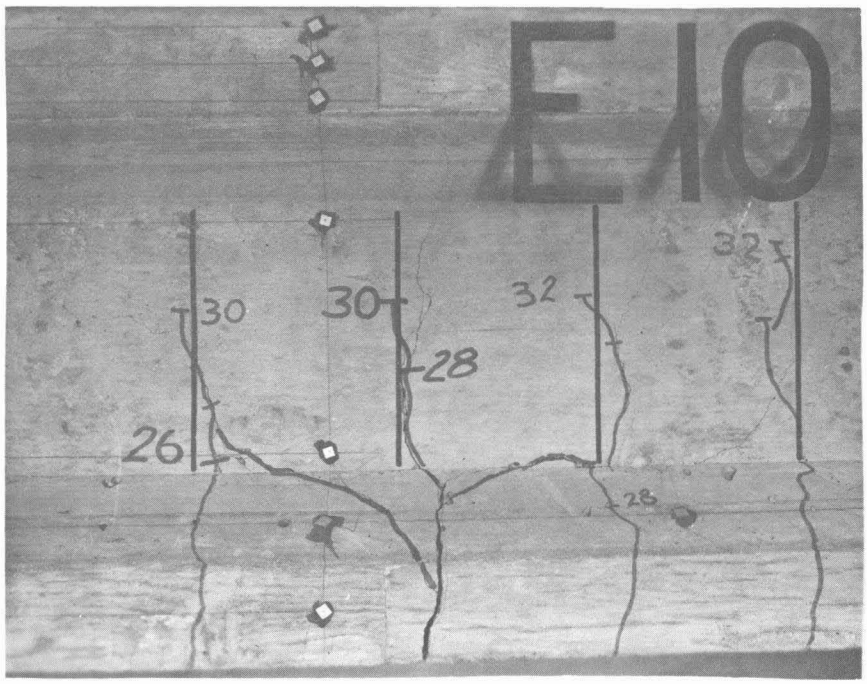

Fig. 24 Strand fatigue failure region in E.10

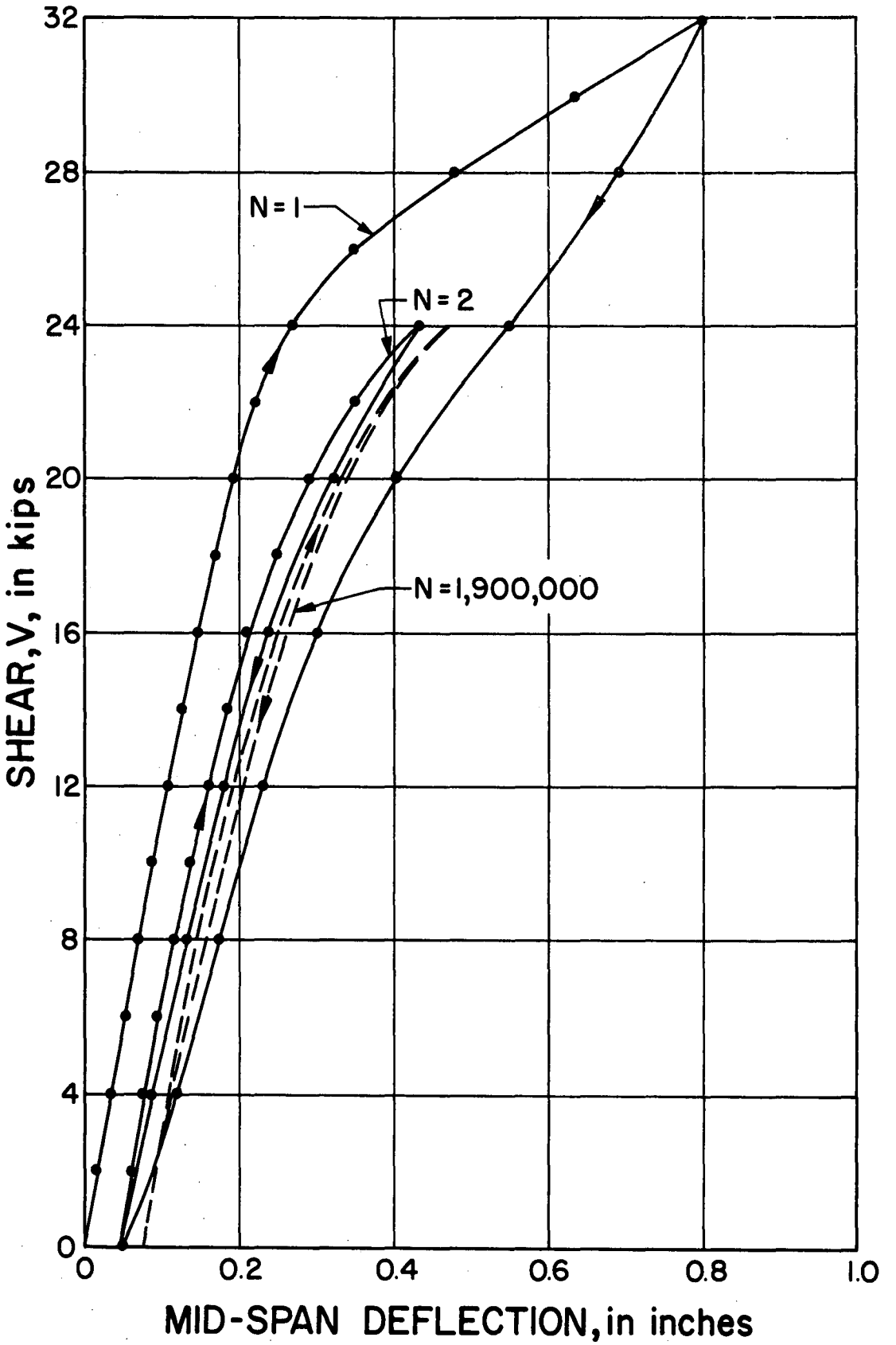

Fig. 25 Load-deflection curve for E.11

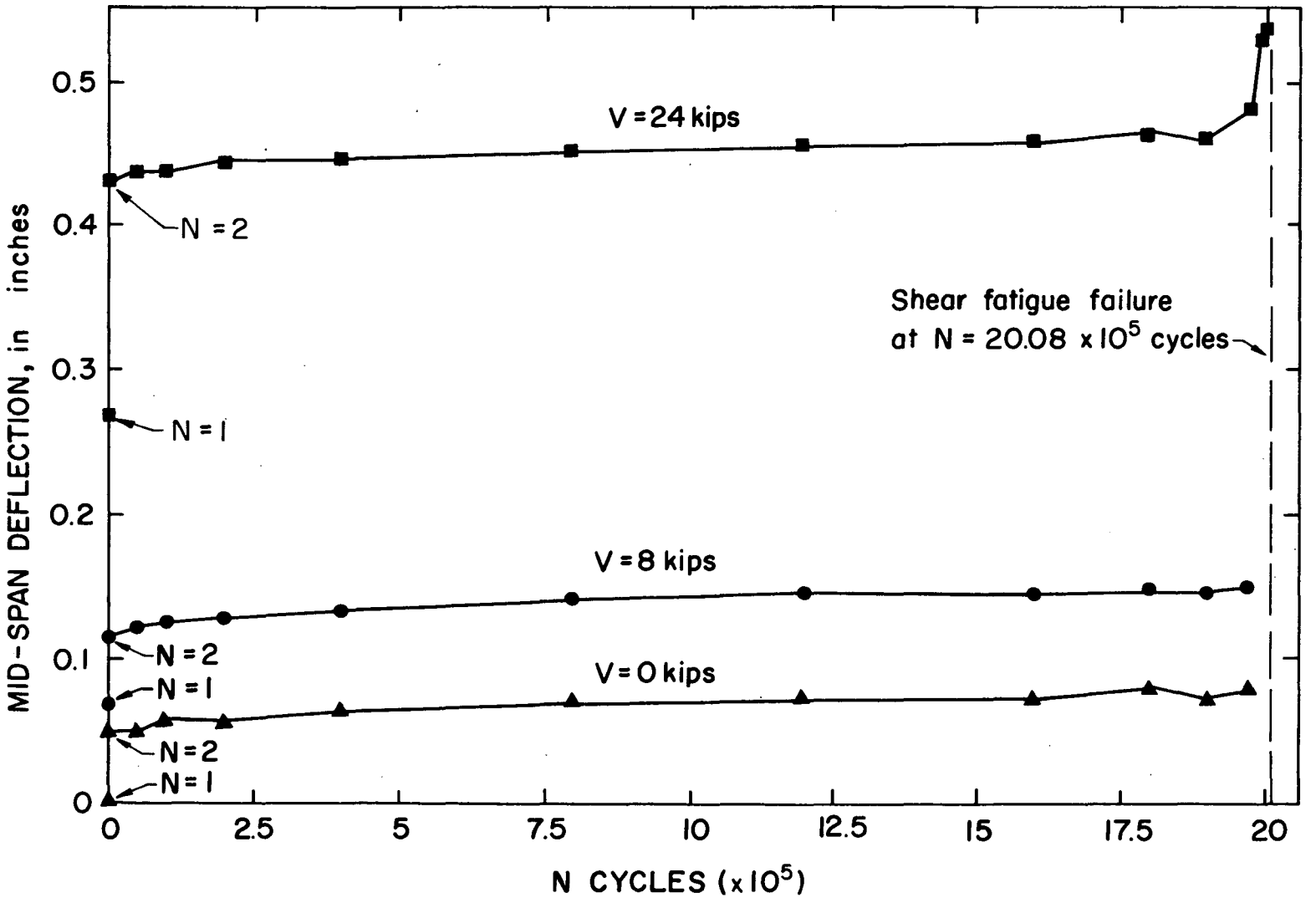

Fig. 26 Deflection-N curves for E.11

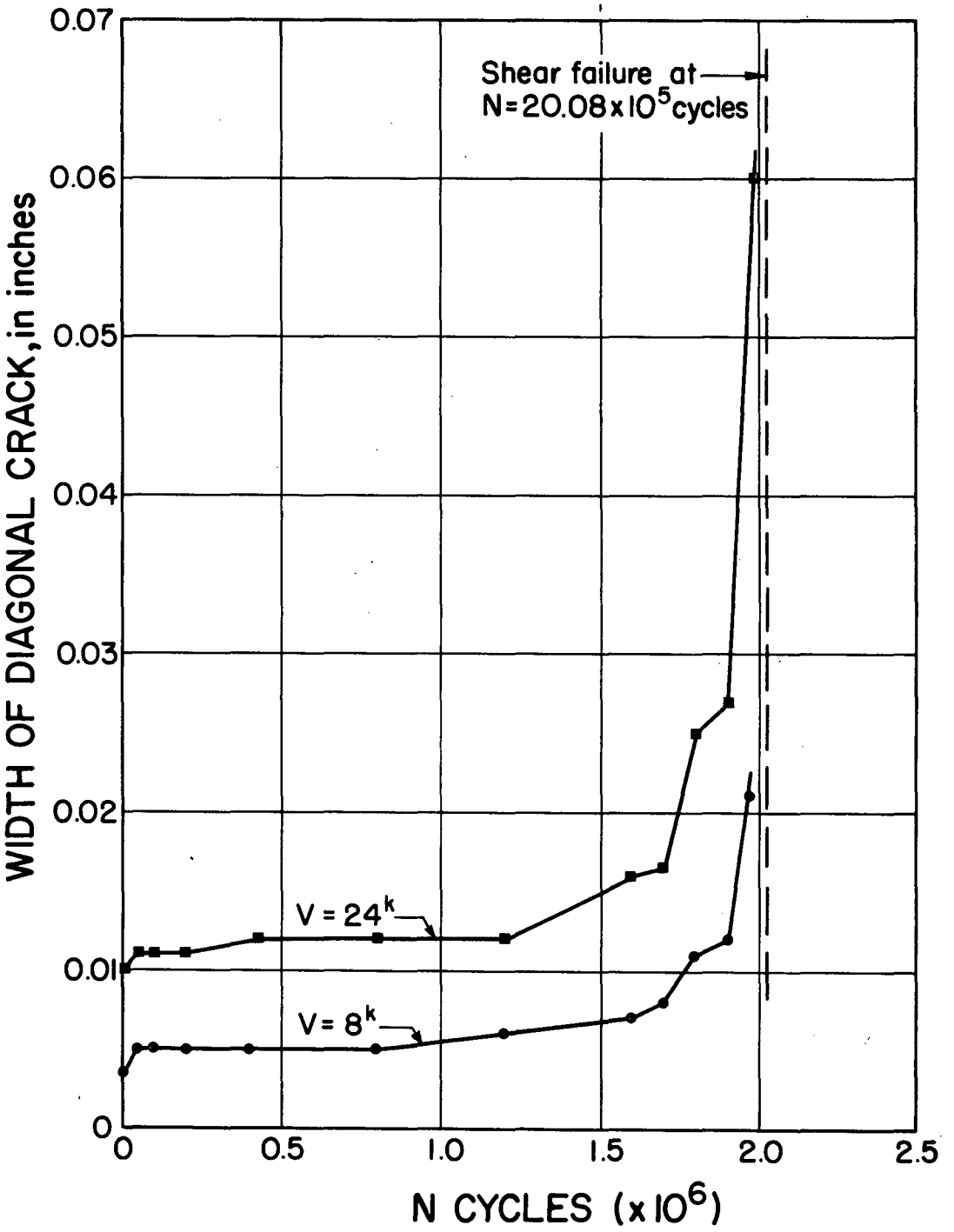

Fig. 27 Variation in width of diagonal crack with N for E.11

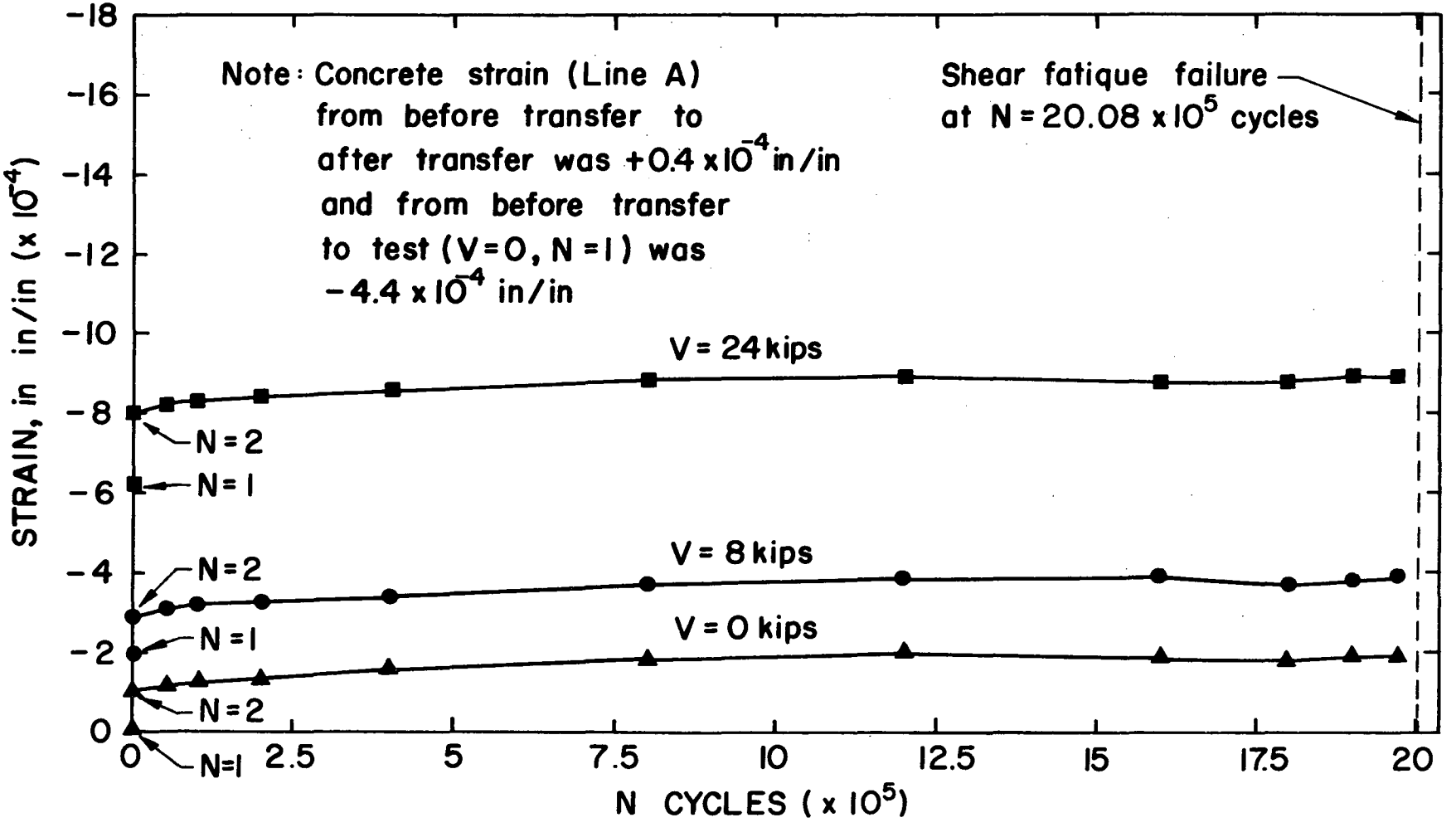

Fig. 28 Variation in concrete strain of top fibers during test of E.11

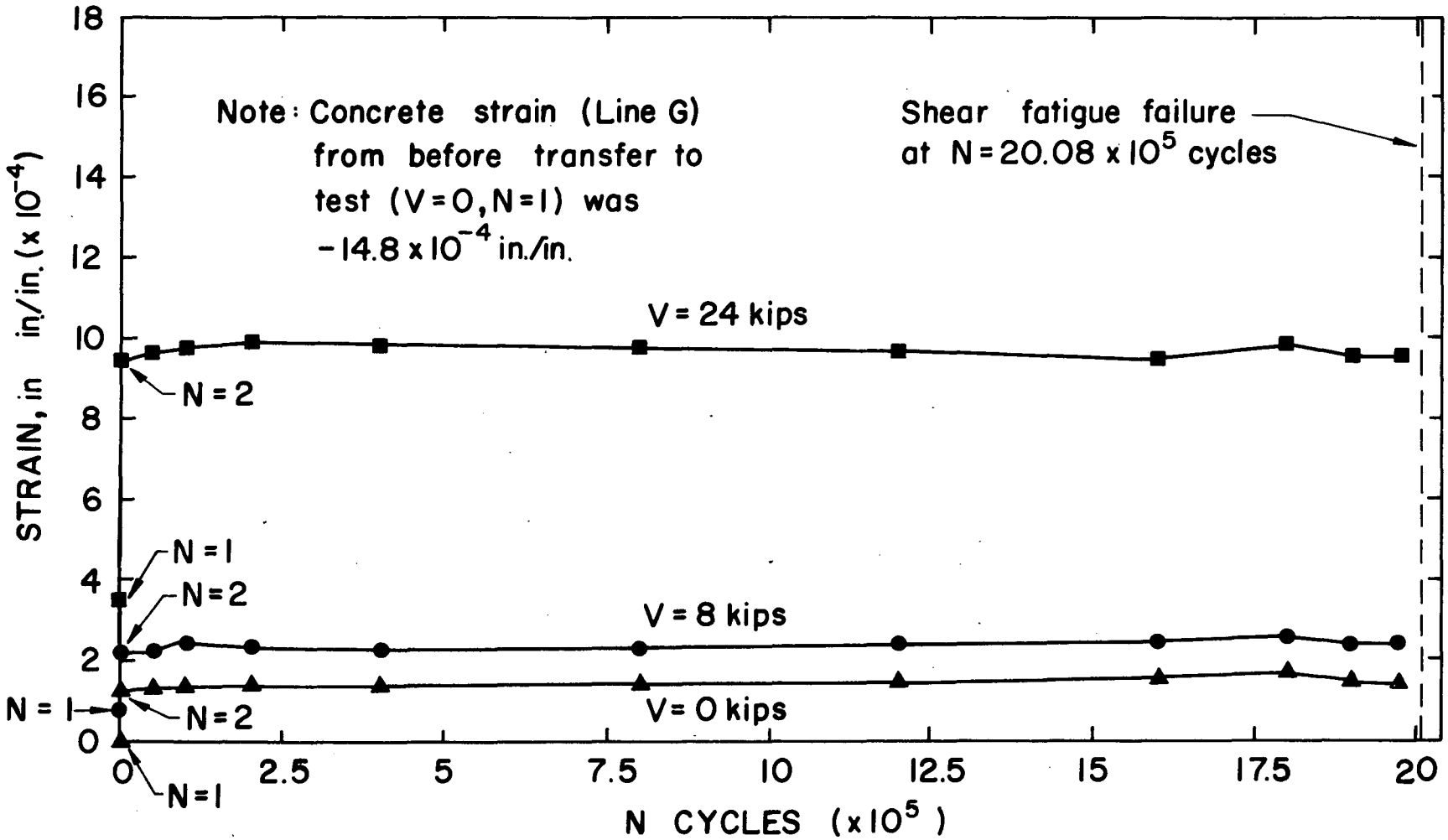

Fig. 29 Variation in concrete strain at level of C.G.S. during test of E.11

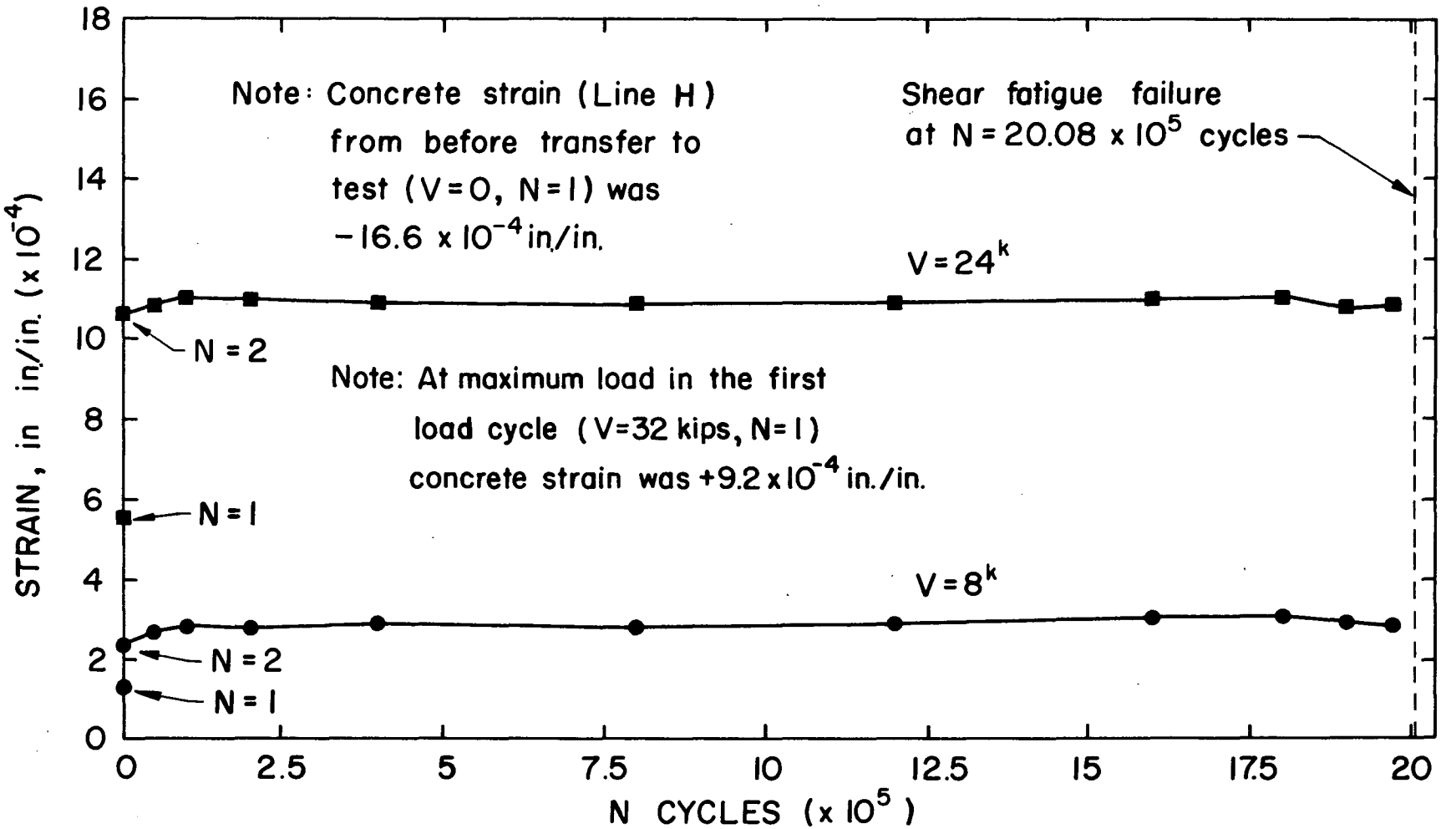

Fig. 30 Variation in concrete strain at level of lower strand during test of E.11

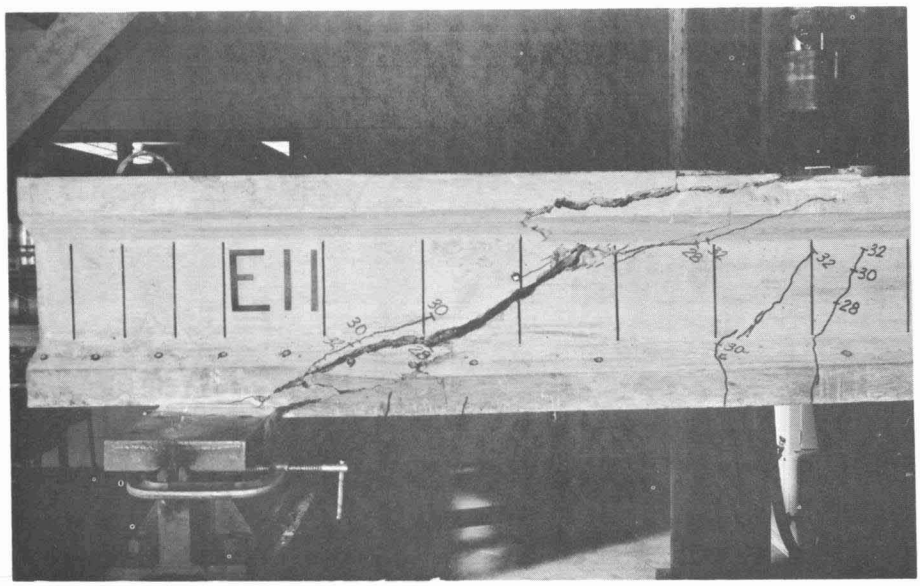

a. View of end (20)

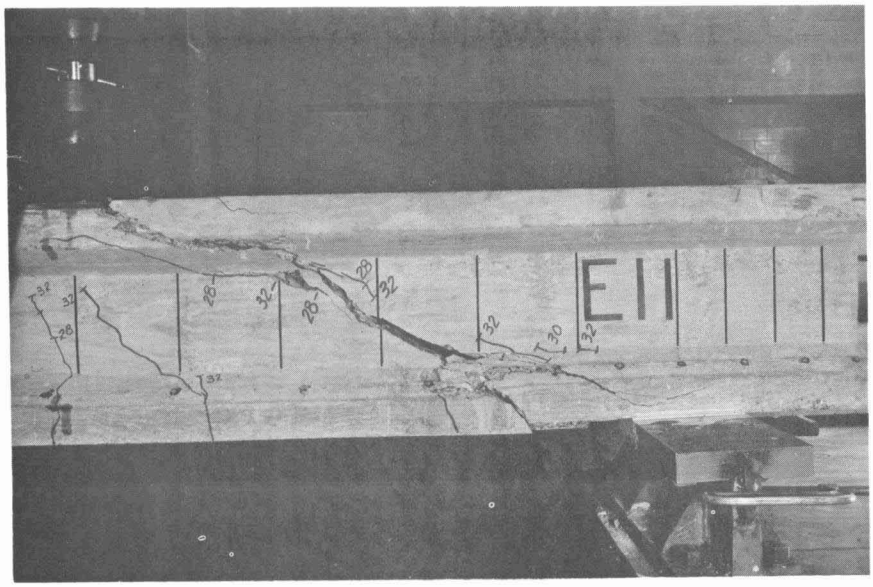

b. Opposite side view of end (20)

Fig. 31 Shear fatigue failure region in E.11

conducted at N equal to 1,970,000 cycles, at which time failure appeared to be imminent. However, the test beam was able to sustain an additional 77,500 load cycles. During this period the diagonal crack continued to grow in width, until at failure the width was estimated as greater than three-sixteenth of an inch, which was wide enough to see completely through the web of the beam. The width of the crack appeared to increase at a non-uniform rate, and seemed to be associated with extensions of the diagonal cracking. Final failure occurred suddenly with the fracture of the third stirrup from the support. This was the exact location at which the width of the diagonal crack had been measured, the data being presented in Fig. 27, as previously noted.

3.6 Re-loaded Static Tests

As previously explained, after a test in either the static or repeated load test group had been completed, the crack patterns were marked and the test specimen photographed. The specimen was subsequently stored in the laboratory for a short period before disposal.

However, several of the test beams had a region away from the location of the failure which was of sufficient length to permit a second ultimate strength test. The physical appearance of these regions indicated a high degree of recovery from the preceding test. Flexure and shear cracks were completely closed, and there was a noticeable camber, indicating that the prestress force was still retained in the region away from the failure.

Consequently four test beams were selected on which a second ultimate strength test was conducted. These four were E.11, E.16, E.17, and E.18, and the results of these tests are summarized in Table 8. No strain measurements or deflection readings were taken during the test, nor was the strength of concrete at the time of the re-loaded test determined, as all cylinder tests had been conducted with the preceding static or repeated load test. The age of the specimens at the time at which the re-loaded test was conducted was as follows: E.11 - 396 days, E.16 - 186 days, E.17 - 190 days, and E.18 - 189 days.

Table 8. Re-loaded Static Tests

Specimen	P_u (kips)	M_u (ft-kips)	Ratio of M_u to Flexural Capacity	Remarks
E.11 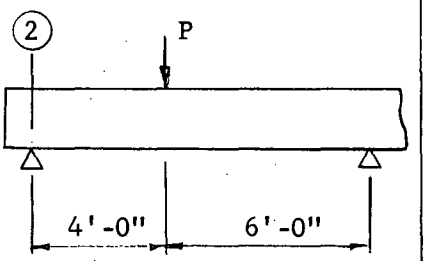	67.8	163	0.98	Existing flexural cracks observed to re-open at P = 38 kips. First inclined crack in 6'-0" shear span at P = 50 kips. Apparent shear compression failure in 4'-0" shear span.
E.16 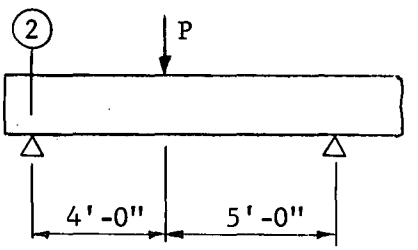	62.5	139	0.84	First inclined crack in 5'-0" shear span at P = 30 kips. Apparent shear compression failure in 5'-0" shear span.
E.17 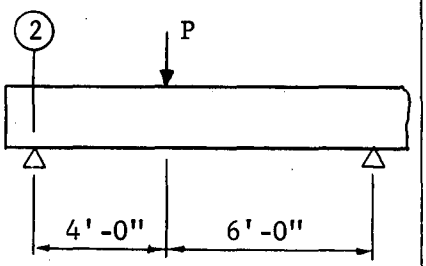	58.0	139	0.84	Existing flexural cracks observed to re-open at P = 27 kips. First inclined crack in 6'-0" shear span at P = 33 kips. Shear failure in 4'-0" shear span due to stirrup fracture.
E.18 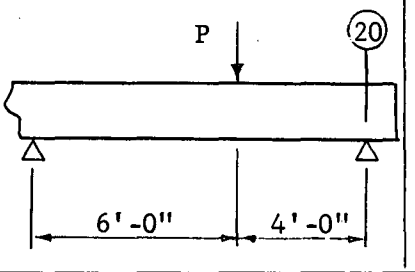	57.2	138	0.83	Existing flexural cracks observed to re-open at P = 20 kips. First inclined crack in 6'-0" shear span at P = 31 kips. Apparent shear compression failure in 6'-0" shear span.

4. DISCUSSION

4.1 Overload Behavior of Prestressed I-Beams

As noted in Section 1.1, knowledge of the ultimate strength of a prestressed beam requires an understanding of the physical behavior of this type of member under load. This behavior may be described with reference to the uncracked or cracked loading range.

In the uncracked range, the familiar formulas of structural mechanics, based on an uncracked section and a linear strain distribution, are applicable. However, at cracking a fundamental change takes place in the way in which the prestressed beam carried load. Two cases are important. Where flexure predominates, the strain distribution remains linear beyond the flexural cracking load up to the ultimate failure condition. With this as a compatibility condition the ultimate flexural capacity can be accurately determined using, for example, the procedure by Mattock, Kriz, and Hognestad.[2] Where shear is significant, inclined cracks develop in the prestressed beam. In the zone of inclined cracking the strain distribution is non-linear. If shear is critical, the inclined cracking leads to a shear failure.

The ultimate shear strength of prestressed concrete members has been studied extensively in recent years. Three important conclusions may be drawn from these investigations: (1) the inclined cracking load in a prestressed beam without web reinforcement is the same as the inclined cracking load in a prestressed beam with web reinforcement; (2) the inclined cracking load in a prestressed beam without web reinforcement and subjected to moving loads is the ultimate load, and (3) the stress in web reinforcement is not significant unless crossed by an inclined crack.

Tests on thirty-three pretensioned I-beams without end blocks by Hulsbos and Van Horn[3] may be regarded as a basis for the first conclusion. The results of their tests indicated that the amount of web reinforcement had no apparent effect on the magnitude of shear causing the formation of inclined cracks. This conclusion is supported by the results of the E Series tests presented in Table 5. Comparison of the values of V_c^{dt} for beams tested on an a/d ratio of 3.39 shows no significant trend with amount of web reinforcement.

McClarnon, Wakabayashi, and Ekberg[4] conducted tests on two pretensioned beams of rectangular cross section without web reinforcement which were

first symmetrically loaded until fully developed flexure shear cracking had occurred. The two beams were then unloaded, and subsequently re-loaded to failure on an increased shear span. In comparison to similar test beams on which the shear span was not changed, the results of their tests indicated a significant reduction in ultimate strength due to moving the load points. This reduction in strength was attributed to loss of restraint on the development of the flexure shear crack as a result of moving the load point. Specifically, with regard to test beams C10 and C11 shown in Fig. 27 of their report, the ultimate load carried by C10 of 12.8 kips may be seen as closely equal to the load which caused the flexure shear crack to form in C11. This work therefore supports the second conclusion for inclined cracking of the flexure shear type. For inclined diagonal tension cracking the second conclusion holds without the restriction that the loads be moving loads, as may be readily seen from the results on E.1 through E.4 presented in Section 3.4.

Work by Mattock and Kaar[5] on the shear strength of continuous prestressed girders with web reinforcement forms a basis for the third conclusion. Their investigation showed that prior to diagonal tension cracking, the web reinforcement was only slightly stressed, in either tension or compression. With diagonal tension cracking, web reinforcement crossed by the cracking yielded immediately.

The importance of the three conclusions discussed in the preceding paragraphs emphasizes the need of being able to accurately determine the inclined cracking strength of a prestressed beam. Consider first the flexure shear type of inclined cracking, which begins as a flexure crack but, because of the presence of shearing forces, becomes inclined in the direction of increasing moment. An important characteristic of this type of cracking is that its development is more rapid than a flexural crack. Therefore the flexure shear inclined cracking load at a particular section in the beam may be conservatively but realistically taken as the load which will cause a flexure crack to first form at some distance in the direction of decreasing moment from this section. The distance from the section must be sufficient to permit the development of a significant inclined crack which would lead to a critical shear condition.

In the tests by Hulsbos and Van Horn, referred to previously, the principal stress method was determined to be a satisfactory method for evaluating

the diagonal tension cracking strength of pretensioned I-beams. Their conclusion was based on a study of the calculated state of stress in the web of the I-beam just prior to inclined cracking, and included an approximation of the stresses due to the stress concentration from the reaction and load point. The inclined cracking load was calculated as the load causing the principal tensile stress to reach a certain limiting value at any point in the web of the I-beam. The limiting value of principal tensile stress recommended by Hulsbos and Van Horn was the stress determined from a tensile test specimen with a 4 by 4 in. cross section.

A very thorough study of the shear at inclined cracking of a large number of prestressed beams has been made by Hernandez, Sozen, and Siess. Design proposals by Hernandez, Sozen, and Siess, based on the findings of their study, have been summarized by Mattock and Kaar[5] and state that the shear at inclined cracking shall be taken as equal to the least shear which will produce either of the following effects: (a) a net tensile stress of $6\sqrt{f'_c}$ in. the extreme fiber in tension at a distance from the section considered equal to the effective depth of the section, measured in the direction of decreasing moment; or (b) a principal tensile stress of $4\sqrt{f'_c}$ at the intersection of the neutral axis with a 45° line drawn in the direction of decreasing moment from the extreme fiber in compression of the section considered.

The significant feature of the proposals by Hernandez, Sozen, and Siess is that only the state of stress at the neutral axis of the member is considered in determining the inclined diagonal tension cracking load. Since the state of stress at the bending neutral axis is simplified because flexural stresses are zero at that point, the inclined cracking load becomes a function of only two variables, the limiting tensile strength of the concrete and the effective prestress force, and can be readily calculated.

Based on the discussion in the preceding paragraphs, consider the behavior of a simply supported prestressed beam with web reinforcement, as shown in Fig. 32, subjected to a uniform load, w, simulating the dead load on the member and a concentrated live load, P, which may have a variable magnitude and location. In the typical design situation, with increasing span length, L, the uniform dead load would become a greater part of the total design load. The crack patterns may develop in several different ways. For beams with the

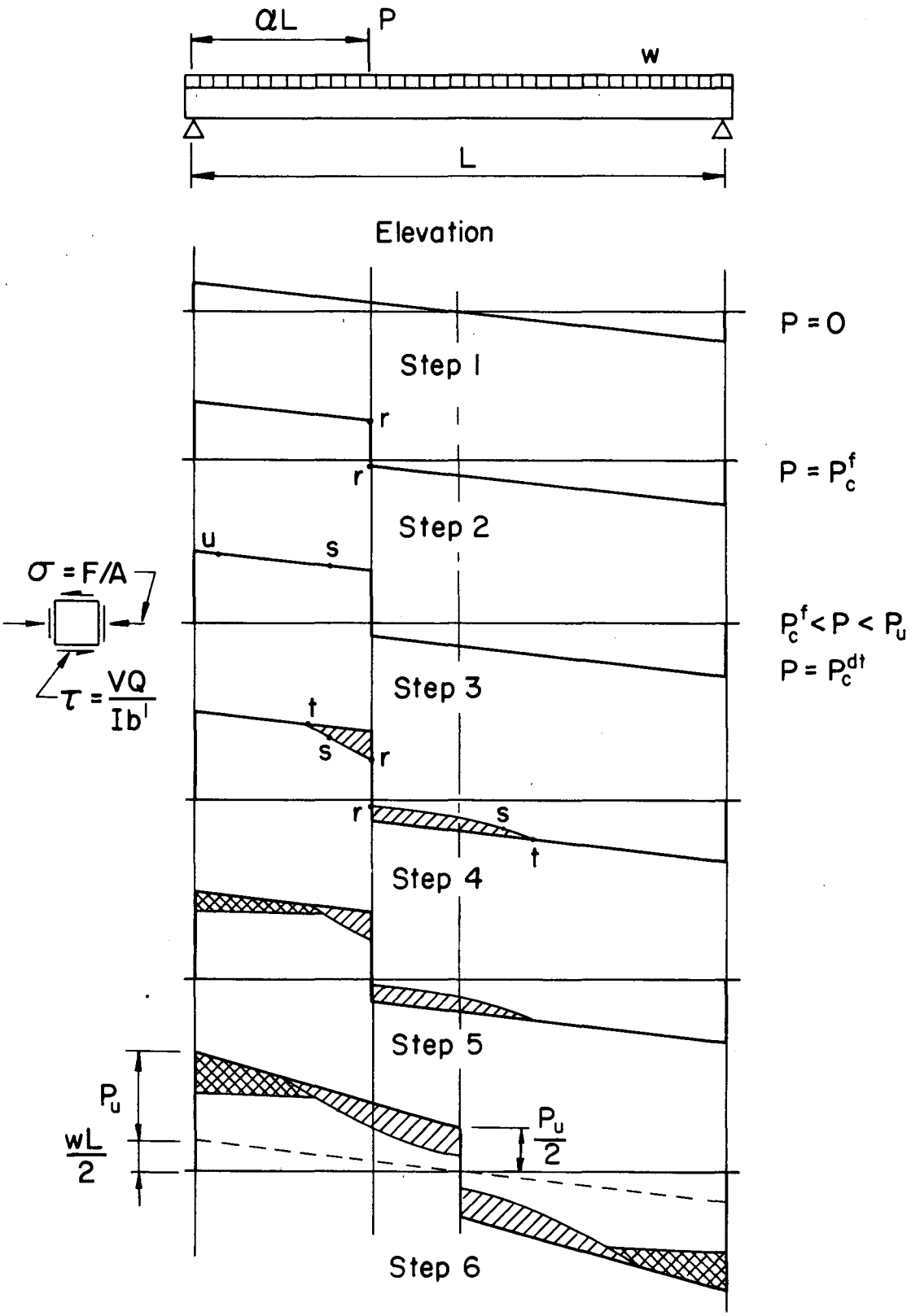

Fig. 32 Behavior of a simply supported prestressed beam

greater span lengths the first cracking in the beam would be flexural cracking, followed by flexure shear cracking adjacent to the concentrated load. For intermediate span lengths diagonal tension cracking may either precede or follow flexure shear cracking. For short spans diagonal tension cracking may precede flexural cracking.

In Fig. 32, let the span be regarded as being of intermediate length; therefore both flexure shear and diagonal tension cracking must be considered. Consider the load to be applied at a particular location, αL. Step 1 shows the shear diagram with only the uniform dead load applied. Next apply a load P of sufficient magnitude to initiate flexural cracking, say P_c^f. Designate the ordinates of the shear diagram, with P_c^f applied, at the section of maximum moment as points r, as indicated in Step 2. If P is increased above P_c^f but less than the load causing failure for any value of α, i.e. the moving ultimate load, P_u, the resulting shear diagram would be that shown in Step 3. Designate the ordinates of this shear diagram which correspond to the sections at which the moment is equal to the flexural cracking moment as points s. The shear diagram shown in Step 4 is drawn for the load P equal to the moving ultimate load P_u. Designate as t the ordinates on the P_u shear diagram where the moment is equal to the flexural cracking moment.

On the P_u shear diagram in Step 4, plot the points r and s. The curve drawn through the three points, r, s, and t may be called the flexural cracking curve. Cross-hatch the area between the flexural cracking curve and the P_u shear diagram. Since a flexure shear crack begins as a flexural crack, the region in which flexure shear cracking may occur is the length along the beam represented by the cross-hatched area.

To include the effect of inclined diagonal tension cracking, return to the shear diagram shown in Step 3. The region of maximum shear must be investigated. The state of stress at the bending neutral axis is assumed to be as shown on the sketch of an element of material adjacent to the Step 3 shear diagram. Knowing the prestress force and the value of the principal tensile strength of the concrete at the bending neutral axis (σ_t^{cg}) at which cracking will occur, the critical shear V equal to V_c^{dt} may be calculated. Represent the

value of V_c^{dt} by the ordinate u. Consider the point at which u is plotted in Step 3 of Fig. 32 to be the location along the bending neutral axis where diagonal tension cracking will first occur, i.e., corresponding to P equal to P_c^{dt}.

As P is increased above P_c^{dt}, other sections will be subjected to a shear equal to or greater than that indicated by the critical ordinate u, and may be expected to develop diagonal tension cracking. Thus at the load P_u, diagonal tension cracking may be expected to occur in the region where the shear is greater than that indicated by the ordinate u.

Step 5 in Fig. 32 summarizes the discussion of the behavior of the simply supported prestressed beam with web reinforcement when the load P_u is applied at a particular location αL. The singly cross-hatched area defines the region where flexure shear cracking may occur; the doubly cross-hatched area defines the region where diagonal tension cracking may be expected.

To consider the effect of P_u as a moving load, the procedure described in the preceding paragraphs could be repeated for selected values of α increasing from 0 to 0.5. More succinctly, the maximum shear envelope may be drawn, and the shear at any section at which flexure shear and diagonal tension cracking may occur may be determined as the shear causing either a flexural stress in the bottom fibers equal to the flexural tensile strength of the concrete or a principal tensile stress at the bending neutral axis equal to the principal tensile strength of the concrete, respectively. This is indicated in Step 6 of Fig. 32, where again the region denoting the length along the beam where flexure shear cracking may occur is singly cross-hatched, and the region where diagonal tension cracking may occur is doubly cross-hatched.

Furthermore, since the web reinforcement in the beam carries essentially no load until crossed by an inclined crack, the ordinate of the cross-hatched area at any particular section represents the amount of shear which must be developed after the web reinforcement begins working in order to sustain the load P_u. It therefore appears that the amount of web reinforcement required is a function of the ordinate of the cross-hatched area.

Consider a section arbitrarily located in the beam in Fig. 32 in the region where inclined cracking would exist, as shown in Fig. 33. A free body

diagram of the portion of the beam to the left of this section may be drawn by separating the beam along the path of an inclined crack, say JK, and by a vertical cut through the concrete at the top of the inclined crack, say KL. Since the path of the inclined diagonal tension crack will not extend through to the bottom flange in the region of J, the section taken along JK may pass through some concrete. The principal forces at this section would be the two components of the resultant force in the strand, F_H and F_V, the two components of the resultant force in the web reinforcement, V_{w_H} and V_{w_V}, and the resultant force transmitted through the concrete which may be represented by a horizontal compressive force C and a shearing force V_c. For prestressed beams with web reinforcement, the horizontal component of the force in the web reinforcement is small, and therefore V_{w_V} may be taken as simply V_w. Likewise the vertical component of shear transmitted across the prestressing elements is small, particularly if the prestressing elements are seven wire strand, and may be neglected. Thus the general free body diagram may be replaced by a simplified free body diagram, also shown in Fig. 33.

Let V_u be the ultimate shear on this section located an x distance from the left support. For equilibrium:

$$V_u = V_c + V_w$$

But V_w may be regarded as known, based on the assumption that web reinforcement crossed by an inclined crack has yielded. Therefore if A_v is the area of a single stirrup and s the spacing:

$$V_w = A_v f_y \cdot \frac{\not{\beta} d}{s}$$

where f_y is the yield stress of the web reinforcement. Solving for A_v gives the equilibrium requirement that:

$$A_v = \frac{(V_u - V_c)\, s}{f_y \cdot \not{\beta} d} \qquad (1)$$

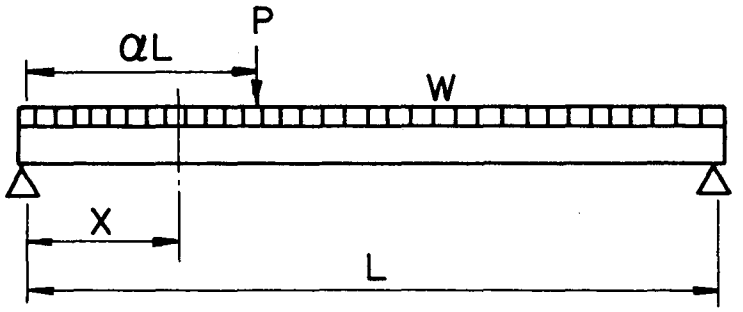

Elevation

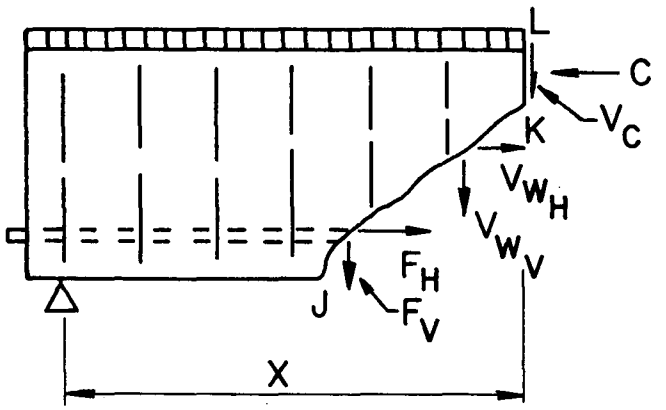

General Free Body Diagram

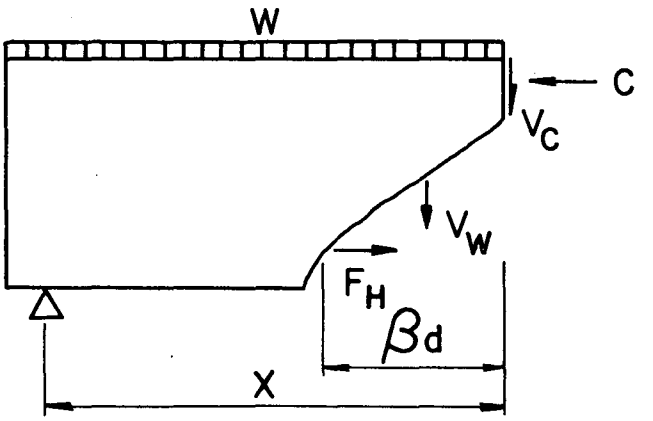

Simplified Free Body Diagram

Fig. 33 Shear equilibrium condition

Equation (1) has several significant features. If V_c and β were known the form of Eq. (1) is such that it could readily be used as a design equation. In fact, with $\beta = 1$, Eq. (1) has been presented as a design proposal by Hernandez, Sozen, and Siess, as reported in an article by Mattock and Kaar,[5] where V_c is taken as the inclined cracking load and calculated according to the recommendations previously given on p. 58 Mattock and Kaar[5] have also presented a design equation of the form of Eq. (1), where V_c is calculated according to the recommendations of Hernandez, Sozen, and Siess and the factor β is taken equal to 3.5 sin (a/d). Mattock and Kaar's proposal correlated excellently with the results of thirteen tests which they conducted on continuous pretensioned beams failing in shear.

The physical justification for taking the shear carried by the prestressed beam just prior to inclined cracking as the shear carried by the concrete, along the cut KL, at failure is by no means apparent. The results of the tests on beams E.1 through E.4 as reported in Section 3.4 support the statement, however. These four beams, all without web reinforcements, were initially loaded until inclined diagonal tension cracking formed, at the shear indicated in Table 5 as V_c^{dt}. At this point in the test the beams, which had become very unstable, were unloaded. Subsequently the beams were re-loaded to failure, indicated as the shear V_u in Table 5. In the re-loading process essentially all of the shear must have been carried by the concrete in the region above the top of the inclined crack. The lowest ratio of V_u to V_c^{dt} is 0.80, in the case of the beam with the longest shear span, while the average ratio of V_u to V_c^{dt} for these four tests is 0.90. Furthermore, there is reason to believe that with even a small amount of web reinforcement, the crack opening in the web would have been sufficiently restricted to increase the ratio of V_u to V_c^{dt} to one or greater.

The angle of inclination of the inclined crack, for diagonal tension cracking, is closely associated with the direction of the compressive stress trajectory, as can be readily seen from the sketches of crack patterns presented in Appendix I. When an increment of load has been applied which causes the diagonal tension crack to form, its initial length, i.e. initial value of β, appears quite arbitrary, probably depending on the relationship between the location of the crack and the position of web reinforcement in the vicinity. Immediately there is a re-distribution of shear in the beams, as the stirrups crossed by the crack pick up an amount of shear at least approximately equal to

$A_v f_y$. Any further increase in shear must be carried either by the concrete above the top of the crack or must cause extension of the inclined crack so as to intersect additional web reinforcement, provided that the contribution to the shear carried by the concrete or strand below the bottom of the crack is neglected. The important feature, however, is not the relationship between this division of load for values of shear on the section less than the ultimate shear, but rather the conditions that exist as the last increment of load is applied before the ultimate shear capacity is reached. The limited observations made from the tests reported herein indicate that before failure would occur the inclined crack will always have developed sufficiently to have crossed all web reinforcement in its projected path. Failure will subsequently occur either as a fracture of the web reinforcement or in the compression zone of the concrete, provided that failure has not occurred prior to this due to web distress, i.e. crushing of concrete in the web. This criteria suggests that β might be reasonaly calculated as the factor which, when multiplied by d, gives the horizontal projection of an inclined diagonal tension crack with inclination approximated as the angle of the compressive stress trajectory at the bending neutral axis, and considered to extend from the junction of the web with the top flange to the lowest depth at which the web reinforcement may be regarded as effective. Formulated, this definition may be expressed as:

$$\beta = \frac{\ell_e}{(\tan \theta)d} \qquad (2)$$

where ℓ_e is the distance from the intersection of the top flange and web to the lowest point at which the web reinforcement may be regarded as effective.

With reference to flexure shear cracking, β could have values varying from zero to greater than one. Experimental observations of test beams critical in shear have indicated that flexure shear cracks forming at β values of less than one are supplanted by more critical flexure shear cracks with values of β greater than one. Therefore it appears conservative to take β equal to one for all flexure shear cracking.

With V_c and β values determined according to the discussion in the preceding paragraphs, Eq. (1) becomes a criteria for proportioning vertical web

reinforcement in a prestressed beam. But Eq. (1) has severe limitations as an ultimate shear strength equation. The purpose of web reinforcement is to permit an increase in the load carrying capacity of the beam above the inclined cracking load. This is accomplished by effecting a re-distribution of forces in the beam at inclined cracking. In effect, the beam action destroyed by inclined cracking must be restored by web reinforcement. The conditions required to insure that this restoration of beam action takes place must be met before Eq.(1) can be regarded as having any meaning; these conditions include limitations on the spacing of the web reinforcement, anchorage and bond requirements, etc., which can be summed up under the heading of good dimensional proportioning. Assuming that the conditions required for the re-distribution of forces are met, the prestressed beam critical in shear may fail in three ways: (a) by fracture of the web reinforcement, (b) by web distress, i.e. by crushing of concrete in the web, and (c) by shear compression, i.e. crushing of concrete in the compression zone. But if failure occurs as fracture of the web reinforcement, the critical stress would be the ultimate stress, f_u, which may be more than 50% greater than f_y. Similarly failure due to web distress or shear compression must be associated with the strength of the concrete. None of these indexes, however, are an explicit part of Eq. (1). Therefore Eq. (1) must be regarded as an equilibrium requirement which holds, approximately, at loads close to but not necessarily at the ultimate load.

4.2 Static Shear Strength of Test Beams

Section 4.1 presented a general discussion of the static overload behavior of prestressed I-beams with web reinforcement. The purpose of this section is to correlate the results of the static tests presented in Section 3.4 with the discussion in Section 4.1.

For this purpose, the test results given in Table 5 and 5A are plotted as applied load shear, V, versus the a/d ratio on which the test was conducted, as shown in Fig. 34. In this form, the results represent the experimentally determined flexural cracking, inclined cracking, and ultimate strength of the type of member being tested. The numbers beside some of the plotted points indicate the number of tests for which that plotted point is an average.

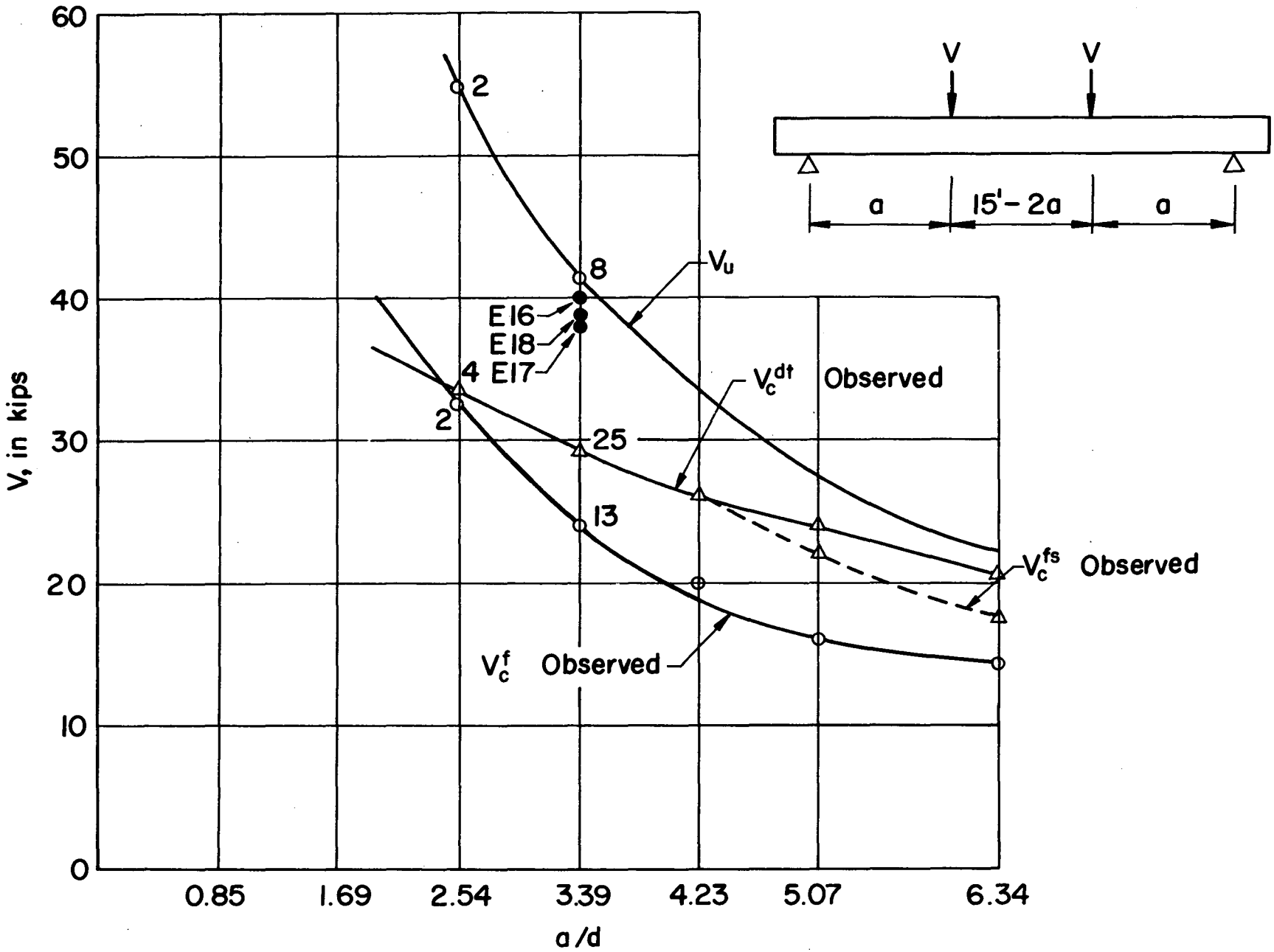

Fig. 34 Static strength of test beams

To be significant, the diagram of shear strength versus the a/d ratio must be associated with a particular concrete strength. The data plotted in Fig. 34 was taken from tests which, as may be seen from Table 3, varied in concrete strength from 6580 psi to 7790 psi; the average for the 16 static tests was 6920 psi. Consider for example the point indicating the inclined cracking strength of the test beams on an a/d ratio of 3.39. These 25 points are plotted in Fig. 35, and indicate little variation in inclined cracking strength with concrete strength over the small range of concrete strengths being considered. Similarly the flexural capacities of the static test beams failing in flexure, presented in Table 6, do not indicate any significant variation with concrete strength. Therefore, in this discussion the data plotted in Fig. 34 will be regarded as associated with a concrete strength of 6920 psi.

The flexural cracking strength of the test members would generally be calculated from the equation:

$$M_c^f = Z^b \left[f_t' + \frac{F}{A} + \frac{F(e)}{Z^b} \right] \qquad (3)$$

Using the properties of the transformed section of the test beams, Eq. (3) becomes:

$$M_c^f = V_c^f(a) + 2900(12) = 450.9 \left[f_t' + \frac{F}{105.3} + \frac{F(5.02)}{450.9} \right] \qquad (4)$$

Solving for f_t':

$$f_t' = \frac{V_c^f(a)+3.48\times10^4}{450.9} - \frac{F}{105.3} - \frac{F(5.02)}{450.9} \qquad (5)$$

Using Eq. (5), values of F from Table 4, and values of V_c^f from Tables 5 and 7, the flexural tensile strength of the concrete, f_t', was calculated, and the values determined are given in Table 9. The average value of the flexural tensile strength determined in this manner was 675 psi, and corresponds to an average ratio of $f_t' / \sqrt{f_c'}$ of 8.07. The minimum ratio of $f_t'/\sqrt{f_c'}$ was 6.60, as determined for E.13. Therefore the recommendation of Hernandez, Sozen, and Siess (page 58) that the critical tensile stress in the extreme fiber in tension be taken as $6\sqrt{f_c'}$ would have conservatively predicted the flexural cracking moment for all the E Series test beams. Their recommendation was based on

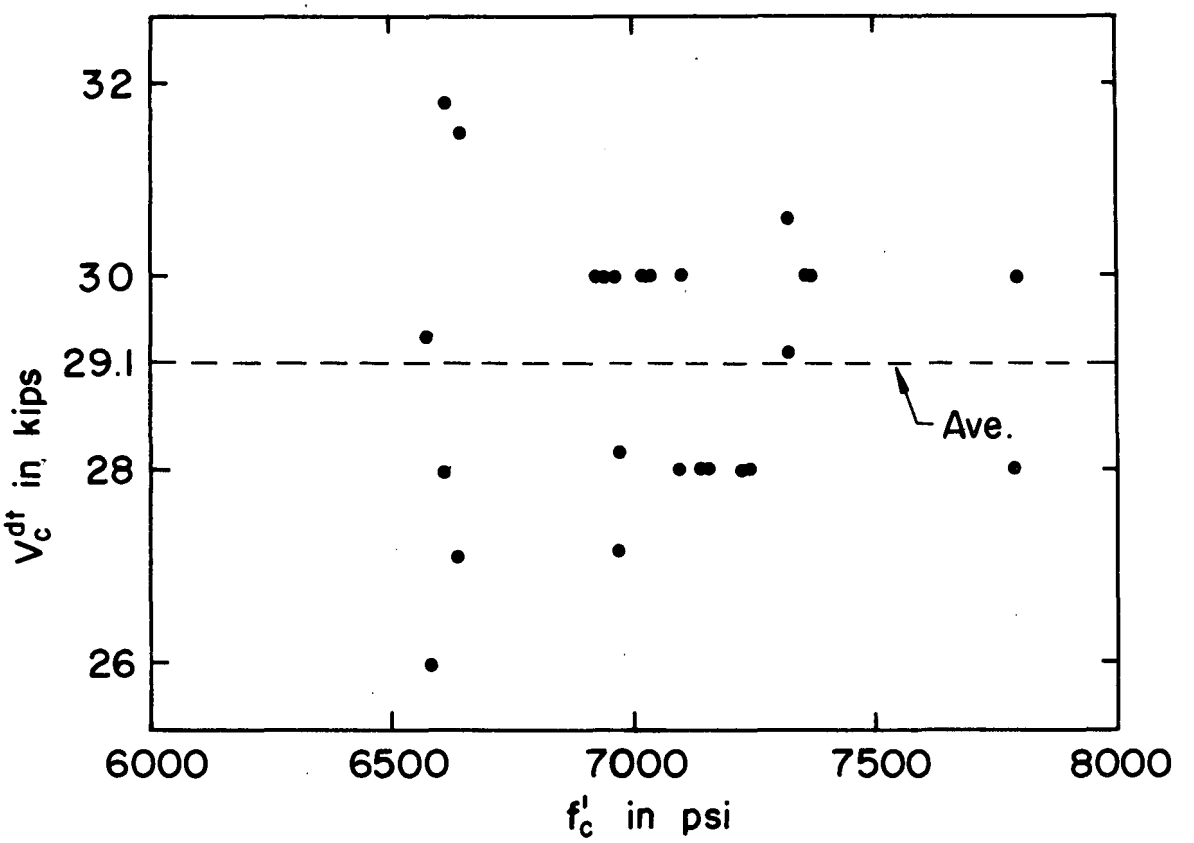

Fig. 35 Variation in V_c^{dt} with concrete strength for a/d = 3.39

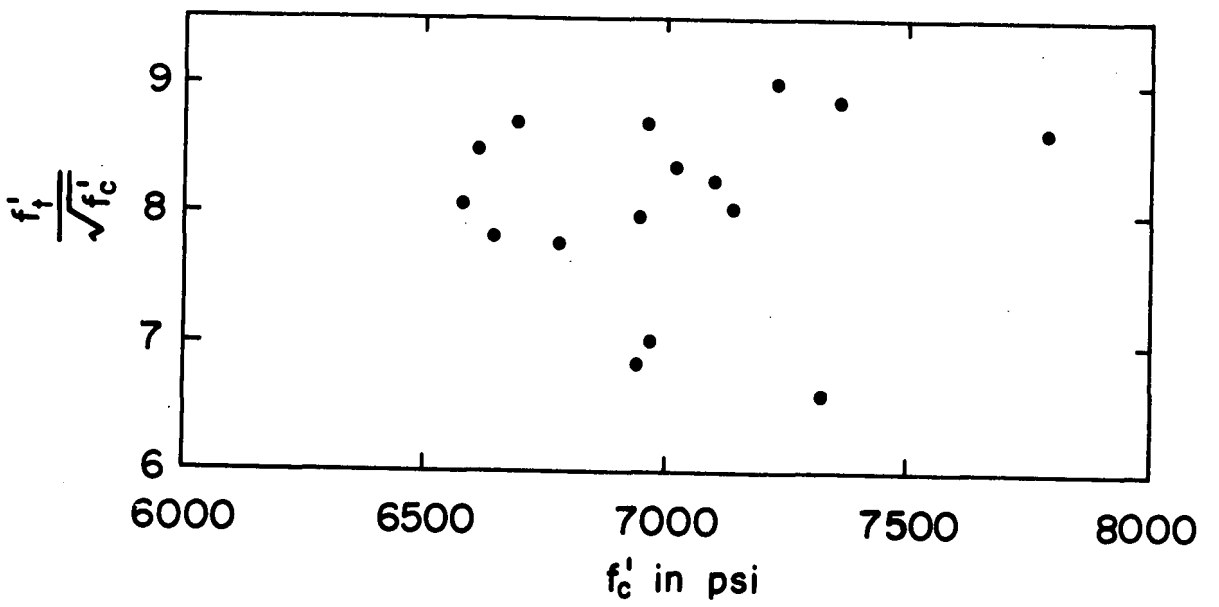

Fig. 36 Variation in flexural tensile strength with compressive strength

Table 9. Flexural Tensile Strength and Principal Tensile Strength Determined from Test Beams

Beam	f'_t (psi)	$\frac{f'_t}{\sqrt{f'_c}}$	σ_t^{cg}		$\sigma_t^{cg}/\sqrt{f'_c}$	
			(2) End (psi)	(20) End (psi)	(2) End	(20) End
E.1	--[1]	--	--[3]	--[2]	--	--
E.2	710	8.68	--[3]	--[2]	--	--
E.3	--[1]	--	--[2]	--[3]	--	--
E.4	725	8.70	435	--[3]	5.22	--
E.5	690	8.49	480	395	5.90	4.85
E.6	695	8.26	445	405	5.29	4.81
E.7	765	9.00	395	395	4.65	4.65
E.8	585	7.01	405	375	4.86	4.50
E.9	680	8.04	400	395	4.74	4.68
E.10	760	8.85	450	455	5.24	5.30
E.11	760	8.62	455	410	5.16	4.66
E.12	700	8.35	440	445	5.25	5.31
E.13	565	6.60	440	410	5.15	4.80
E.14	640	7.77	480	500	5.83	6.08
E.15	570	6.84	490	520	5.88	6.25
E.16	665	7.97	440	440	5.28	5.28
E.17	655	8.08	355	425	4.38	5.24
E.18	645	7.82	370	475	4.54	5.83
Ave.	675	8.07	430		5.16	

Notes: 1. Values of f'_t calculated for these beams regarded as unrealistically high, and indicate that the corresponding experimentally determined values of V_c^f are too high.

2. Not applicable because of prior flexure shear cracking.

3. Diagonal tension cracking at other end only.

an investigation which covered a much wider range of concrete strengths than were included in the E Series tests. However, Fig. 36 shows a plot of f'_c versus $f'_t/\sqrt{f'_c}$, and indicates no significant trend of the flexural tensile strength with compressive strength in the range of concrete strengths investigated. Based on the results of the E Series tests, the flexural tensile strength of the concrete may be conservatively determined as:

$$f'_t = 6.5\sqrt{f'_c} \qquad (6)$$

The V_c^f design curve shown in Fig. 37 was determined using Eq. (5), with f'_t calculated from Eq. (6) based on the average concrete strength of 6920 psi, and F taken as the average prestress force which, from Table 4, is 91.4 kips.

To understand the experimentally determined inclined cracking curve shown in Fig. 34 as V_c^{dt} and V_c^{fs} observed, reference should be made to the presentation of results in Section 3.4. The analytical approach used to determine the inclined cracking strength, as discussed in conjunction with Fig. 32, depends upon whether the inclined cracking was classified as flexure shear or diagonal tension. Consider first the flexure shear cracking. The V_c^{fs} design curve shown in Fig. 37 was constructed by displacing the V_c^f curve a distance d in the direction of increasing moment. It is a conservative estimation of the V_c^{fs} observed curve, as it must be since the flexure shear cracking was not considered critical until, by definition, it occurred approximately a distance d away from the load point.

The transition from flexure shear to diagonal tension cracking may be seen, from Fig. 34, to take place in the neighborhood of an a/d ratio of 4. From an examination of the figures in Appendix I, the critical principal tensile stresses (σ_t^{cg}) at the intersection of the path of the diagonal tension crack as it first formed and the centroid of the concrete section may be estimated, and are recorded in Table 9. The average value of σ_t^{cg} determined in this manner was 430 psi, which corresponds to an average ratio of $\sigma_t^{cg}/\sqrt{f'_c}$ of 5.16. The minimum ratio of $\sigma_t^{cg}/\sqrt{f'_c}$ was 4.38, as determined for E.17. The recommendation of Hernandez, Sozen, and Siess (page 58) was that diagonal tension inclined cracking should be considered to occur, for design purposes, when a principal tensile stress of $4\sqrt{f'_c}$ occurs at the intersection of the

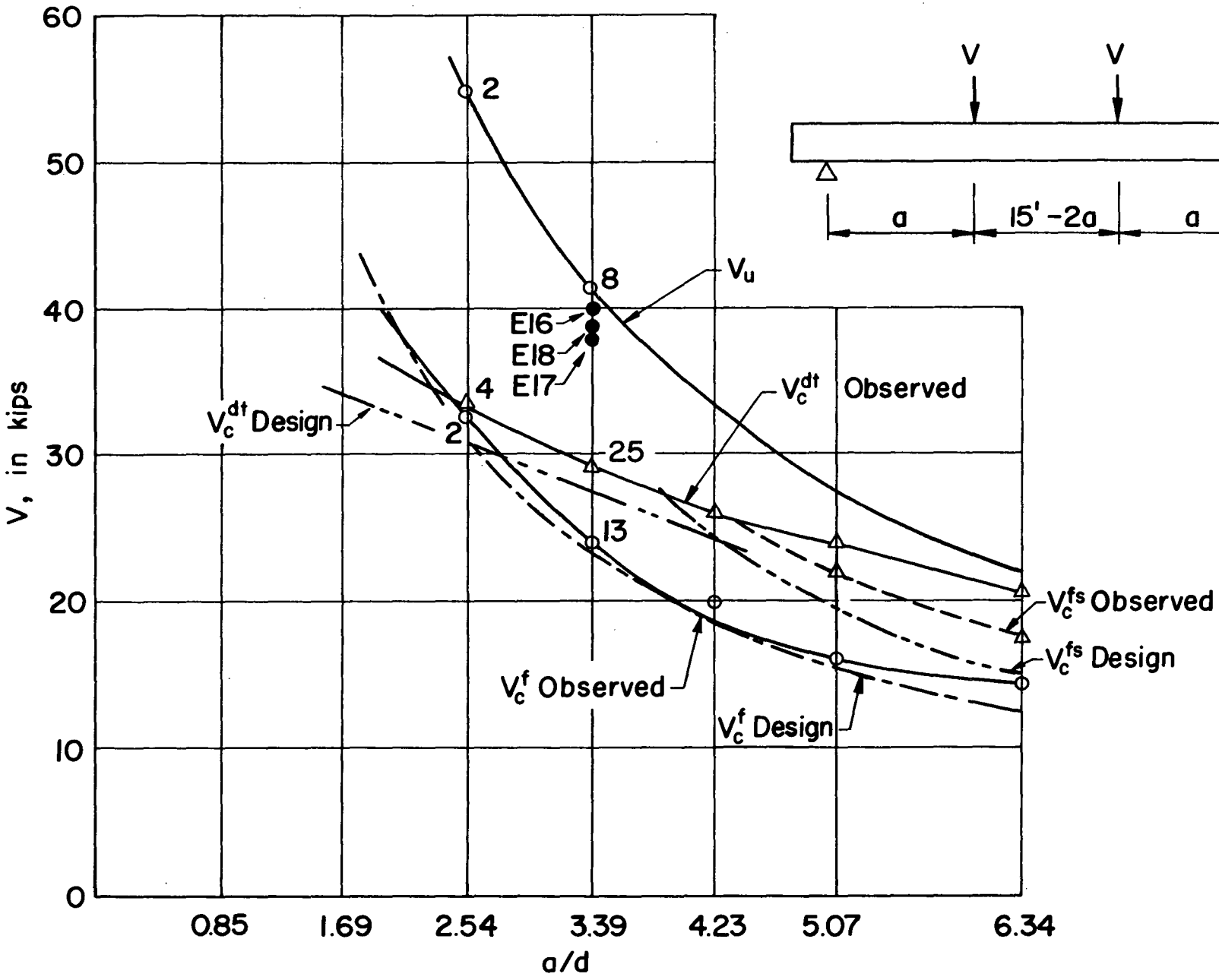

Fig. 37 Static strength of test beams associated with a concrete strength of 6920 psi

neutral axis with a 45^{o} line drawn in the direction of decreasing moment from the extreme fiber in compression of the section considered. As may be noted from the figures in Appendix I, the values of the principal tensile stress along the neutral axis are relatively constant, because the dead load of the test beams is a small proportion of the total load at inclined cracking; therefore the location of the section considered for diagonal tension cracking is not critical, and can be taken as the section at which the diagonal crack formed. Thus it may be concluded that the recommendation of Hernandez, Sozen, and Siess would have conservatively predicted the diagonal tension inclined cracking strength of all of the test beams in the E Series.

Values of $\sigma_t^{cg}/\sqrt{f'_c}$ are plotted against concrete strength in Fig. 38 and the a/d ratio in Fig. 39. In Fig. 38, the four points with the circle around the solid point correspond to the four points in Fig. 39 on the a/d ratio of 2.54; the remaining points all correspond to the a/d ratio of 3.39. From Fig. 38 it may be seen that, in the range of concrete strengths investigated, the principal tensile strength, expressed as a function of $\sqrt{f'_c}$, is relatively insensitive to changes in concrete strength. But from Fig. 39 it would appear that the value of σ_t^{cg} varies with the a/d ratio.

In examining the figures in Appendix I, it should be again noted that the indicated values of principal tensile stress were determined in the conventional way; that is, the section was assumed uncracked, and only stresses due to the prestress force, weight of the test beam, and applied test loads were considered. To determine more closely the true state of stress in the web, consideration must also be made of the stress concentrations due to the prestress transfer zone and the concentrated load points. However, all of the test beams had an overhang at the reaction of 15 inches which, as may be noted from Table 4, was in general greater than the transfer distance. Furthermore the location of diagonal tension cracking did not in any instance appear influenced by proximity to the end of the test beam. Therefore the stresses due to the prestress force, at the locations considered in the shear span, should be closely determined by the elementary stress formulas.

To consider the effect of stress concentration due to the reaction and load points, use was made of an approximate method suggested by Hulsbos and Van Horn,[3] in which the stresses due to the concentrated force points are calculated from Timoshenko and Goodier's[6] equations for stresses due to a concentrated

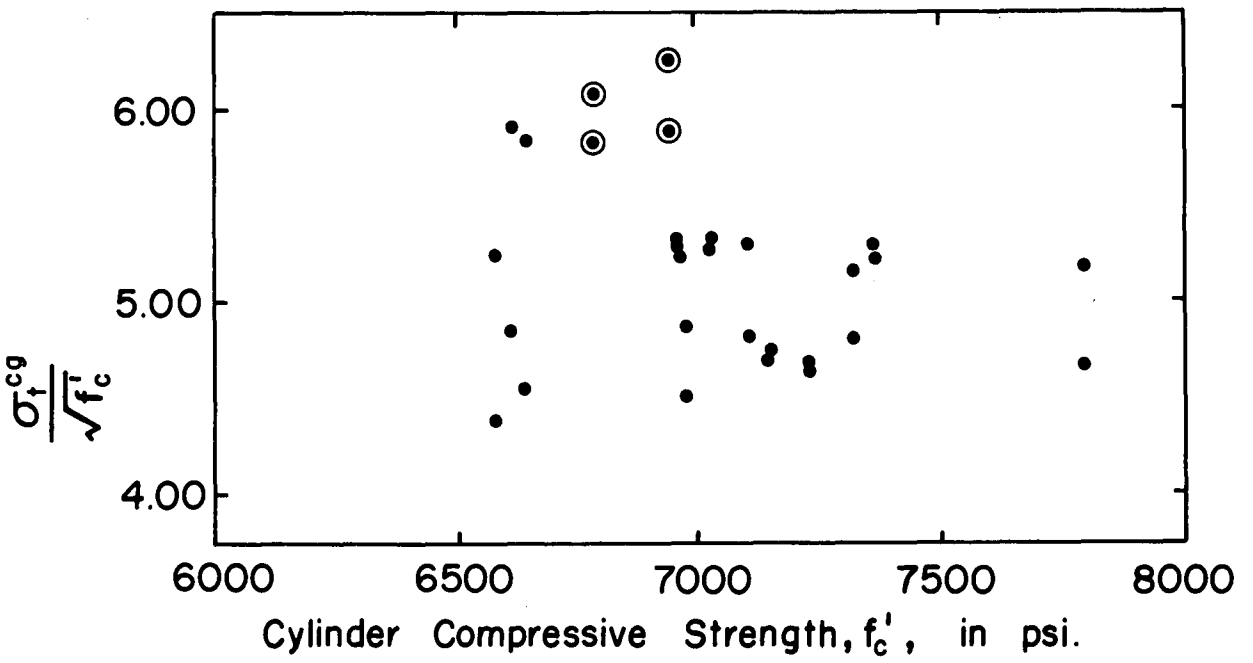

Fig. 38 Relationship between principal tensile strength along C.G.C. at diagonal tension cracking and compressive strength of concrete

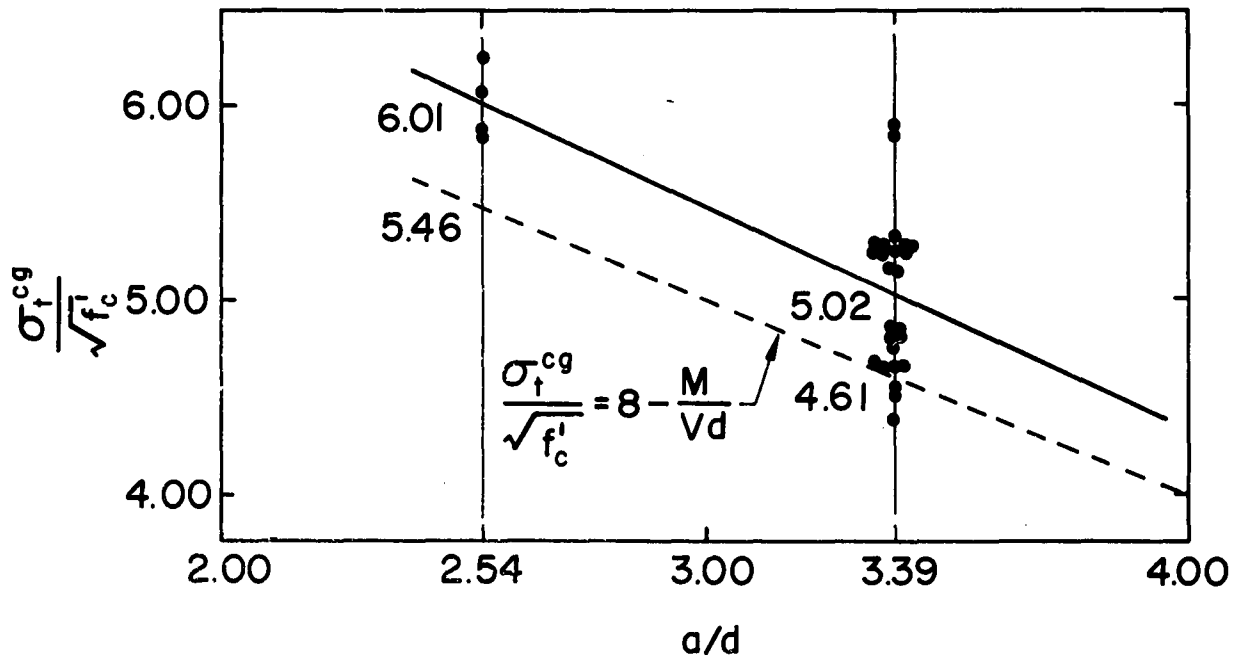

Fig. 39 Relationship between principal tensile strength along C.G.C. at diagonal tension cracking with the a/d ratio

force on the edge of a semi-infinite plate. In addition to the limitations implied by the use of these equations, which are discussed by Hulsbos and Van Horn, the further assumption was made that 90 percent of the concentrated force applied to the top or bottom surface of the I-beam should be used as the edge force applied to the semi-infinite plate having a width equal to the width of the web of the I-beam. With these assumptions, the equations for vertical, horizontal, and shearing stress, respectively, become:

$$\sigma_v = 0.573 \quad V_c^{dt} \cos^4 \varphi / y$$

$$\sigma_h = 0.573 \quad V_c^{dt} \sin^2 \varphi \cos^2 \varphi / y \qquad (7)$$

$$\tau_{vh} = 0.573 \quad V_c^{dt} \sin \varphi \cos^3 \varphi / y$$

where

$$\tan \varphi = x/y,$$

and y and x are the vertical and horizontal distances, respectively, from the concentrated force to the point at which the stress is being calculated. The vertical and horizontal stresses are compression, and the shearing stress adds to the elementary shearing stress. These equations do not satisfy the boundary conditions on the bottom surface of the I-beam, and therefore must be regarded as very approximate.

The results of the calculations from the preceding paragraph are summarized in Fig. 40 for the two shear spans on which inclined diagonal tension cracking occurred, i.e., on the 3'-0" and 4'-0" shear spans corresponding to a/d ratios of 2.54 and 3.39 respectively. With reference to the results in Table 5 or Fig. 34, it may be seen that the average value of V_c^{dt} for these tests on the 3'-0" and 4'-0" shear spans is 29.1 kips and 33.4 kips, respectively. As shown in Fig. 40, principal tensile stresses have been calculated at the intersections of the grid lines with the junction of the web and top flange, the centroid of the concrete section, and the junction of the web and the bottom flange. At a particular point, the upper left hand corner number is the principal tensile stress determined in the same manner as the principal stresses given on the figures in Appendix I, including only the effect of shear, bending moment, and the average prestress force which, considering all of the test beams, was 91.4 kips. The principal tensile stress recorded as the upper right hand corner number includes the additional effect of the stress

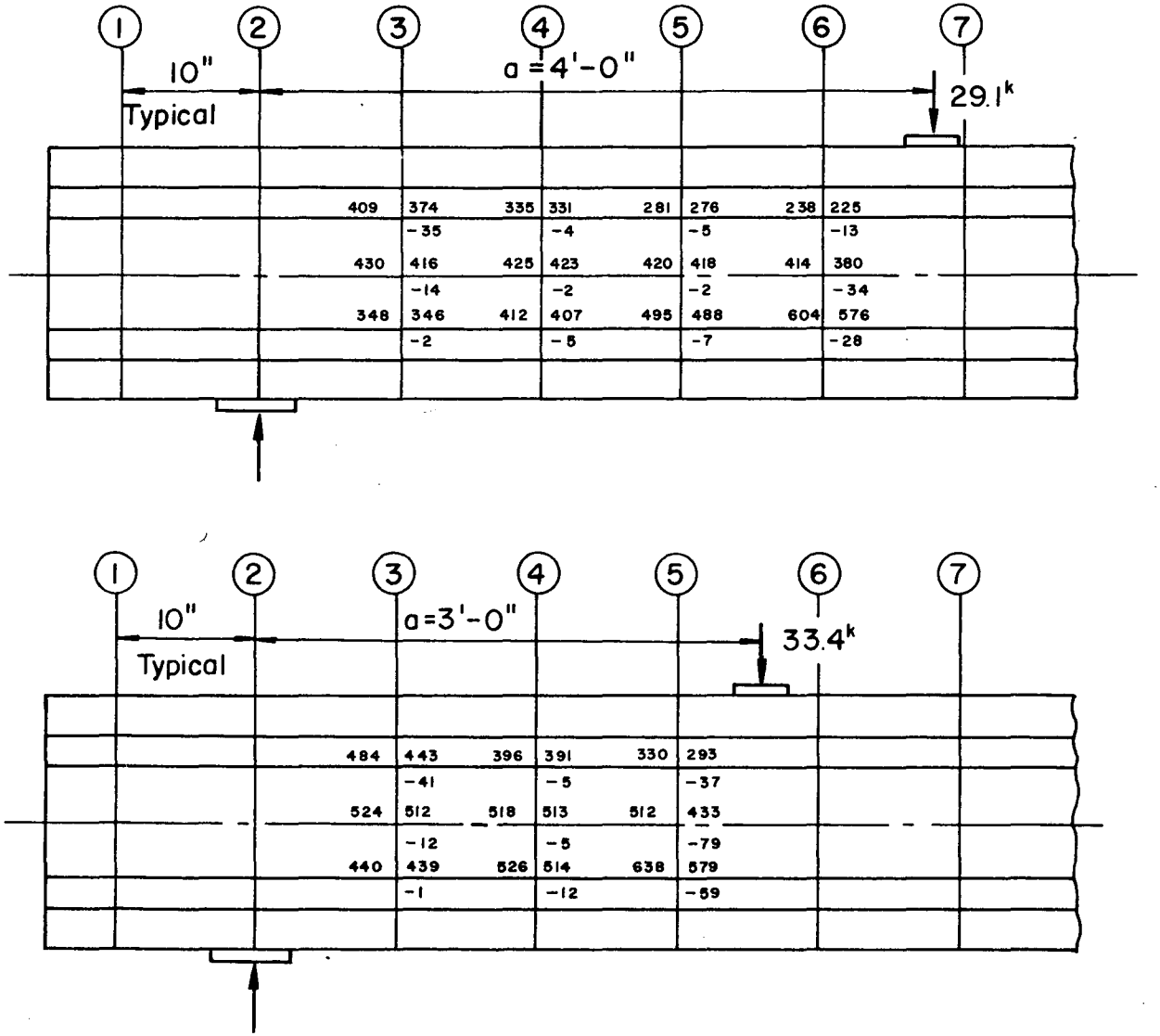

Fig. 40 Corrections to calculated values of principal tensile strength due to stress concentration from load points

concentration from the concentrated forces determined using Eqs.(7). The difference between these two principal stresses, recorded as the lower right hand corner number, may be regarded as an approximate indication of the effect of the stress concentration due to the load points on the state of stress in the web of the I-beam.

With this indication of the effect of the stress concentration, consider the figures in Appendix 1, for example, of E.5, E.6 and E.14. Examining the (2) end of E.5, which was tested with 4'-0" shear spans, it would seem that the crack should form in the region close to line (6) and the junction of the web and bottom flange where σ_t is equal to 723 psi. However, the stress concentration from the load point reduces the value of σ_t in this region; furthermore any crack forming in this region would be quickly restrained at its lower extremity by the bottom flange and at its upper extremity by the proximity of the load point. Thus the inclined crack apparently tends to form further back into the web, as very typically indicated by the crack in the (2) end of E.5. In this situation, the inclination of the crack is very closely associated with the direction of the compressive stress trajectory at the centroid of the section, and the direction of the crack is in line with the intersection of the load point and the top surface of the beam. As may be seen from the other figures in Appendix 1, numerous other inclined cracks seem to have these two essential characteristics.

In the case of the (20) end of E.5, the initial inclined crack appears to have been influenced by the higher principal tensile stresses along the intersection of the web and bottom flange. The significant feature here, as may be seen from the photograph of E.5 after failure in Fig. 8 ((2) end on the right side), is that additional inclined cracks subsequently formed further out in the shear span, and it is these cracks which would have been critical if a shear failure had occurred in this shear span. By contrast, it may be seen from Fig. 8 that the initial diagonal tension crack in the (2) end remained the critical crack throughout the test.

The initial cracking in E.6, as may be seen from the figure in Appendix 1, formed well back from the load point at both ends. These cracks exhibited the characteristic that their inclination is closely associated with the direction of the compressive stress trajectory, but the direction of the cracks did

not pass through the point defined by the intersection of the load point and the top surface of the beam. In the beam test the magnitude of the maximum shear is essentially constant throughout the shear span, and in the case of E.6 it would appear that the moment did not influence the location of the crack. As noted in the preceding paragraph, however, in the majority of cases the moment did seem to influence the location of the crack, by tending to pull the crack forward to the load point. An important feature of the initial inclined cracking shown in E.6 is that if a plot is made of the magnitude of the values of σ_t along the crack, the maximum in both cases was sufficiently close to the centroid of the section to be considered at the centroid. This feature may be noted from the figures of many of the other beam tests where the cracking was not influenced by the higher values of σ_t adjacent to and below the load point. And as noted before, where such cracking was the first to occur, in general additional more critical inclined cracking would form at higher loads further back from the load point.

In the case of E.14, tested with a 3'-0" shear span, the initial diagonal cracking at both ends formed closer to the load point than to the reaction, and therefore appeared to be influenced by the moment. This was also true for both ends of the other beam tested on a 3'-0" shear span, E.15. Thus in comparing the 3'-0" and 4'-0" shear spans, it would seem that the diagonal tension cracking was influenced more by the moment for the shorter shear span. This suggests that the maximum moment to shear ratio, M/V, is a factor in the formation of the diagonal tension cracking. Expressed in non-dimensional form, the moment to shear ratio may be written as M/Vd, and thus for the E Series test beams which have a maximum moment given by M equal to V·a the M/V ratio becomes the a/d ratio. These observations of the influence of the M/V ratio on the location of cracking support the previous discussion in conjunction with Fig. 39.

For the two tests on the 3'-0" shear span, it is important to note that in each end of both beams, additional inclined cracks subsequently formed at higher loads further back from the load point than the inclined cracks which formed initially. These inclined cracks which formed at slightly higher loads had the two characteristics previously noted, that is, that the inclination of the cracks were closely associated with the angle of the compressive

stress trajectory at the centroid of the section and that the direction of the cracks would approximately pass through the point defined by the intersection of the load point and the surface of the beam. Furthermore, it is these cracks which appeared to be the critical shear cracks as the test progressed.

Thus, from the tests reported herein, it would appear that critical diagonal tension cracking has the important characteristic that is inclination may be closely determined as the direction of the compressive stress trajectory at the centroid. Furthermore, these tests indicate that to be critical the extended direction of the inclined crack must lie either on or outside the point defined by the intersection of the reaction or load point and the top or bottom surface of the beam. Applied to the situation shown in Fig. 41, the critical crack must form somewhere between lines a-a and b-b. In the region between lines a-a and b-b, any line on which diagonal tension cracking might occur would in general have the maximum principal tensile stress at or near the centroid of the section. Therefore σ_t^{cg} may be regarded as approximately equal to σ_t. Thus with the principal tensile strength of the concrete known or assumed, the value of the diagonal tension cracking load can be calculated by considering only the state of stress at the centroid.

However, the critical principal tensile strength is not easily defined, because of the difficulty of determining the stress concentrations in the web. The method suggested by Hulsbos and Van Horn, the results of which are summarized in Fig. 40, indicates approximately the effect of the concentrated load points, but does not explain the difference in apparent principal tensile strength of concrete associated with the development of a significant inclined crack on different shear spans, indicated by Fig. 39.

If the critical principal tensile stress causing diagonal tension cracking is empirically related to the M/Vd ratio, a reasonable expression for this stress is:

$$\sigma_t^{cg} = (8 - \frac{M}{Vd}) \cdot \sqrt{f'_c} \qquad (8)$$

where M is the maximum moment in the shear span being investigated.

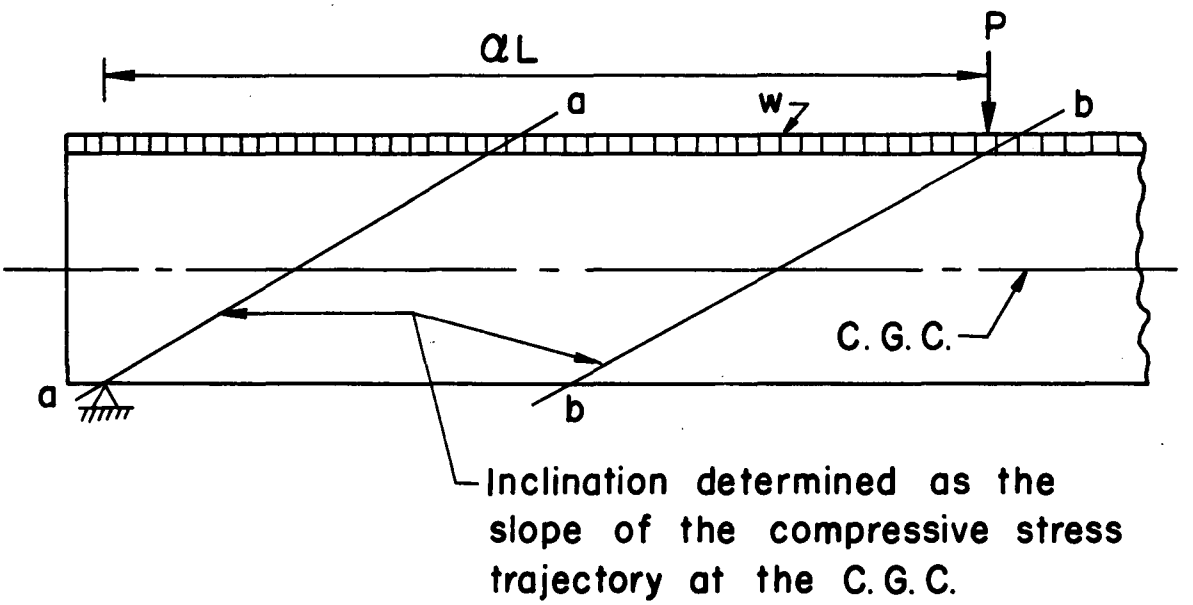

Fig. 41 Region in which critical diagonal tension inclined cracking may occur

This expression has been plotted in Fig. 39 for comparison with the test data, and has been used to determine the V_c^{dt} design curve in Fig. 37.

This concludes the general discussion of the results of the static tests. Further discussion of the individual tests on E.13, E.14, E.16, E.17, and E.18, however, is required.

Beams E.13 and E.14, tested on a/d ratios of 3.39 and 2.54, respectively, had inverted L-shaped stirrups for web reinforcement rather than the U-shaped stirrups used on all of the other test beams. E.13 failed in flexure; however, E.14 failed in shear because of a bond failure in one of the L-shaped stirrups, as was described in Section 3.4 and shown in Fig. 12. The inclined diagonal tension crack which led to this failure was initially fully contained in the web of the test beam. As the load was increased above the load causing the crack to form, the crack extended along its inclined path both upwards towards the load point and downward towards the reaction. The upward development of the crack, however, was restrained by the compressive forces in the top flange. The downward development of the crack penetrated the bottom flange, and at failure had resulted in a complete separation of the bottom flange along the path of the crack, as may be seen from Fig. 12. In this case it is evident that the last stirrup crossed by the inclined crack in its downward development did not have sufficient embedment below the crack to develop the strength required for the redistribution of forces in the member. Therefore the conclusion follows that, where required for ultimate strength, web reinforcement should be provided with a hook in the bottom flange.

As was noted in Section 3.4, the failure in E.18 may possibly also have been a bond failure in the web reinforcement, which in this case was U-shaped stirrups. The bottom leg of the U-shaped stirrup was oriented perpendicular to the longitudinal axis of the beam. Thus if the plane of the inclined crack intersects the bottom leg of the stirrup, or just above the bottom leg, the embedment of the lower leg may not be effective.

The two test beams with web reinforcement which failed in shear were E.17 and E.18. As discussed in Section 3.4, the failure mechanism for E.17 was characterized by crushing of the concrete in the web, while the failure mechanism for E.18 was characterized by fracture of the web reinforcement, if the possibility that the failure in E.18 may have been triggered by a bond failure is excluded. Beam E.17 and E.18 had $rf_y/100$ values of 121 and 97, respectively. Values of $rf_y/100$ required to satisfy the equilibrium condition discussed in conjunction with Eq. (1) may be determined. Since:

$$\frac{rf_y}{100} = \frac{A_v}{b's} \cdot f_y \tag{9}$$

Eq. (1) may be written as:

$$\frac{rf_y}{100} = \frac{V_u - V_c}{b'\not{\phi}d} \tag{10}$$

From Eq. (10) values of $rf_y/100$ required to satisfy the equilibrium condition discussed in conjunction with Eq. (1) may be calculated. For the a/d ratio of 3.39, V_c^{dt} is less than V_c^{fs}, and is therefore the appropriate value for V_c. Since V_c^{dt} is calculated from a consideration of the state of stress at the centroid, as shown adjacent to Step 3 in Fig. 27:

$$\sigma_t^{cg} = \sqrt{\left(\frac{F/A}{2}\right)^2 + \left(\frac{VQ}{Ib'}\right)^2} - \frac{F/A}{2} \tag{11}$$

Using the properties of the transformed section given in Fig. 1, the average prestress force for all of the test beams equal to 91.4 kips, and a value of σ_t^{cg} determined from Eq. (8) based on the average concrete strength of 6920 psi, Eq. (11) may be solved for V equal to V_c^{dt}:

$$384 = \sqrt{(433)^2 + (0.025\ V_c^{dt})^2} - 433$$

$$V_c^{dt} = 27{,}700 \text{ lb}$$

Also, the inclination of the compressive stress trajectory may be determined from the equation:

$$\tan 2\theta = \frac{\frac{VQ}{Ib}}{\frac{1}{2} \cdot \frac{F}{A}} \qquad (12)$$

For the above conditions:

$$\tan 2\theta = \frac{0.025(27,700)}{433} = 1.6$$

$$\theta = 29^{o}$$

Taking ℓ_e as the distance from the junction of the web and top flange to the lowest level of strand, ℓ_e is equal to 11-1/2 inches, and from Eq. (2):

$$\cot = \frac{11.5}{(\tan 29^{o})(14.18)} = 1.43$$

Substituting these values of V_c^{dt} and $\cot$ into Eq. (10), the required value of $rf_y/100$ to develop a shear, V_u, equal to 41.3 kips corresponding to the ultimate flexural capacity of the section is:

$$\frac{rf_y}{100} = \frac{41,300 - 27,700}{3(1.43 \times 14.18)} = 224$$

Therefore the amount of web reinforcement provided in E.17 and E.18 did not satisfy the requirement of Eq. (1).

Test beams E.15 and E.16 failed in flexure, although the web reinforcement in these beams was less than $rf_y/100$ equal to 224. While many factors are involved, this would appear to indicate most probably that the value of V_c at failure was greater than V_c^{dt}.

4.3 Repeated Load Shear Strength of Test Beams

As previously noted, the purpose of the two shear fatigue tests, E.10 and E.11, was to determine if a prestressed beam subjected to a single load cycle of sufficient magnitude to cause inclined diagonal tension cracking

could subsequently be critical in fatigue of the web reinforcement under repeated loadings of lesser magnitude. Test procedure and results for these two tests has been presented in Section 3.5.

Three loading ranges were used during the course of the two fatigue tests. E.10 was first subjected to N equal to 4,000,000 cycles of symmetrical loading in which the applied shear ranged between 8 and 18 kips. From N equal to 4,000,000 cycles to N equal to 4,526,900 cycles, at which failure due to a fatigue fracture in one wire of one of the lower level strands occurred, the applied load shear ranged from 8 to 28 kips. E.11 was able to withstand N equal to 2,007,500 cycles of symmetrical loading, which ranged between 8 and 24 kips applied shear, before failure due to fracture of the web reinforcement occurred.

From the work of Warner and Hulsbos[7] the probable fatigue life of E.10 and E.11 may be determined, assuming that failure occurs as a fatigue fracture in the prestressing strand. The essential information required is the variation in steel stress with load in the most critically stressed strand, which for E.10 and E.11 is any one of the three lower strands. Since the Whittemore strain readings taken on line H are at the same level as the three lower strands, the assumption that the strain in the concrete is equal to the change in the strain in the strand from the initial prestressing strain permits the determination of the steel strain for any value of N directly from Figs. 23 and 30.

Selecting representative values of strain from Figs. 23 and 30, and subtracting these values from the initial strain of 0.00646 in./in. corresponding to an initial average strand tension of 18.95 kips, the strains in the lower strand at the maximum shear in the loading range can be determined, and are presented in Table 10. These strains may be converted to stress using the stress-strain curve for the strand presented in Fig. 2. In the last column in Table 10 the stress is expressed as a percentage of the static ultimate stress for the strand of 252.5 ksi.

Table 10. Stress Variation in Lower Level Strand

Beam	Loading Range (V in kips)	Lower Level Strand		
		Strain (in./in.)	Stress (ksi)	Percentage of Ultimate Stress
E.10	8	0.00500	133.0	52.6
	18	0.00525	140.5	55.6
	28	0.00645	173.5	68.6
E.11	8	0.00505	135.0	53.4
	24	0.00585	157.5	62.3

Using the equations for R and S_L in Fig. 49 of Progress Report No.24, and noting that the dotted line corresponding to P equal to 0.206 is directly applicable because the number of strands at the lower level is three, the predicted N for failure due to strand fatigue can be determined. This work is summarized in Table 11. The results indicate that the 8-18 kip and 8-24 kip loading ranges of E.10 and E.11 are below the fatigue limit, and thus an infinite number of these load cycles could be applied without a fatigue fracture of the strand occurring. The calculations for the 8-28 kip loading range of E.10, however, indicate a probable fatigue failure after 398,000 load cycles. E.10 actually took 526,900 cycles of this loading range before failure occurred, which may be regarded as good correlation.

The 18, 24, and 28 kip shears are 43.6, 58.1, and 67.8 percent of the static ultimate shear, respectively, corresponding to the ultimate flexural capacity of the section. The results of the tests indicate that a prestressed beam with sufficient web reinforcement subjected to a single overload causing diagonal tension inclined cracking will not subsequently be critical in fatigue of the web reinforcement under normal design loadings, i.e., loadings less than approximately 45 percent of the ultimate flexural capacity. To define what is meant by sufficient web reinforcement is not possible. However, any member with web reinforcement proportioned in accordance with the T.R.P.C. specifications is in all probability sufficient.

Table 11. Predicted N for Strand Fatigue Failure

Beam	Loading Range (V in kips)	S_L	R	Log N	N
E.10	8-18	65.1	Negative	--	∞
	8-28	65.1	3.5	5.6	398,000
E.11	8-24	65.7	Negative	--	∞

The load deflection curves for E.10 and E.11 in Fig. 17 and Fig. 25, respectively, suggest a further criteria for judging if fatigue may be critical in a prestressed beam with a diagonal tension crack. After cracking, the load deflection response for E.10 was essentially linear for V from 0 to 18 kips, but definitely non-linear as the shear is increased to 28 kips. Similarly for E.11, the load deflection response is non-linear as V approaches 24 kips. Since both the 8-24 and 8-28 kip loading ranges produced failures, while the 8-18 kip loading range gave no indication of failure in 4,000,000 load cycles, the requirement that the load deflection curve be linear may be an appropriate criteria for precluding the possibility of a shear fatigue failure.

Finally, and perhaps most important, the results of the tests indicate that there are loadings which, for a given prestressed beam, are more critical in fatigue of the web reinforcement than in fatigue of the prestressing strand. The principal parameters involved would appear to be the magnitude of the load, number of load cycles, amount of web reinforcement, and the inclined cracking load, but no insight into the relationship between these parameters is evident from the two shear fatigue tests reported herein.

4.4 Shear Strength of Re-Loaded Test Beams

The results of the static re-load tests have been presented in Section 3.6. These tests were conducted for purely exploratory reasons; that is, after a failure had occurred in a regular static test there remained in some cases a segment of the beam away from the failure region of sufficient length to conduct a second test. Prior cracking in these segments had completely closed, and camber was visually evident indicating that some part of the prestress force was retained.

The test results in Table 8 indicate a reduction in shear strength in the re-loaded tests attributable, at least in part, to the effects of prior cracking and to a loss in prestress force from the first test. Consider the test on E.11. Prior to the re-load test, the applied moment from the repeated load test had never exceeded 68% of the flexural capacity (168.2 ft.-kips, including 2.9 ft.-kips for dead load moment) of the section, and therefore of insufficient magnitude to cause significant yielding of any of the prestressing strand. Consequently the re-load test developed a moment very nearly equal to the ultimate moment of E.9, which had exactly the same web reinforcement.

On the other hand, prior to the re-load tests on E.16, E.17, and E.18, the applied load moments from the static tests were 96, 92, and 93 percent, respectively, of the flexural capacity of the section, and therefore of sufficient magnitude to cause yielding of the prestressing strand. In these three cases the ultimate moments at failure in the re-load tests were 84, 84, and 83 percent, respectively, at the flexural capacity of the section. Although the geometry of loading differed between the static test and corresponding re-load test, the M/V ratio in the shorter shear span of the re-load test was exactly the same as the M/V ratio in the failure shear span in the first static test. Furthermore, had the re-load tests on E.16, E.17, and E.18 actually been first tests, the failure in all three cases would have been expected in the shorter shear spans. The fact that failure occurred in the longer shear spans of the re-load tests on E.16 and E.18 indicates that the high moment in this region from the first static test reduced the ultimate shear strength.

In the case of the re-load test on E.17, failure occurred in the shorter span in which the M/V ratio from the first test was exactly reproduced. However, in the re-load test the shorter shear span carried only 92% of the shear that it had previously carried in the first test. Failure was sudden and complete, due to the fracture of a stirrup. Furthermore, since this failure occurred in a region which had not been subjected to the maximum moment in the first test, it would appear that the failure was influenced by the effect of the cracking incurred in the first test.

The results of these tests are significant because they suggest that ultimate shear strength determined from single cycle static load tests may be more than that which would be obtained if a multiple cycle loading procedure were used. Therefore a better ultimate strength shear test than the conventional single cycle symmetrically loaded test may be when the load is applied in increasing increments, the test beam being unloaded after each increment of loading, until failure occurs.

Finally, these tests show that a re-loading technique of the type used in these exploratory tests does provide results of value. By judiciously locating the web reinforcement, the value of the results obtained can be increased; for example, had the region between the load points in the first static test on E.16 and E.18 been more heavily reinforced with stirrups, the failure in the re-load test would have been forced into the shorter 4'-0" shear span, thereby giving two failures in the same length of shear span from one test beam (as was obtained for E.17). Furthermore, employing such a procedure in no way jeopardizes the results of the first test.

5. SUMMARY AND CONCLUSIONS

The following summarization and conclusions may be drawn from the E Series test beams and from the general discussion of the overload behavior of prestressed beams presented herein. While the concrete strengths of the E Series tests varied between 6580 psi and 7790 psi., the good correlation of these tests with other investigations covering a wider range of concrete strengths indicate that the conclusions presented may be considered valid for concrete strengths greater than 5000 psi.

1. Flexural cracking was observed at loads corresponding to computed tensile stresses in the extreme fiber in tension greater than:

$$f'_t = 6.5 \sqrt{f'_c} \tag{6}$$

The shear causing the development of significant inclined flexure shear cracking was greater than, although realistically predicted as, the shear expected to cause a flexure crack, based on Eq. (6), to form a distance from the section being considered in the direction of decreasing moment equal to the effective depth of the member.

2. The shear causing the development of inclined diagonal tension cracking was realistically predicted as the shear causing a principal tensile stress at the intersection of the path of the crack and the bending neutral axis of:

$$\sigma_t^{cg} = (8 - \frac{M}{Vd}) \sqrt{f'_c} \tag{8}$$

where M is the maximum moment in the shear span being investigated. The path of the crack was assumed to be straight, inclined at the angle of the compressive stress trajectory determined at the bending neutral axis, and to intersect the section being considered at the junction of the web and top flange.

3. Flexural failures occurred at strains in the extreme fiber in compression which varied between 0.0025 and 0.0028.

4. Of the seven test beams which failed in shear, five failed due to crushing of concrete in the web (four of which did not have web reinforcement), one failed due to fracture of the web reinforcement, and the other failed in bond in the web reinforcement.

5. For regions in which inclined diagonal tension cracking is critical, the test results indicated that the TRPC equation for design of web reinforcement:

$$A_v = \frac{1}{2} \frac{(V_u - V_c)s}{f_y jd}$$

was conservative by a factor of roughly 3.

6. An equation for design of web reinforcement of the form:

$$A_v = \frac{(V_u - V_c)s}{f_y \beta d} \tag{1}$$

where β is calculated from:

$$\beta = \frac{\ell_e}{(\tan \theta)\, d} \quad \text{for diagonal tension cracking} \tag{2}$$

or $\beta = 1$ for flexure shear cracking

and V_c = shear at inclined cracking determined from paragraph 1 or 2

would have conservatively predicted, by a factor of approximately 1.5, the amount of web reinforcement required to prevent shear failures in the tests reported herein.

7. A prestressed beam subjected to an overload of sufficient magnitude to develop diagonal tension inclined cracking may be more critical in fatigue of the web reinforcement than in fatigue of the longitudinal prestressing strand. A criteria for determining if the member is critical in fatigue after inclined cracking is the linearity of the load deflection curve. That is, if the repeated loadings are in a range such that the deflection of the member remains essentially linear, the probability of a fatigue failure within the normal life of the member is low.

8. By properly designing the web reinforcement in a test beam, in general more than one ultimate strength shear test can be obtained from each beam specimen.

6. APPENDIX I

STATE OF CRACKING AT THE TIME OF INCLINED CRACKING

Note: Explanation of the figures in Appendix I is presented on page 22.

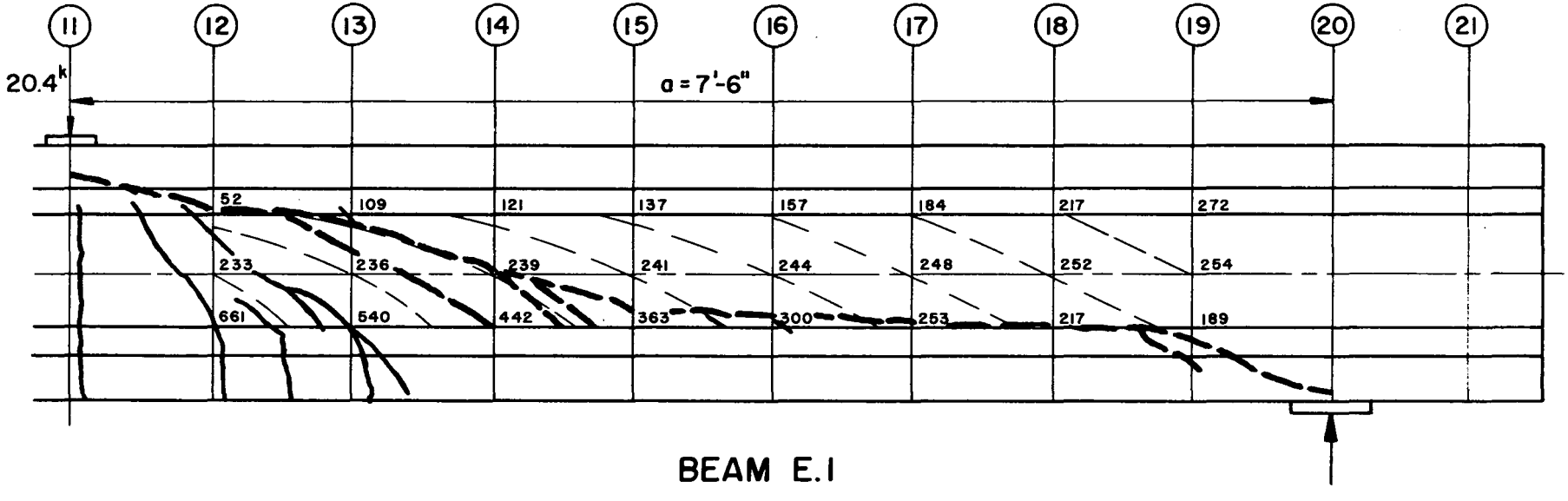
11
12
13
14
15
16
17
18
19
20
21
20.4k
a = 7'-6"
52
109
121
137
157
184
217
272
233
236
239
241
244
248
252
254
661
540
442
363
300
253
217
189

BEAM E.1

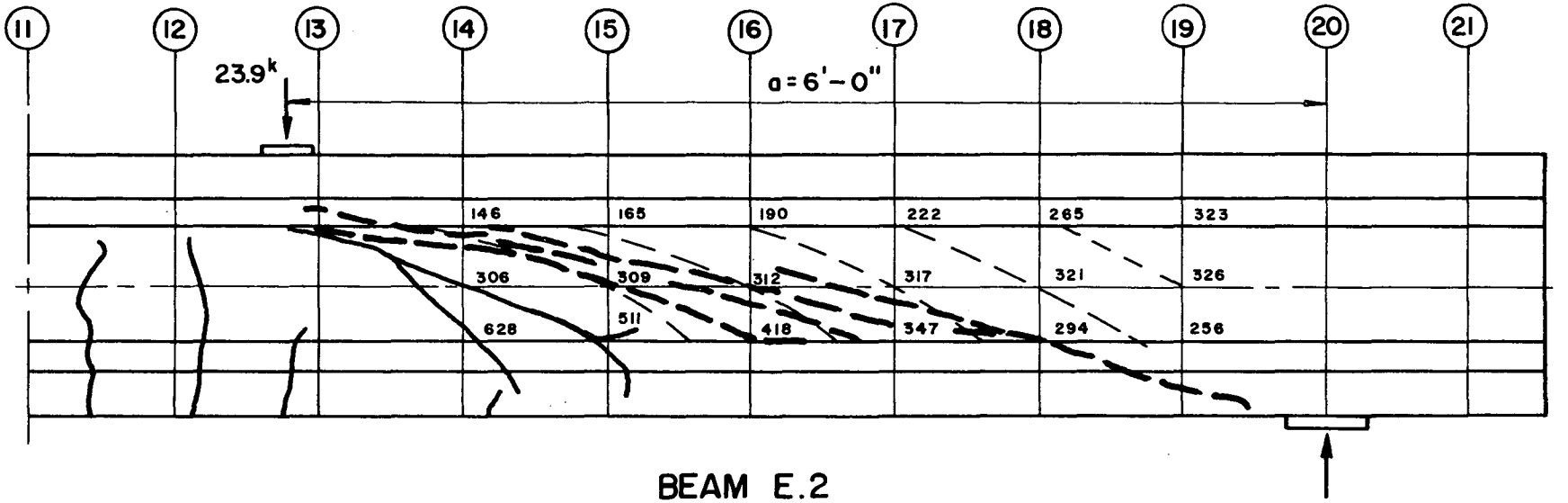
11
12
13
14
15
16
17
18
19
20
21
23.9k
a = 6'-0"
146
165
190
222
265
323
306
309
312
317
321
326
628
511
418
347
294
256

BEAM E.2

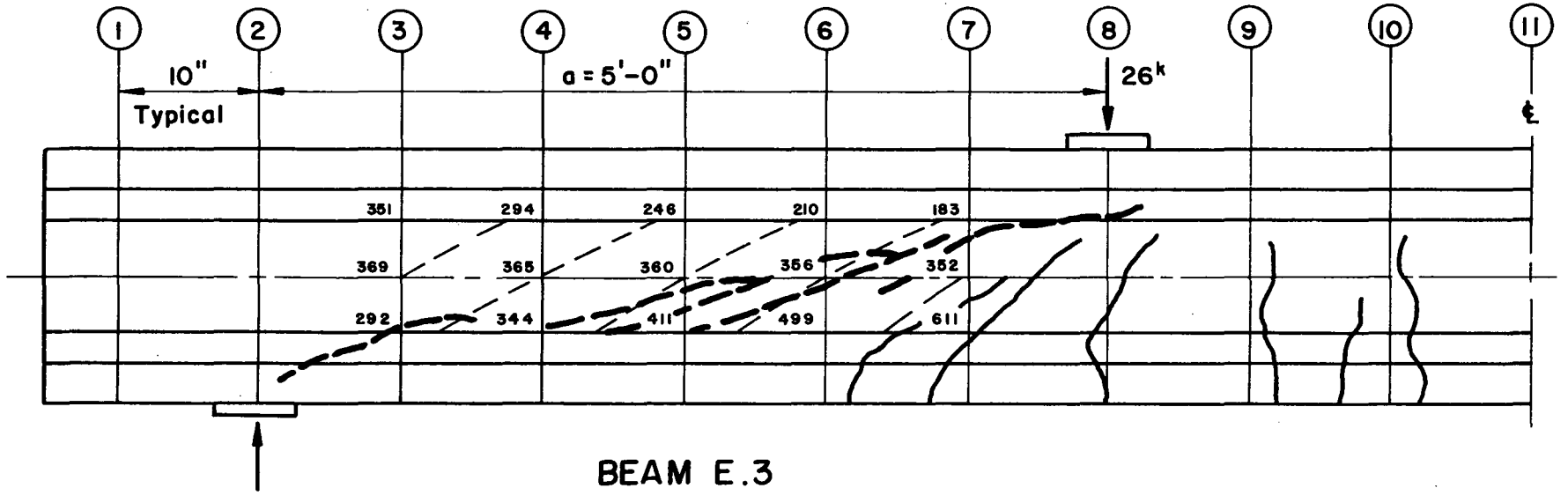
1
2
3
4
5
6
7
8
9
10
11
10"
Typical
a = 5'-0"
26k
℄
351
294
246
210
183
369
365
360
356
352
292
344
411
499
611

BEAM E.3

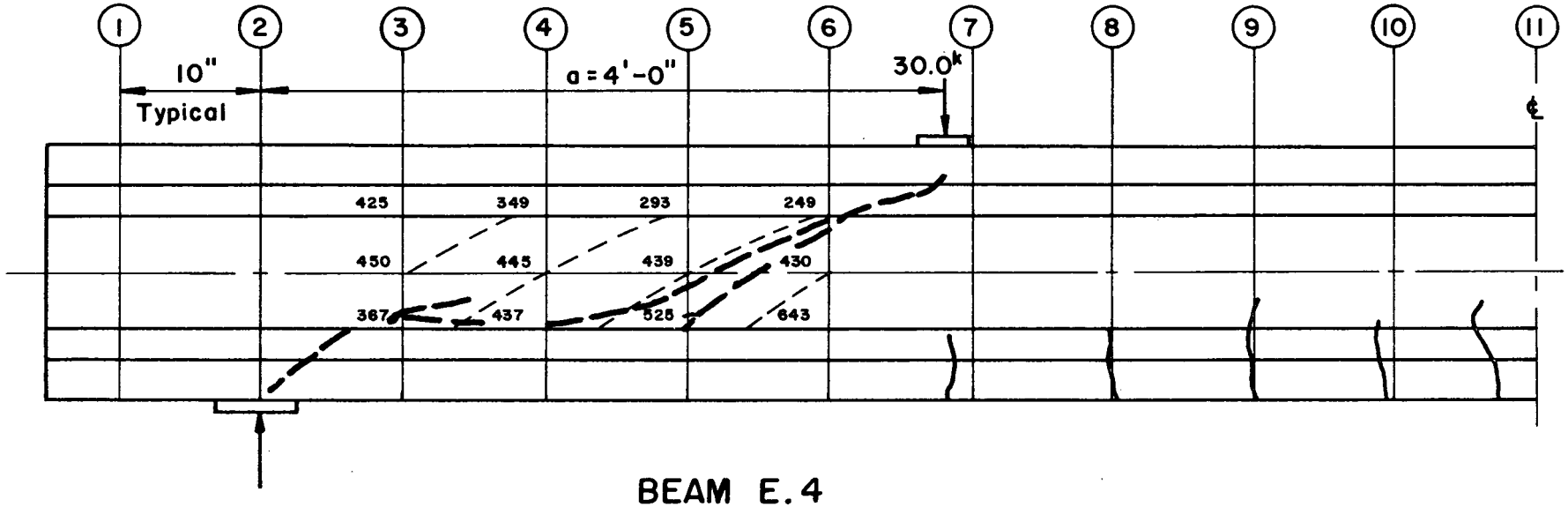
1
2
3
4
5
6
7
8
9
10
11
10"
Typical
a = 4'-0"
30.0k
℄
425
349
293
249
450
445
439
430
367
437
525
643

BEAM E.4

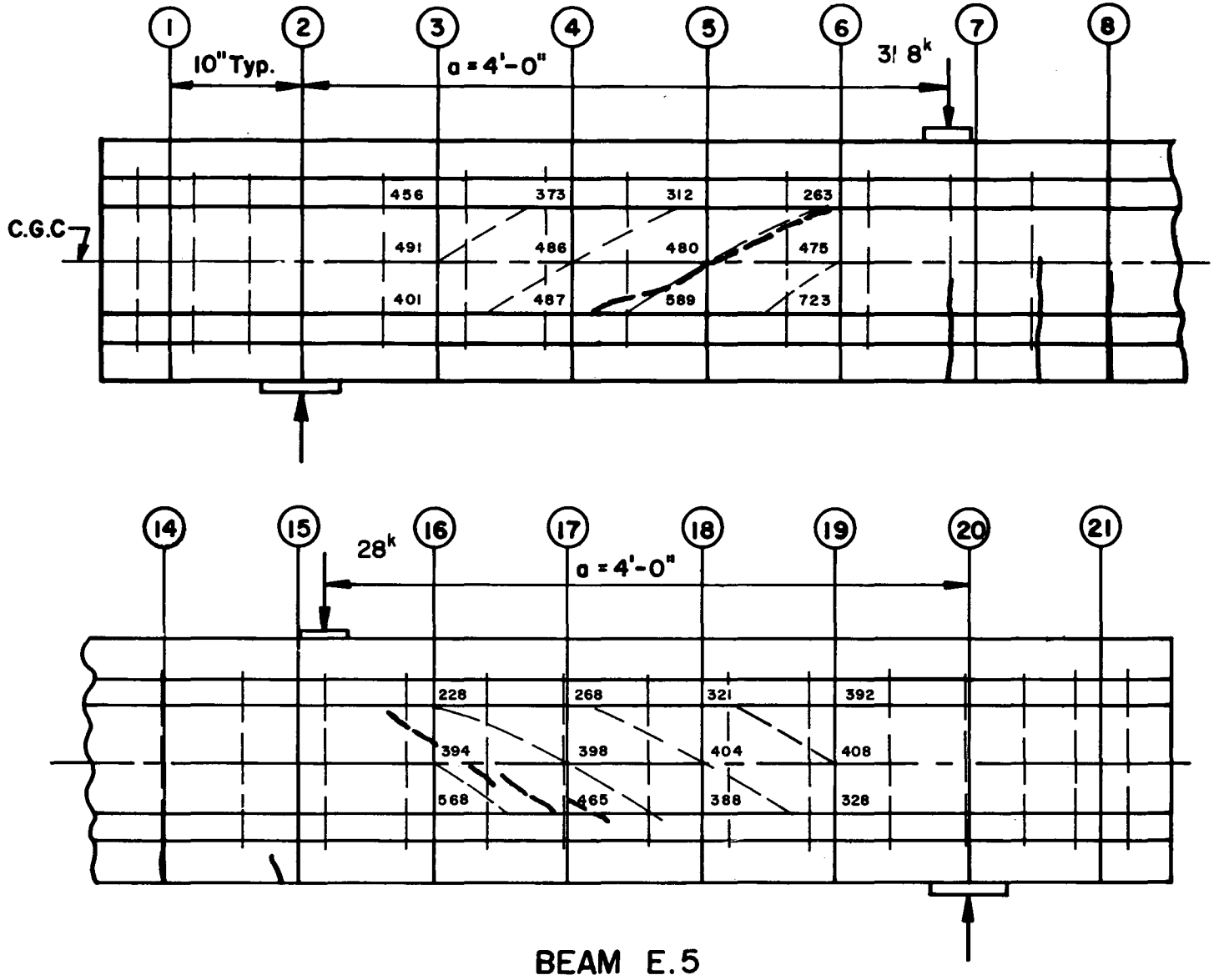
1
2
3
4
5
6
7
8
10"Typ.
a = 4'-0"
31 8k
C.G.C
456
373
312
263
491
486
480
475
401
487
589
723
14
15
16
17
18
19
20
21
28k
a = 4'-0"
228
268
321
392
394
398
404
408
568
465
388
328

BEAM E.5

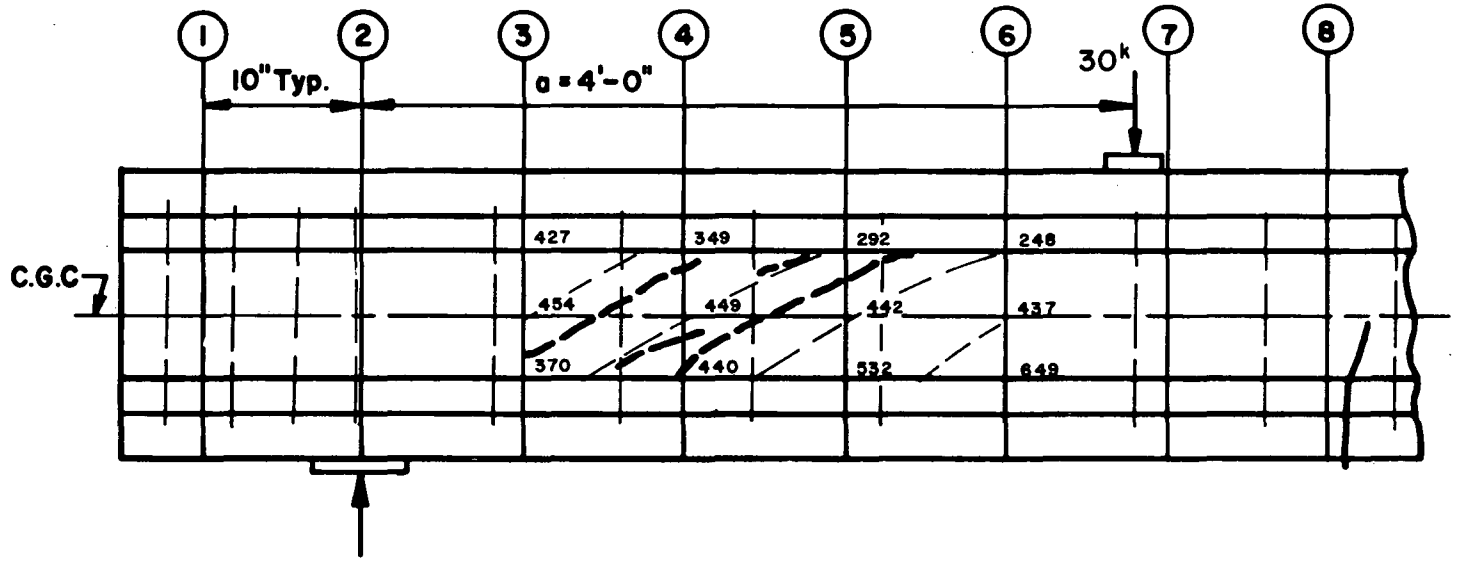
1
2
3
4
5
6
7
8
10" Typ.
a = 4'-0"
30k
C.G.C
427
349
292
248
454
449
442
437
370
440
532
649

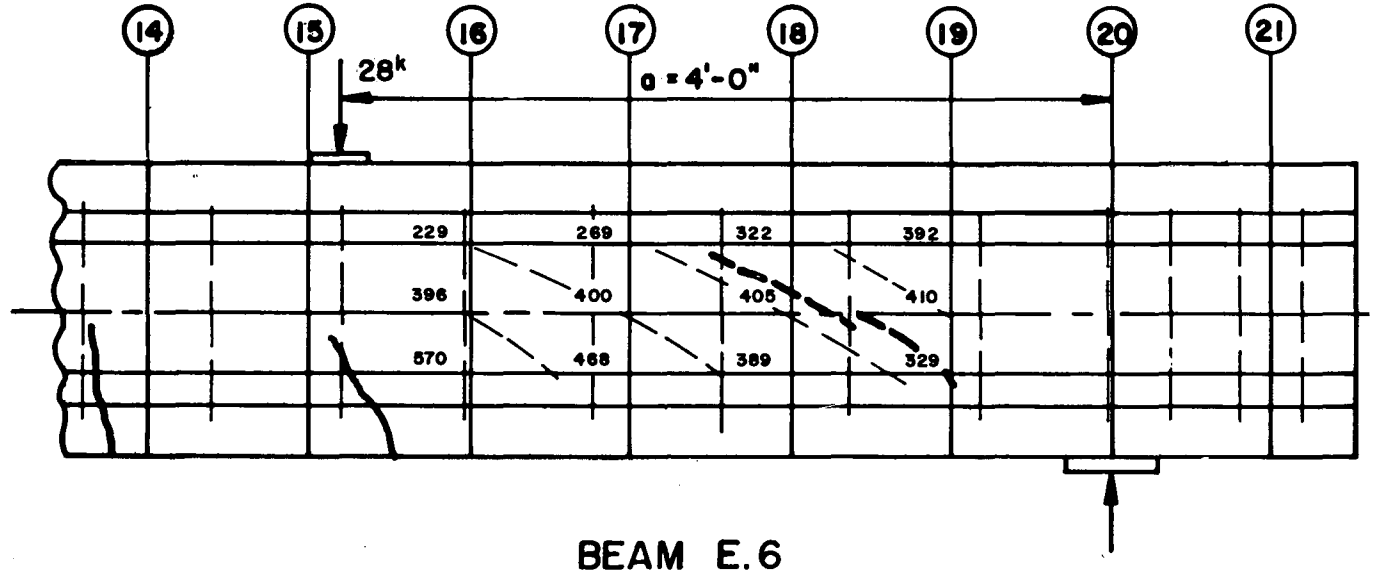
14
15
16
17
18
19
20
21
28k
a = 4'-0"
229
269
322
392
396
400
405
410
570
468
389
329

BEAM E.6

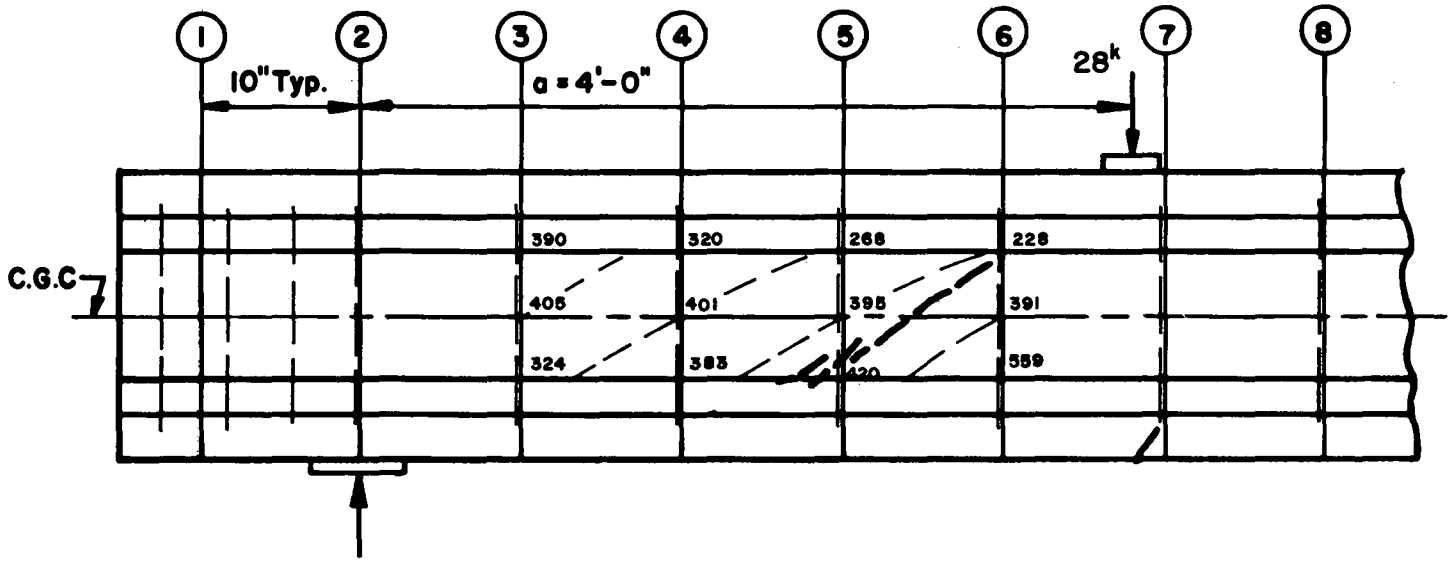
1
2
3
4
5
6
7
8
10"Typ.
a = 4'-0"
28k
C.G.C
390
320
268
228
405
401
395
391
324
383
420
559

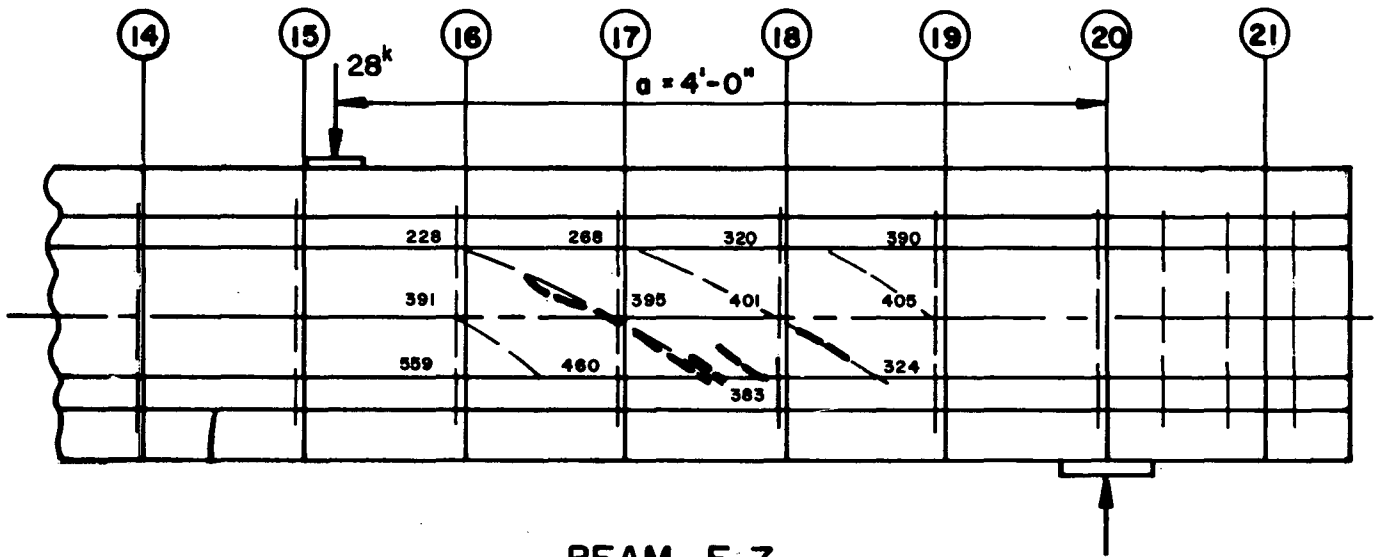
14
15
16
17
18
19
20
21
28k
a = 4'-0"
228
268
320
390
391
395
401
405
559
460
324
383

BEAM E.7

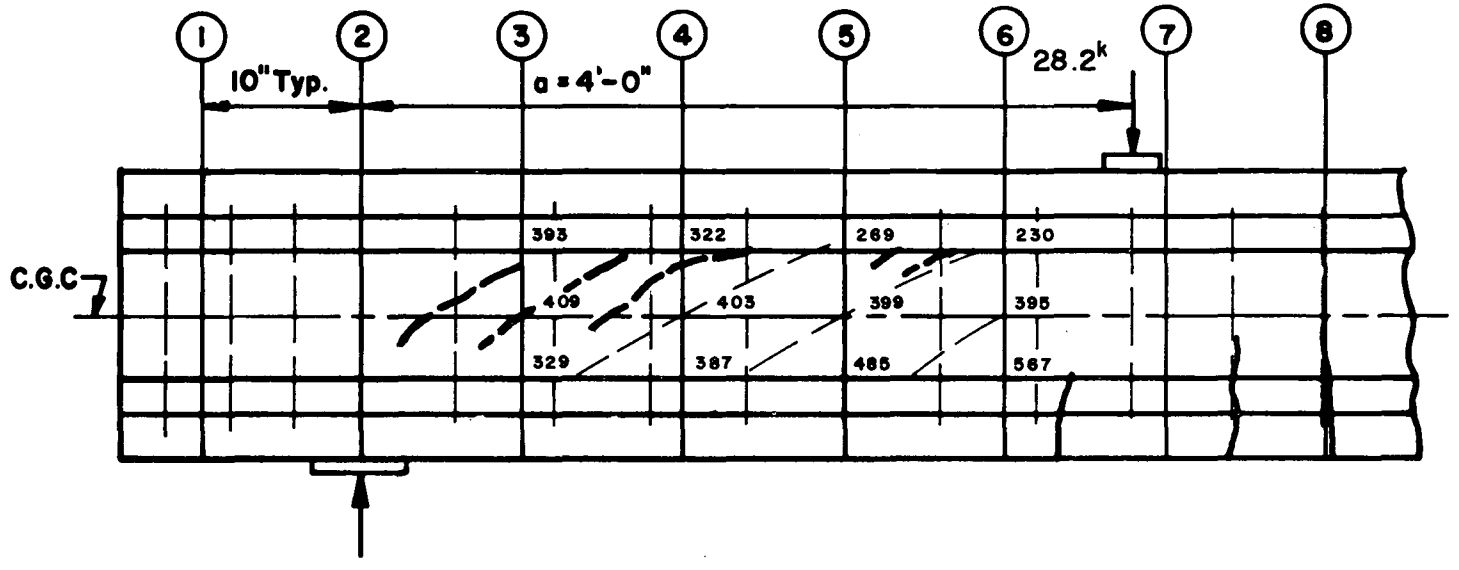
1
2
3
4
5
6
7
8
10" Typ.
a = 4'-0"
28.2k
C.G.C
393
322
269
230
409
403
399
395
329
387
485
567

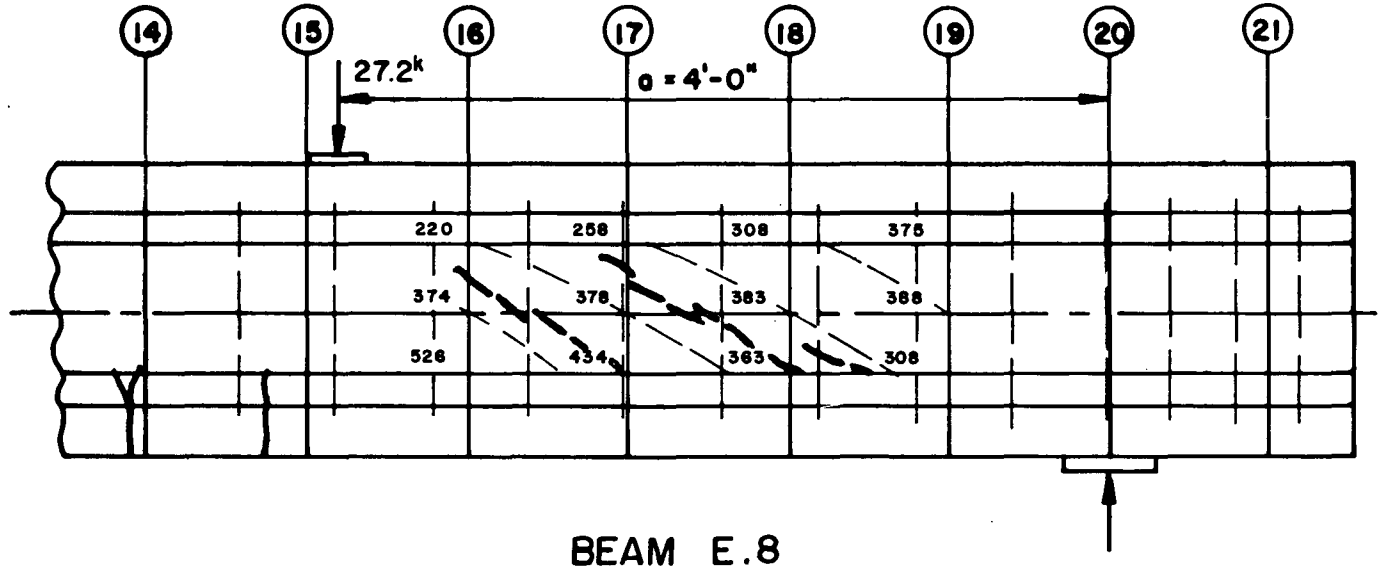
14
15
16
17
18
19
20
21
27.2k
a = 4'-0"
220
258
308
375
374
378
383
388
526
434
363
308

BEAM E.8

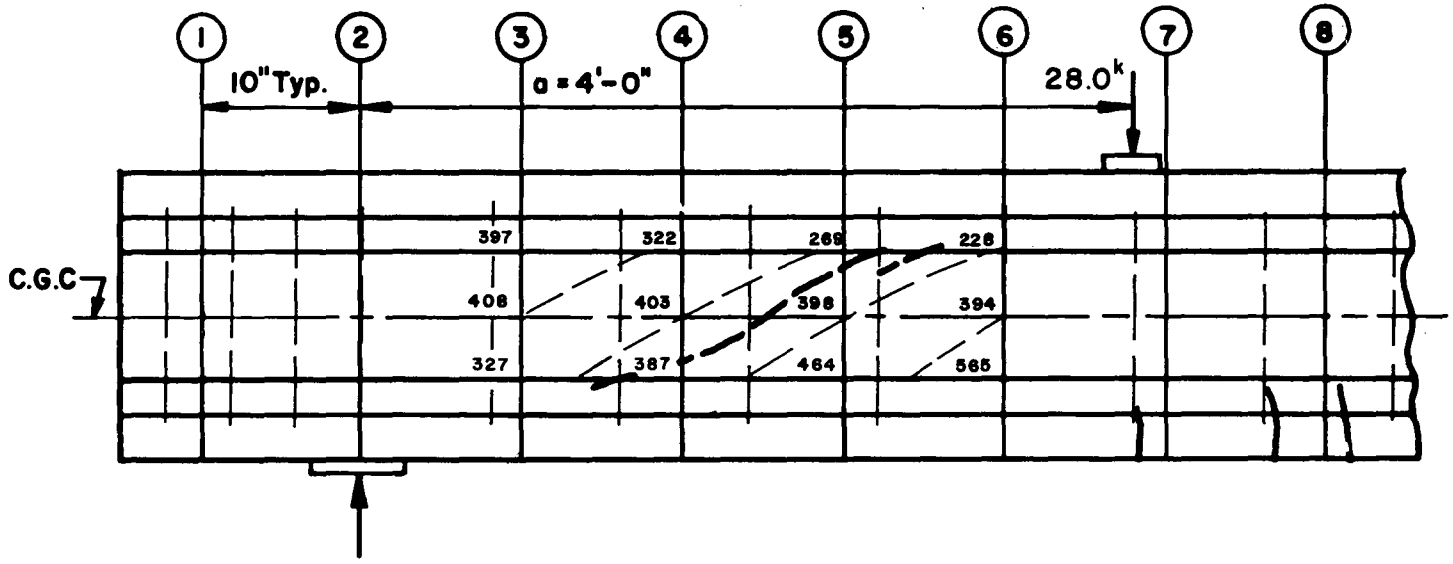
1
2
3
4
5
6
7
8
10"Typ.
a = 4'-0"
28.0k
C.G.C
397
322
269
228
408
403
398
394
327
387
464
565

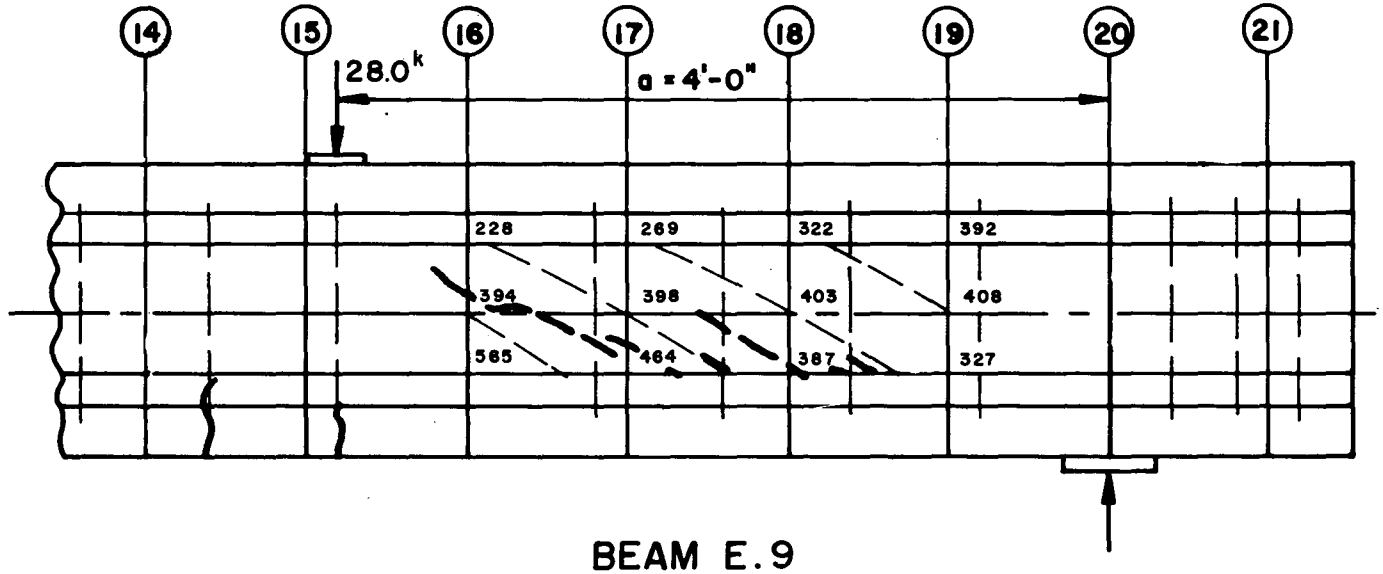
14
15
16
17
18
19
20
21
28.0k
a = 4'-0"
228
269
322
392
394
398
403
408
565
464
387
327

BEAM E.9

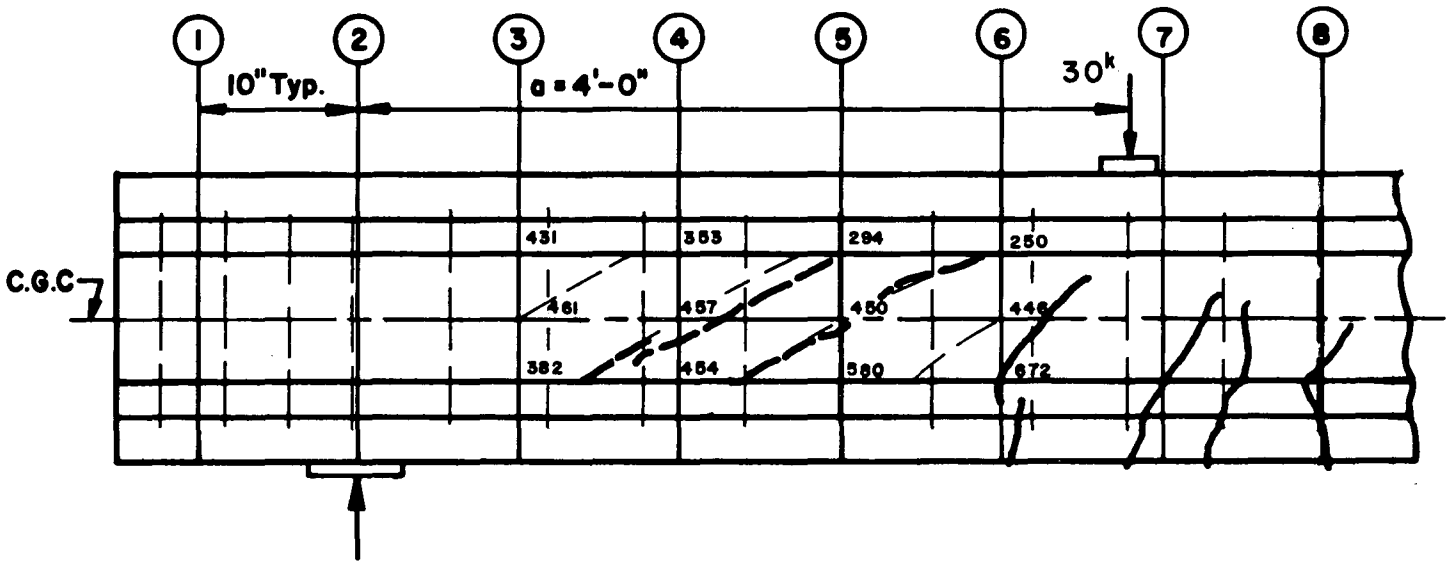
1
2
3
4
5
6
7
8
10" Typ.
a = 4'-0"
30k
C.G.C
431
353
294
250
461
457
450
446
382
454
380
672

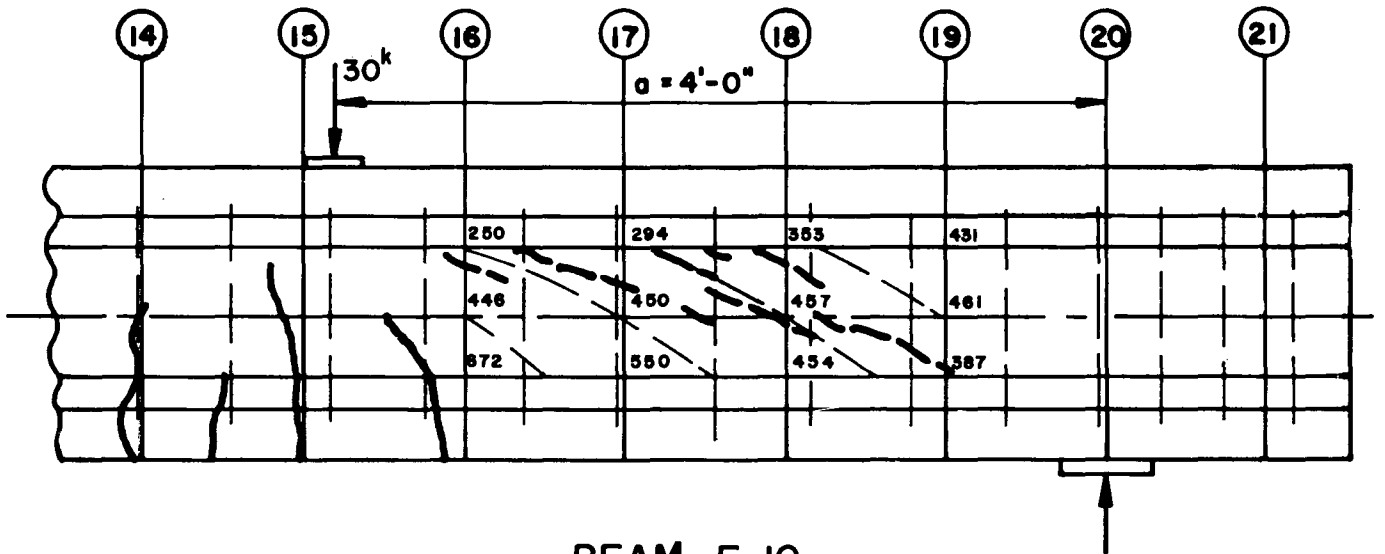
14
15
16
17
18
19
20
21
30k
a = 4'-0"
250
294
353
431
446
450
457
461
372
550
454
387

BEAM E.10

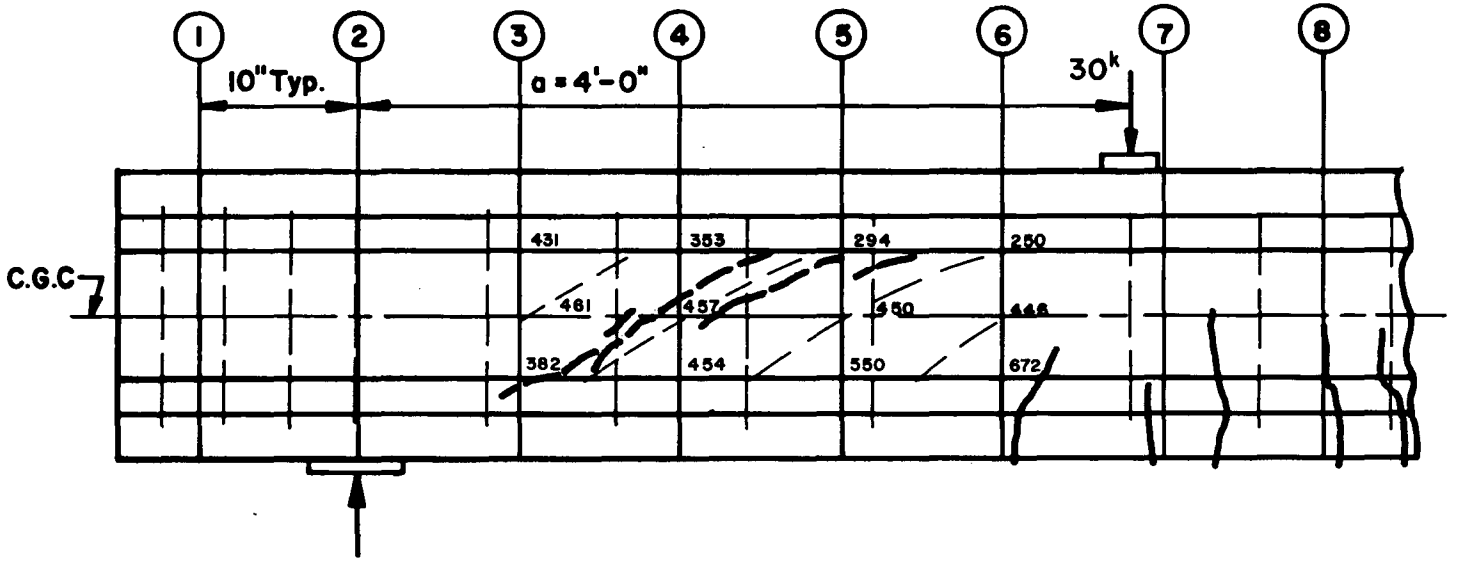
1
2
3
4
5
6
7
8
10"Typ.
a = 4'-0"
30k
C.G.C
431
383
294
250
461
457
382
454
550
672

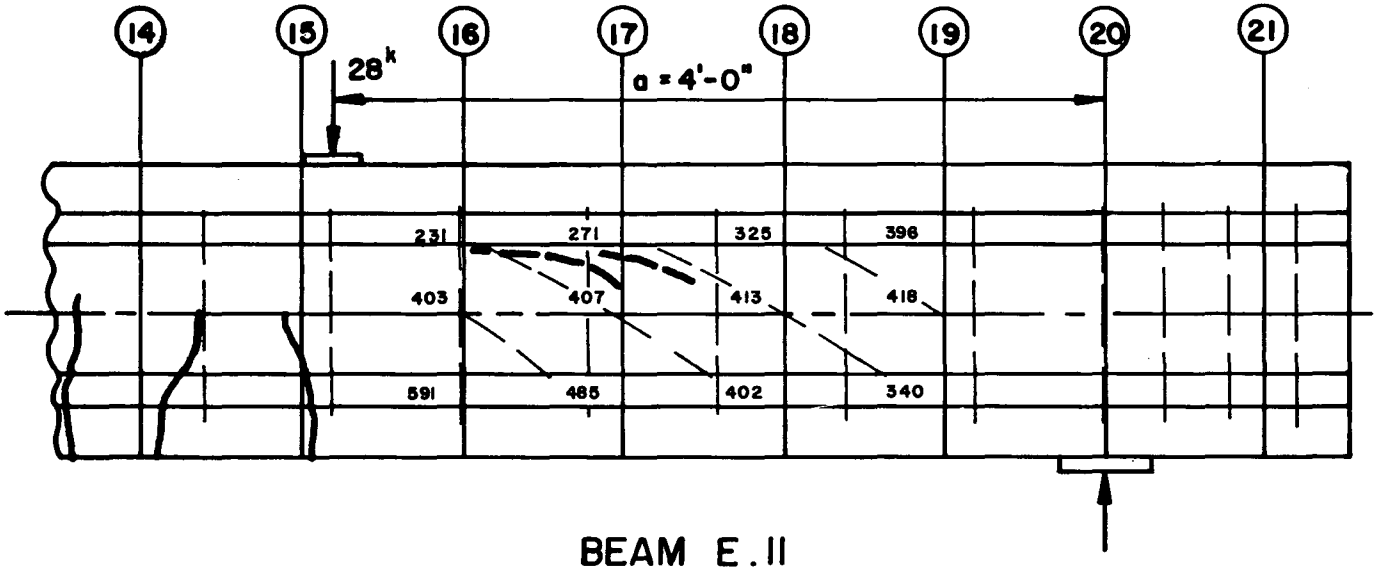
14
15
16
17
18
19
20
21
28k
a = 4'-0"
231
271
325
396
403
407
413
418
591
485
402
340

BEAM E.11

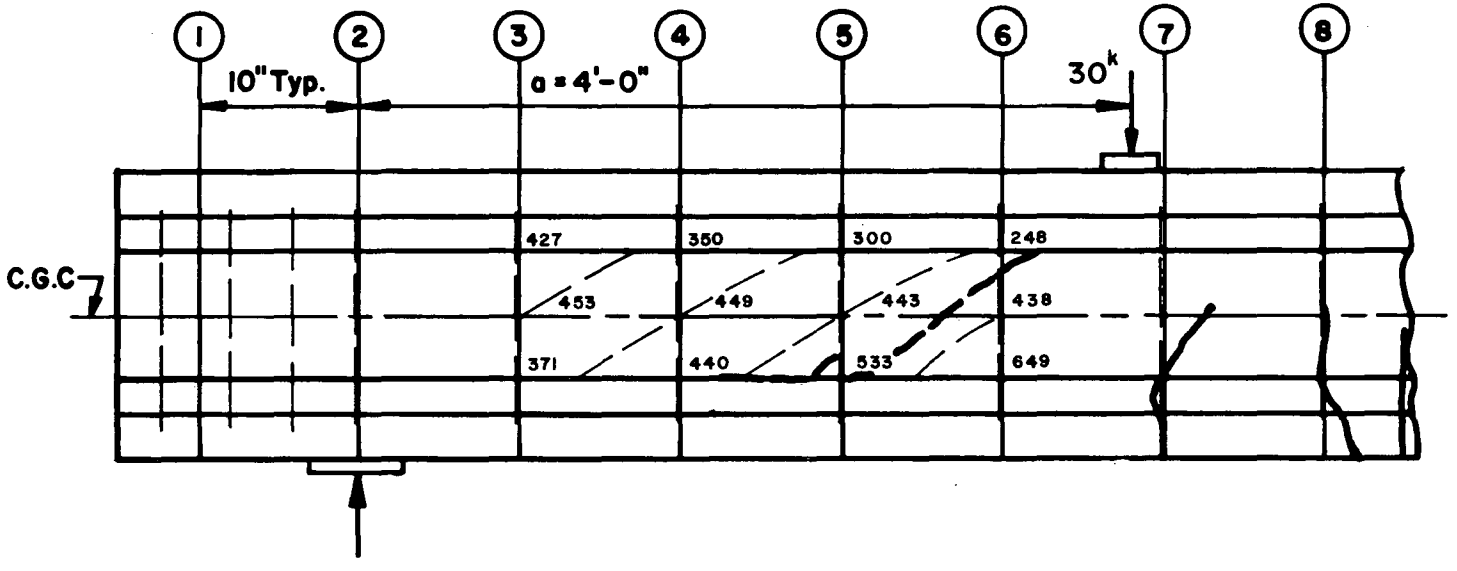
1
2
3
4
5
6
7
8
10" Typ.
a = 4'-0"
30k
C.G.C
427
350
300
248
453
449
443
438
371
440
533
649

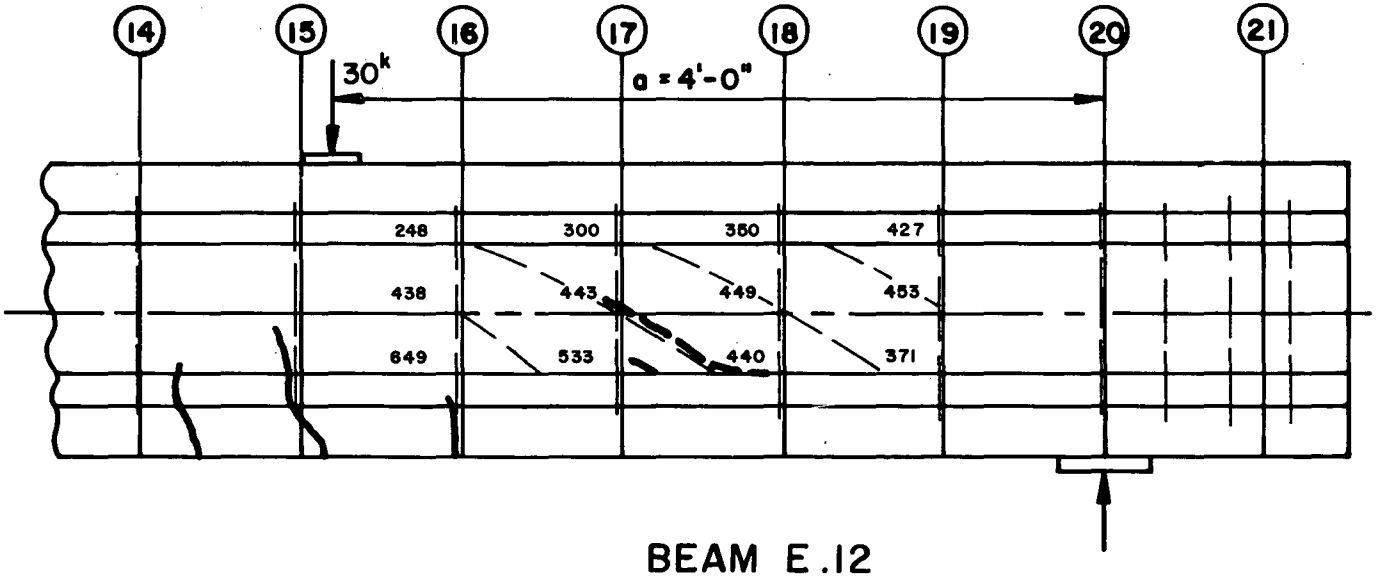
14
15
16
17
18
19
20
21
30k
a = 4'-0"
248
300
350
427
438
443
449
453
649
533
440
371

BEAM E.12

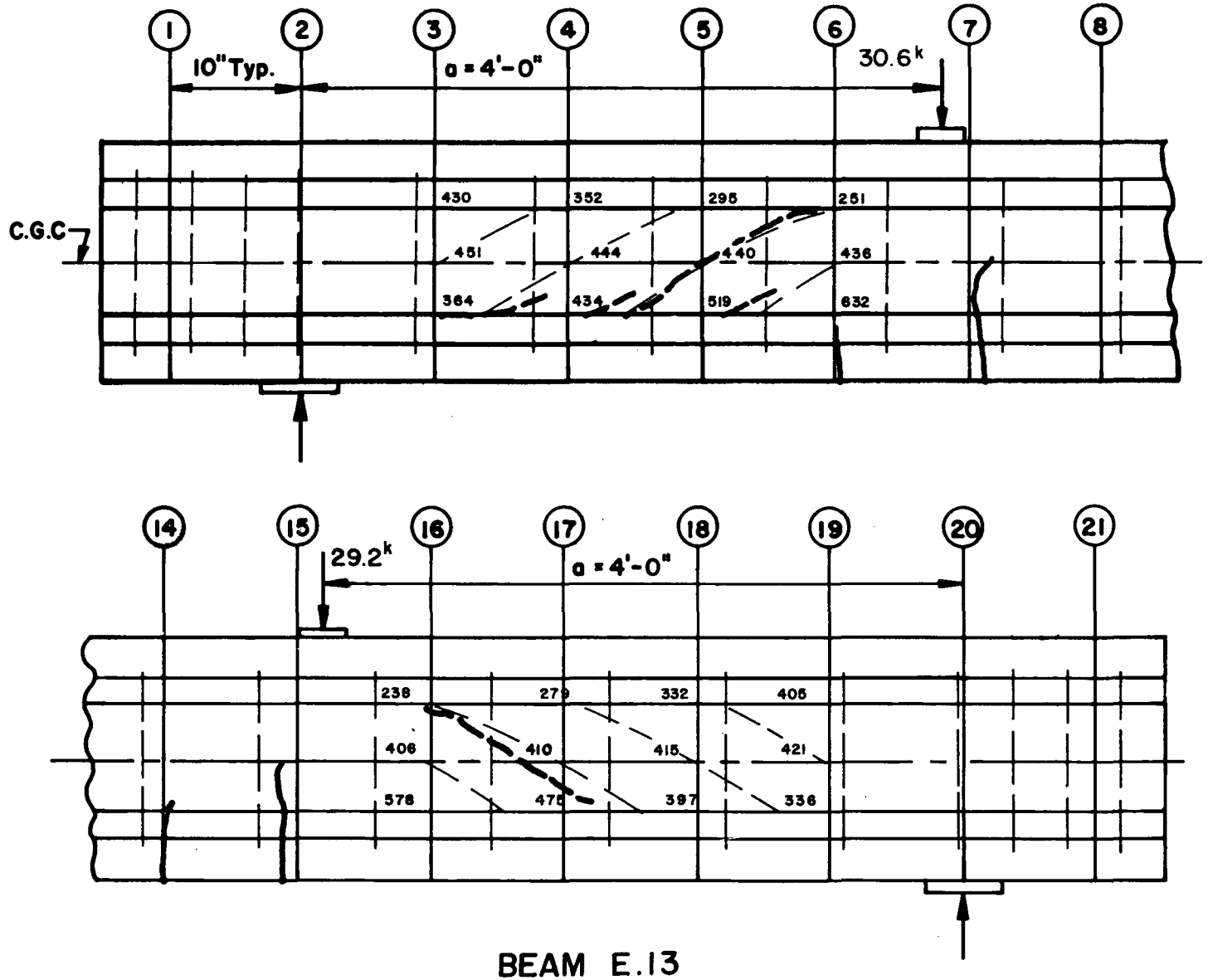
1
2
3
4
5
6
7
8
10" Typ.
a = 4'-0"
30.6k
C.G.C
430
352
295
251
451
444
440
436
364
434
519
632
14
15
16
17
18
19
20
21
29.2k
a = 4'-0"
238
279
332
406
406
410
415
421
578
475
397
336

BEAM E.13

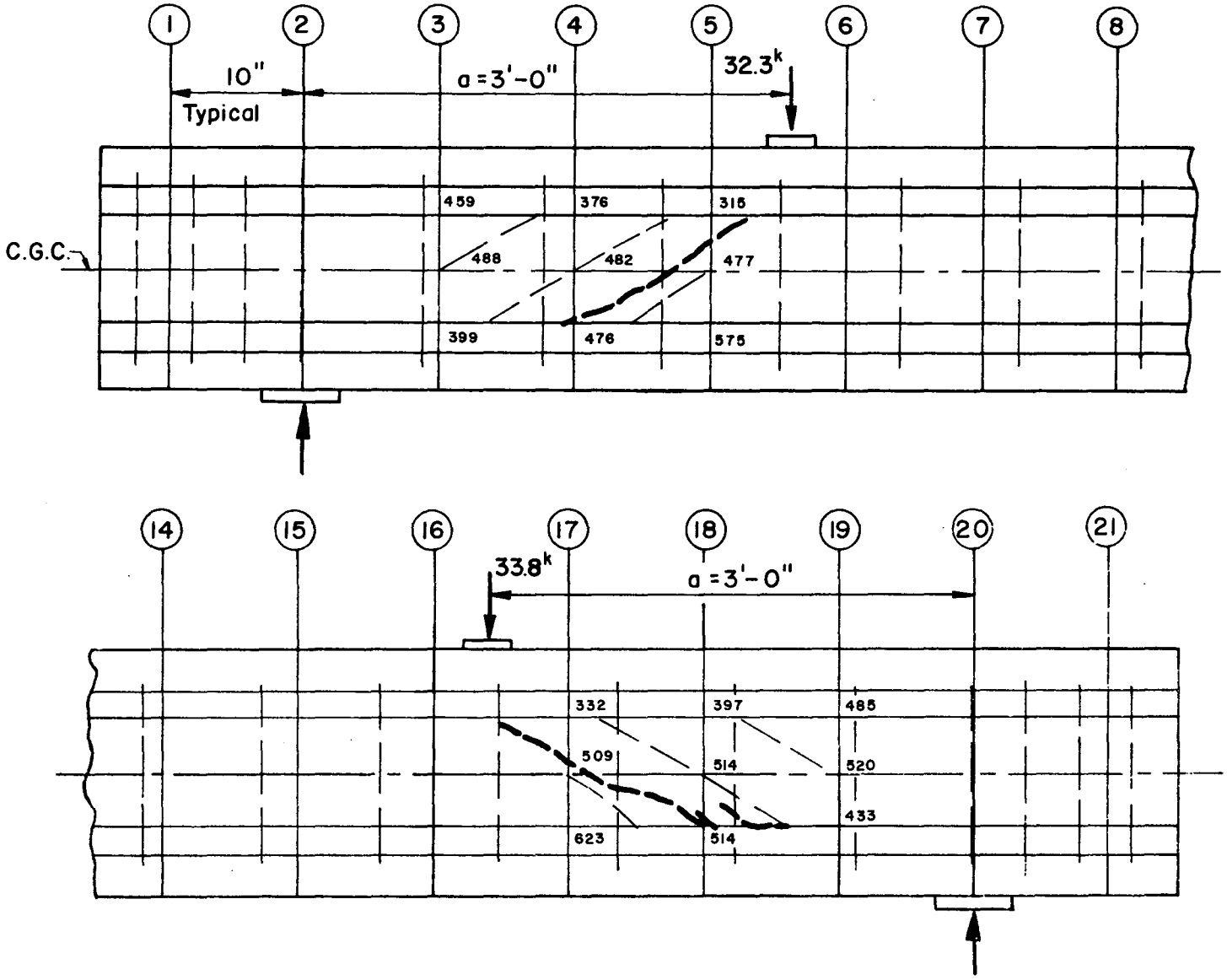
1
2
3
4
5
6
7
8
10"
Typical
a = 3'-0"
32.3k
C.G.C.
459
376
315
488
482
477
399
476
575
14
15
16
17
18
19
20
21
33.8k
a = 3'-0"
332
397
485
509
514
520
433
623
514

BEAM E.14

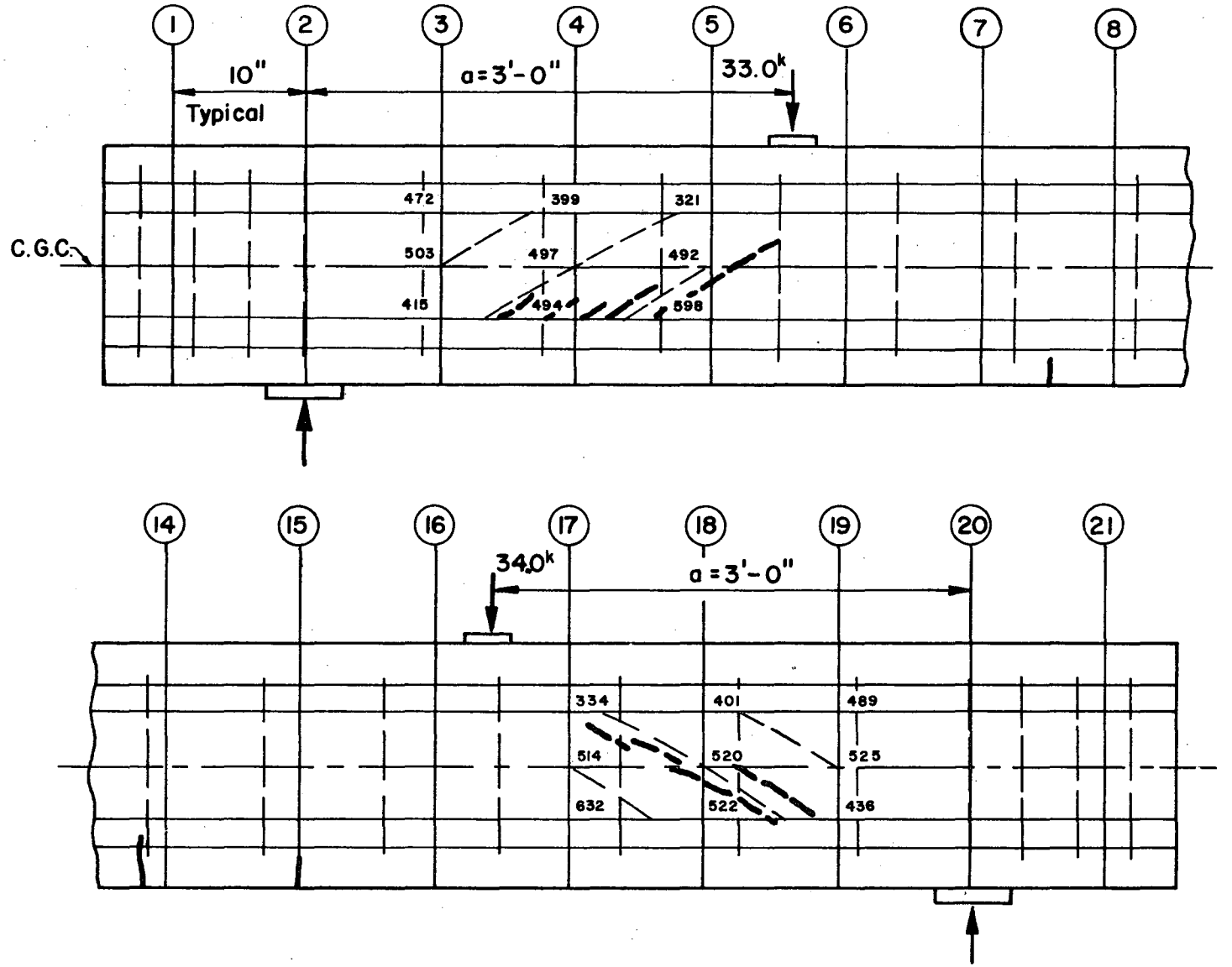
1
2
3
4
5
6
7
8
10"
Typical
a=3'-0"
33.0k
C.G.C.
472
399
321
503
497
492
415
494
598
14
15
16
17
18
19
20
21
34.0k
a=3'-0"
334
401
489
514
520
525
632
522
436

BEAM E.15

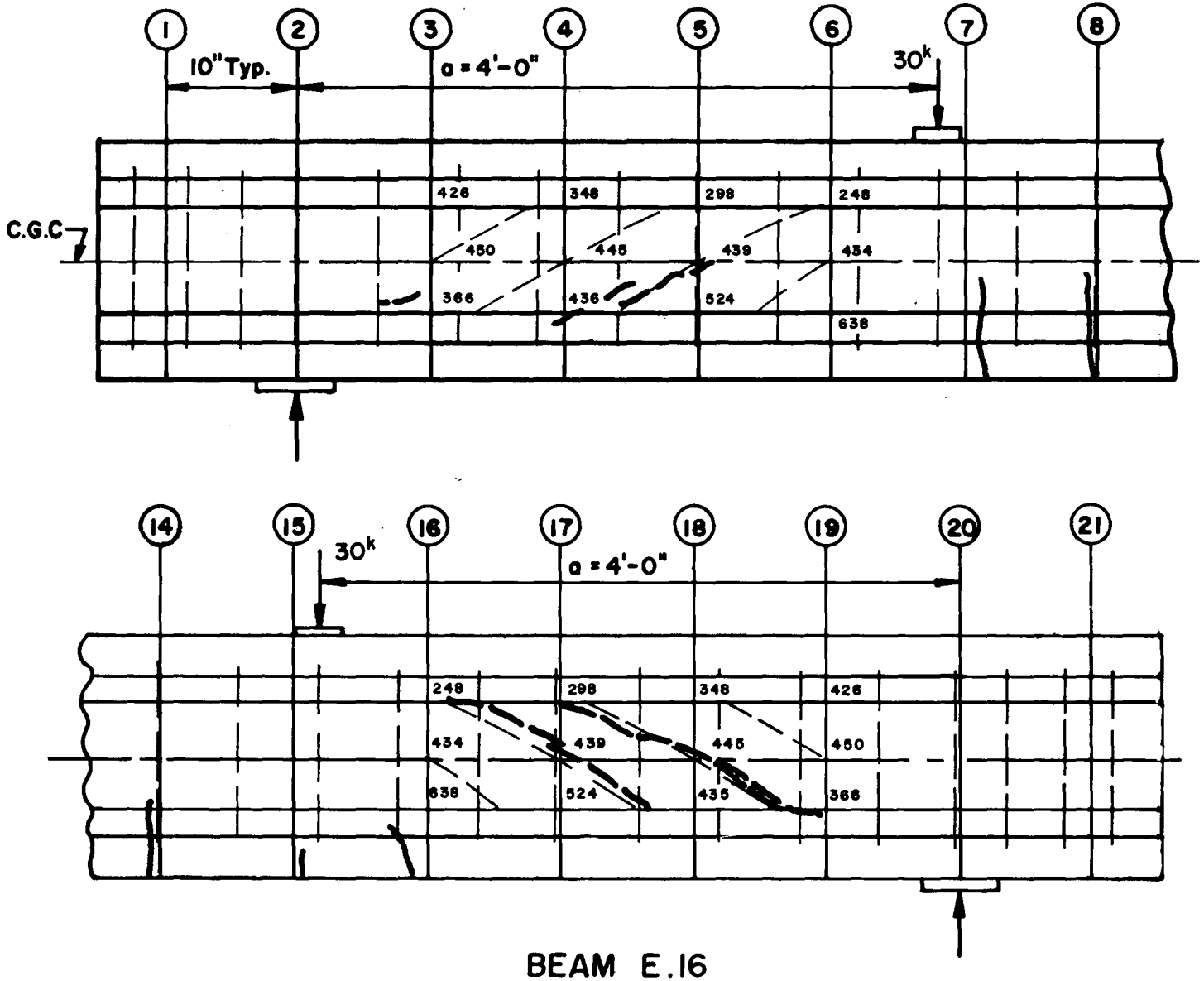
1
2
3
4
5
6
7
8
10"Typ.
a = 4'-0"
30k
C.G.C
426
348
298
248
450
445
439
434
366
436
524
638
14
15
16
17
18
19
20
21
30k
a = 4'-0"
248
298
348
426
434
439
445
450
638
524
435
366

BEAM E.16

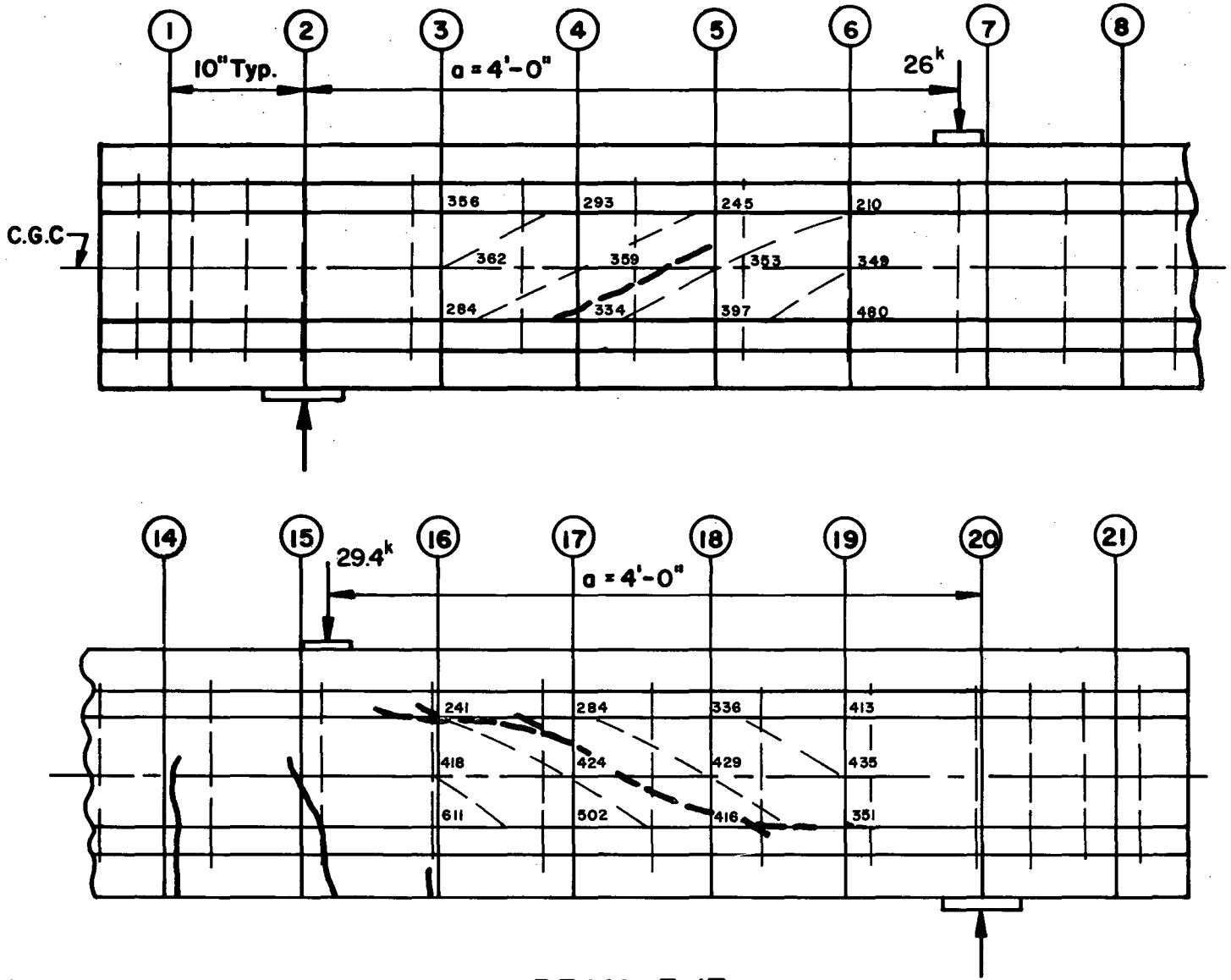
1
2
3
4
5
6
7
8
10" Typ.
a = 4'-0"
26k
C.G.C
356
293
245
210
362
359
353
349
284
334
397
480
14
15
16
17
18
19
20
21
29.4k
a = 4'-0"
241
284
336
413
418
424
429
435
611
502
416
351

BEAM E.17

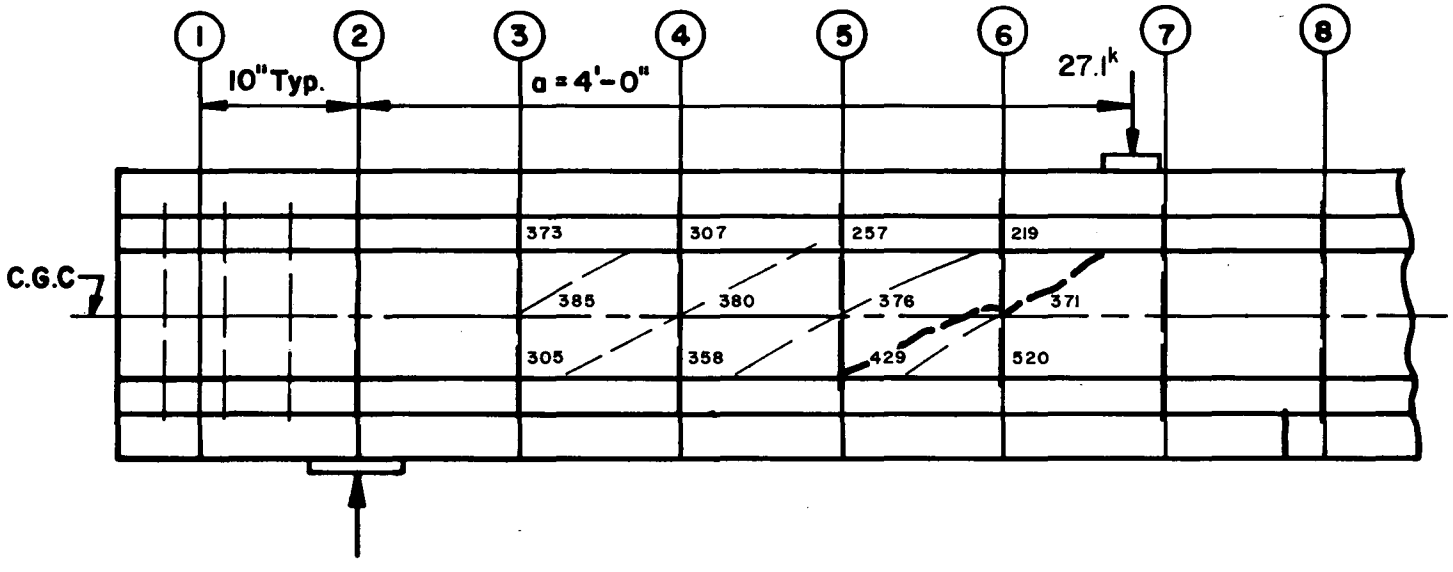
1
2
3
4
5
6
7
8
10" Typ.
a = 4'-0"
27.1k
C.G.C
373
307
257
219
385
380
376
371
305
358
429
520

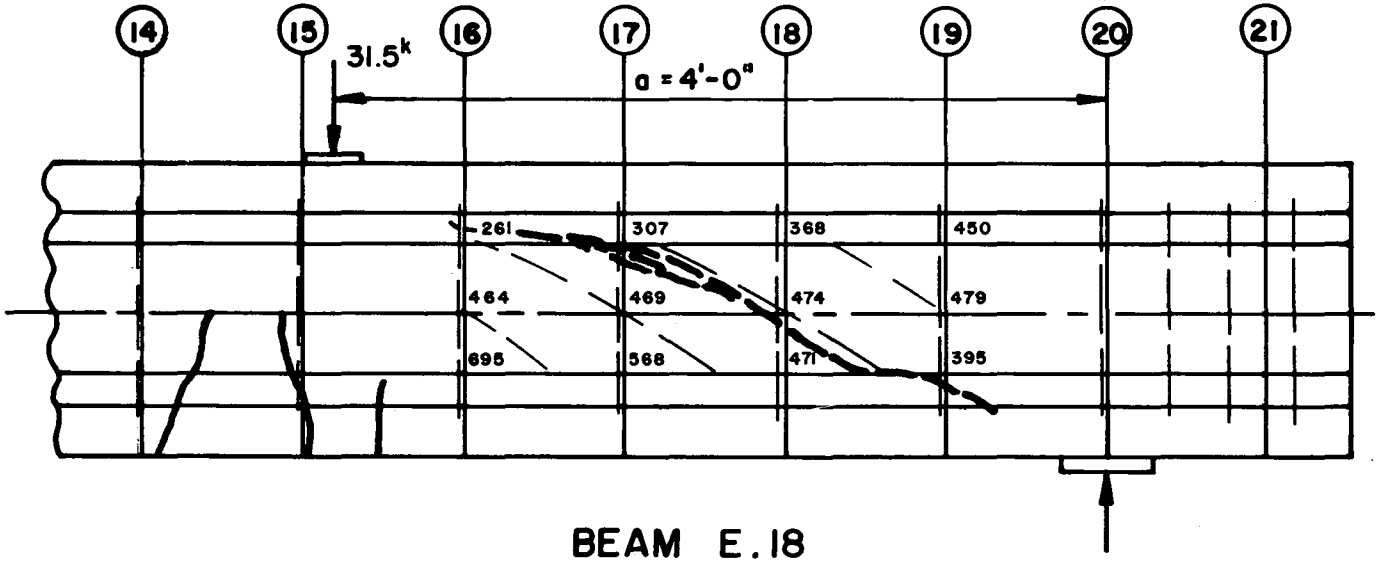
14
15
16
17
18
19
20
21
31.5k
a = 4'-0"
261
307
368
450
464
469
474
479
695
568
471
395

BEAM E.18

7. APPENDIX II

LOAD - DEFLECTION CURVES

FOR THE STATIC TESTS

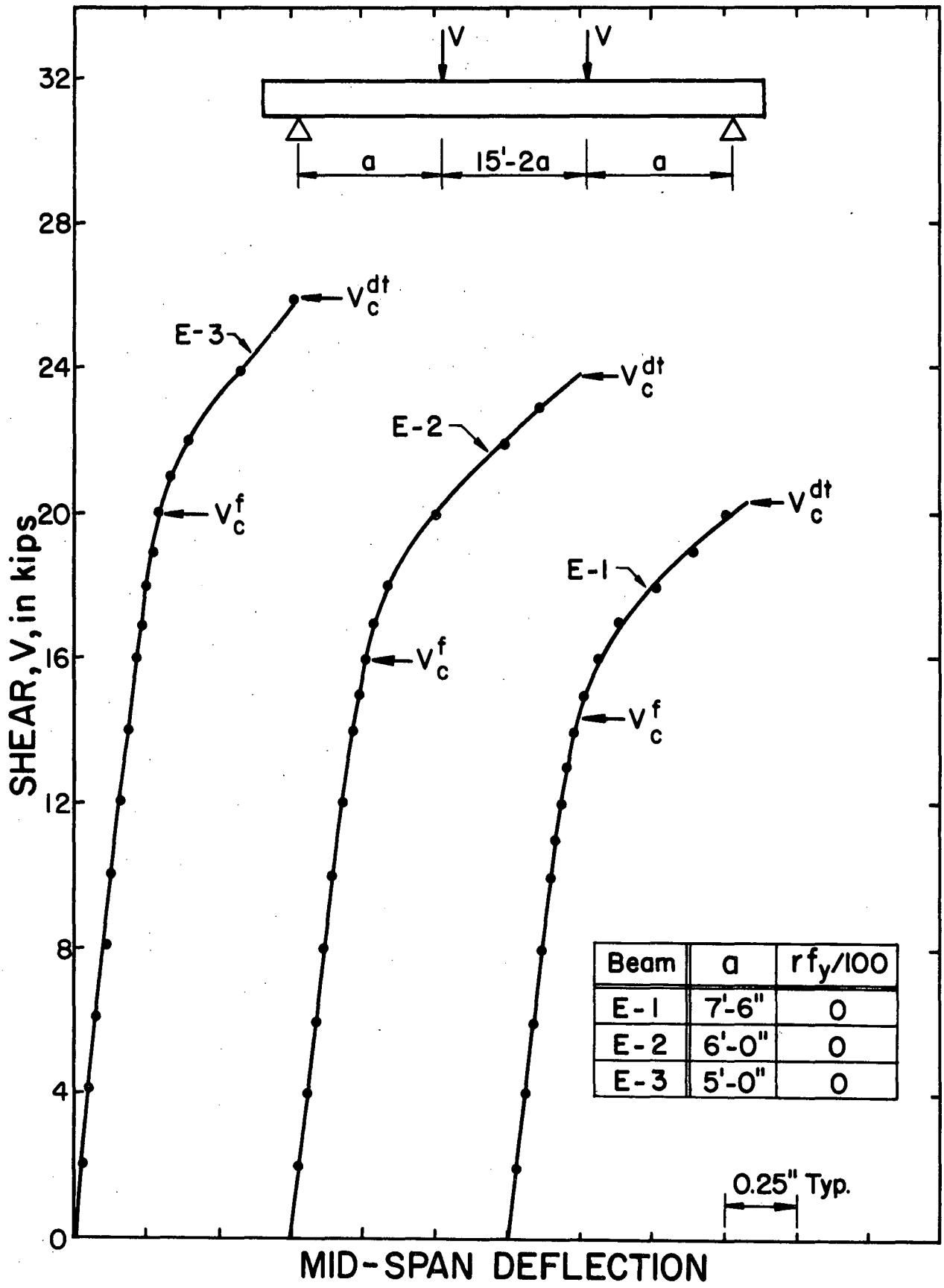

Beam	a	$rf_y/100$
E-1	7'-6"	0
E-2	6'-0"	0
E-3	5'-0"	0

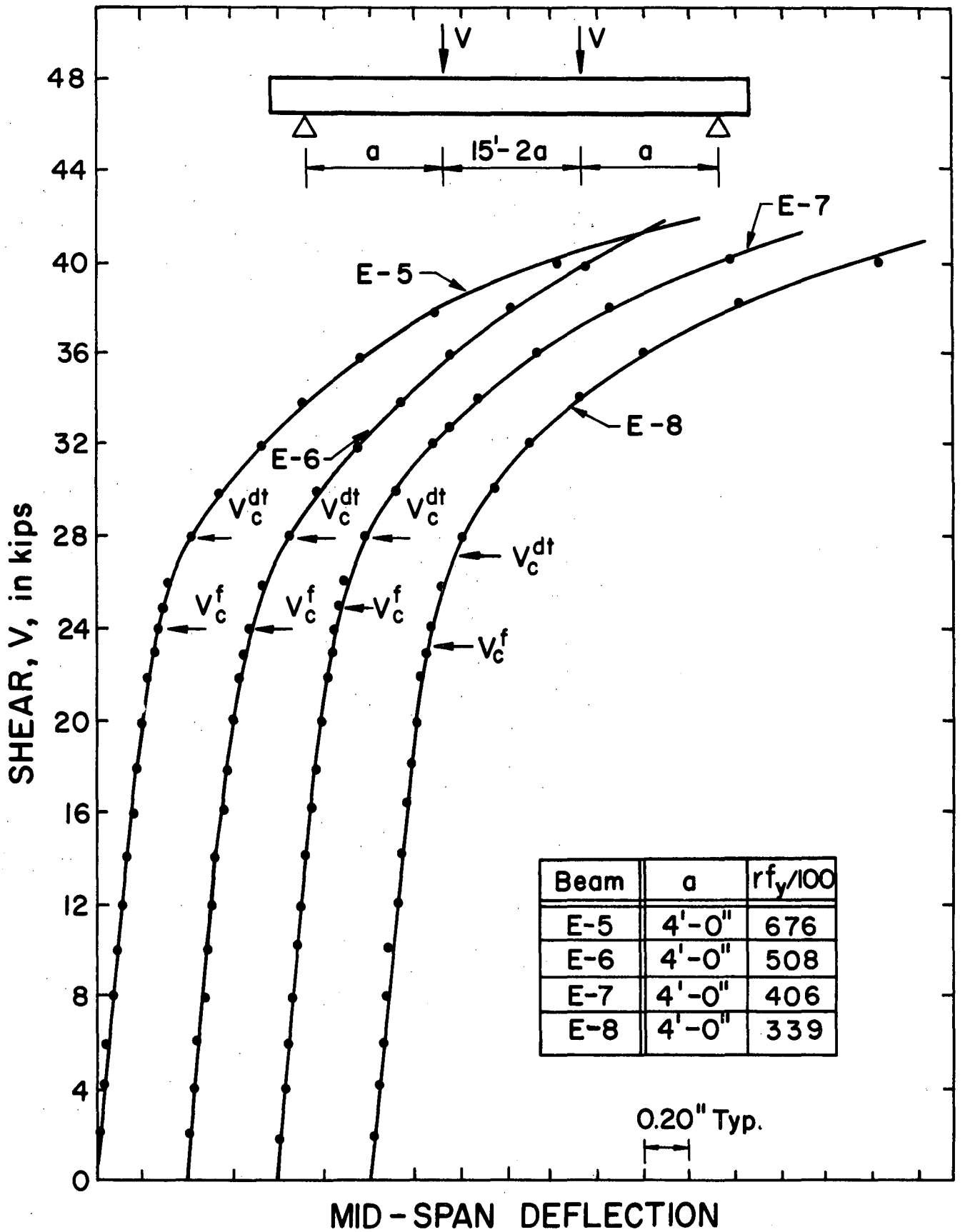

Beam	a	$rf_y/100$
E-5	4'-0"	676
E-6	4'-0"	508
E-7	4'-0"	406
E-8	4'-0"	339

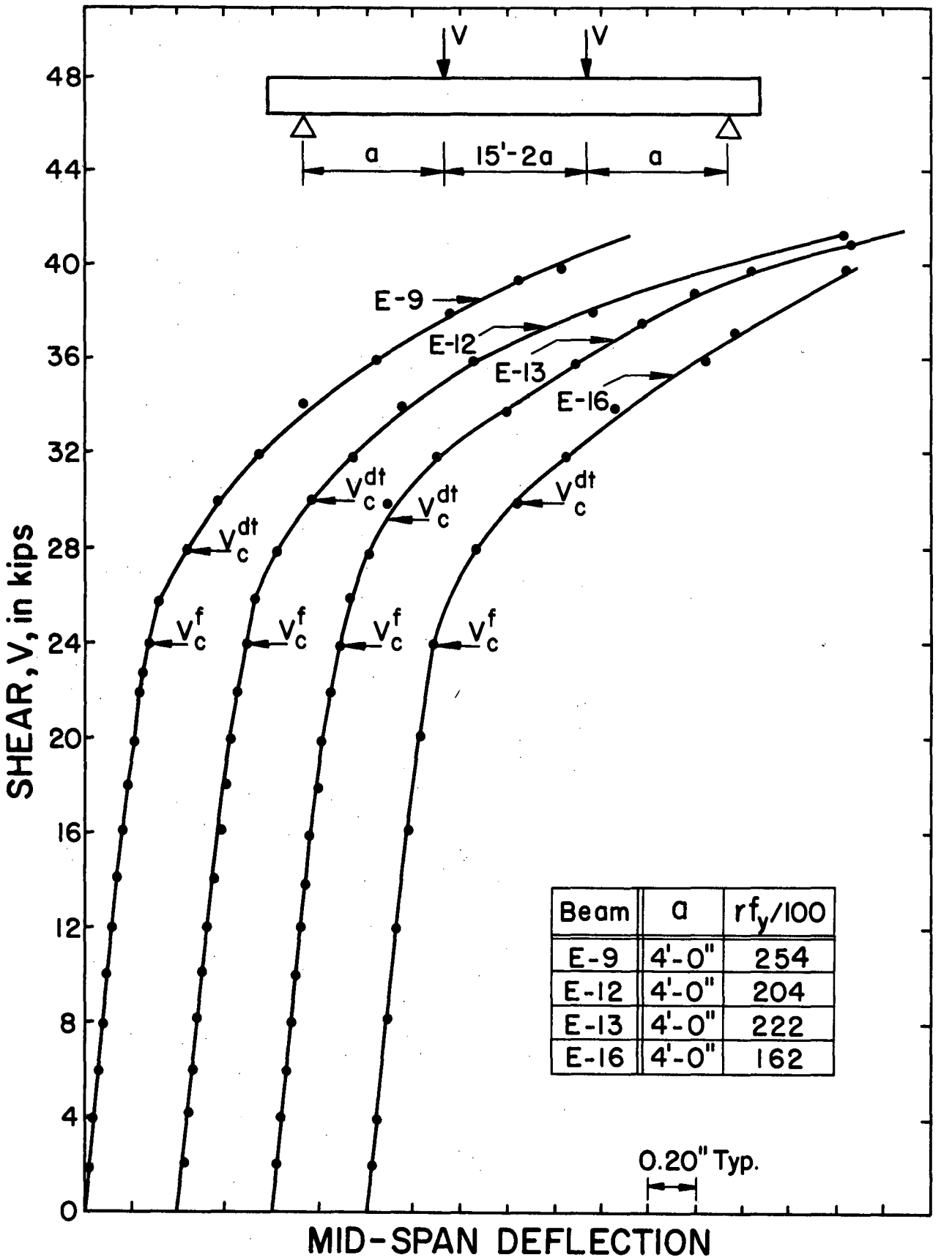

Beam	a	$rf_y/100$
E-9	4'-0"	254
E-12	4'-0"	204
E-13	4'-0"	222
E-16	4'-0"	162

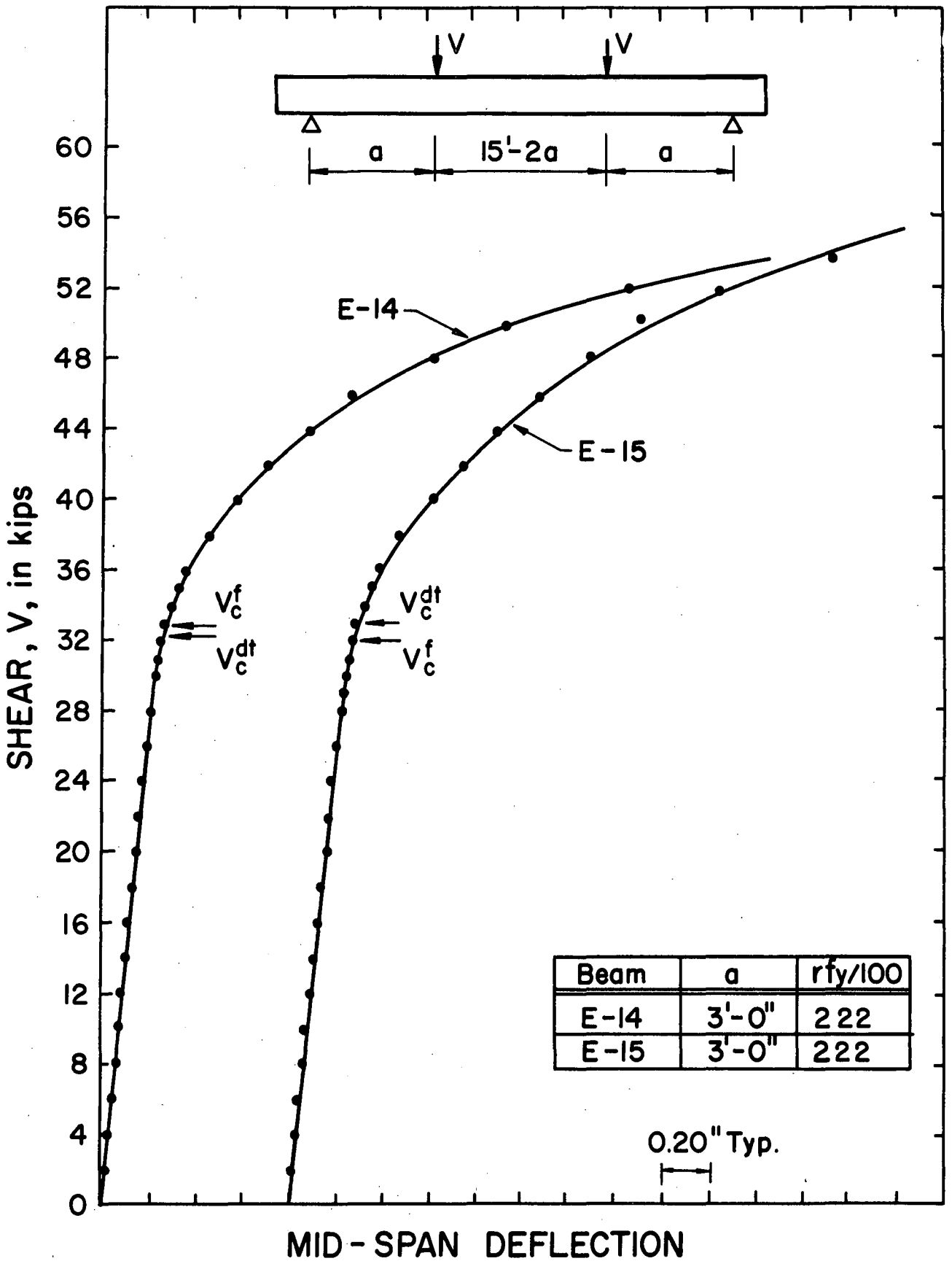
V
V
a
15'-2a
a
60
56
52
48
44
40
36
32
28
24
20
16
12
8
4
0
SHEAR, V, in kips
E-14
E-15
V_c^f
V_c^{dt}
V_c^{dt}
V_c^f
Beam | a | rfy/100
E-14 | 3'-0" | 222
E-15 | 3'-0" | 222
0.20" Typ.
MID-SPAN DEFLECTION

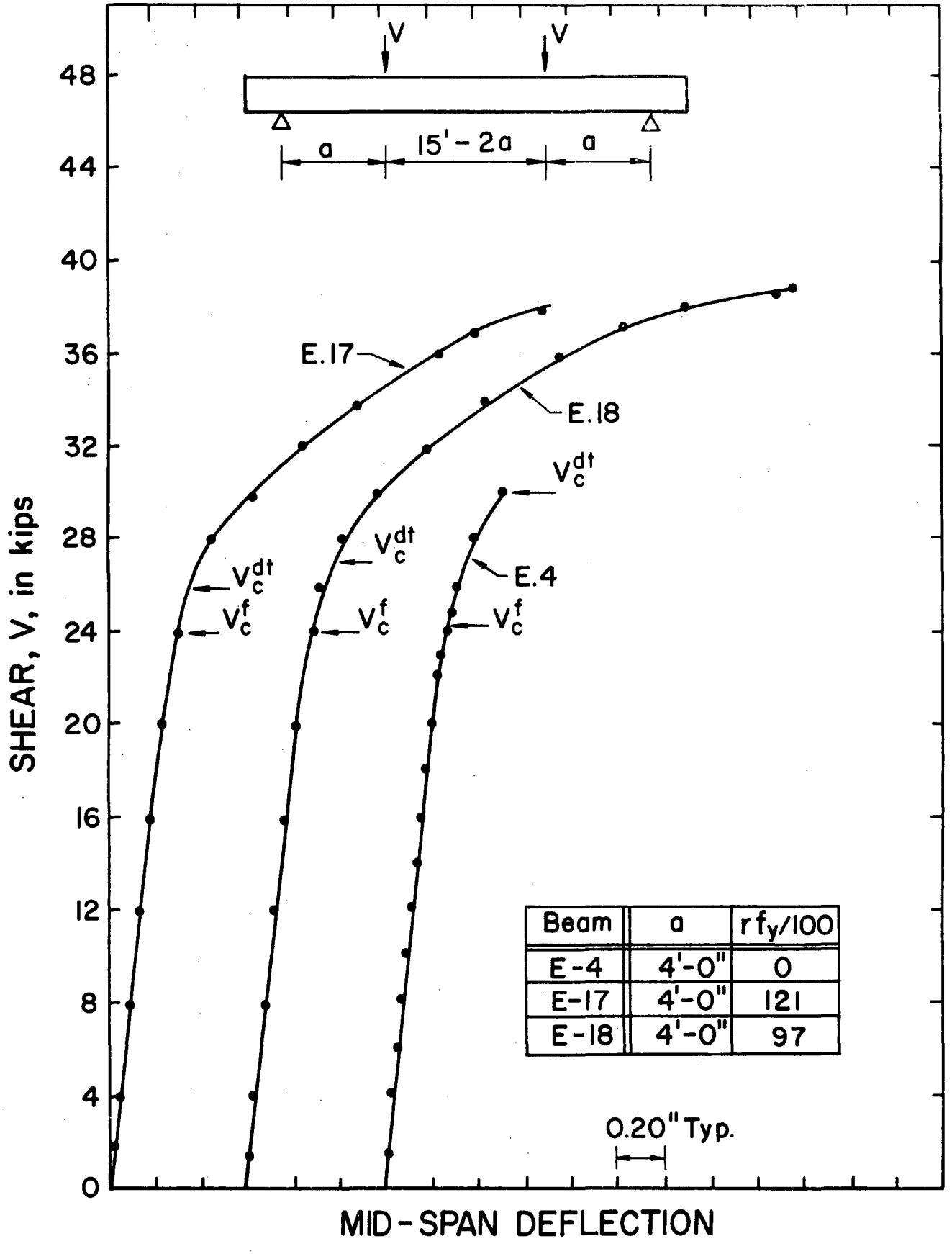

Beam	a	$r f_y/100$
E-4	4'-0"	0
E-17	4'-0"	121
E-18	4'-0"	97

8. REFERENCES

1. ACI - ASCE Joint Committee 323
TENTATIVE RECOMMENDATIONS FOR PRESTRESSED CONCRETE
Journal of the American Concrete Institute, Proceedings V. 54, No. 7, January 1958, pp. 545-578

2. Mattock, A. H., Kriz, L. S., Hognestad, E.
RECTANGULAR CONCRETE STRESS DISTRIBUTION IN ULTIMATE STRENGTH DESIGN
Journal of the American Concrete Institute, Proceedings V. 57, No. 8, February 1961, pp. 875-928

3. Hulsbos, C. L., Van Horn, D. A.
STRENGTH IN SHEAR OF PRESTRESSED CONCRETE I-BEAMS
Progress Report, Iowa Engineering Experiment Station, Iowa State University, April 1960

4. McClarnon, F. M, Wakabayashi, M., Ekberg, C. E. Jr.
FURTHER INVESTIGATION INTO THE SHEAR STRENGTH OF PRESTRESSED CONCRETE BEAMS WITHOUT WEB REINFORCEMENT
Fritz Engineering Laboratory Report No. 223.22, Lehigh University, January 1962

5. Mattock, A. H., Kaar, P. H.
PRECAST-PRESTRESSED CONCRETE BRIDGES 4.
SHEAR TESTS OF CONTINUOUS GIRDERS
Journal of the PCA Research and Development Laboratories, V. 3, No. 1, January 1961, pp. 19-46

6. Timoshenko, S., Goodier, J. N.
THEORY OF ELASTICITY
Second Edition, McGraw-Hill Book Company, Inc., New York, 1951

7. Warner, R. F., Hulsbos, C. L.
PROBABLE FATIGUE LIFE OF PRESTRESSED CONCRETE FLEXURAL MEMBERS
Fritz Engineering Laboratory Report No. 223.24A, Lehigh University, July 1962